

**Contract No:**

This document was prepared in conjunction with work accomplished under Contract No. DE-AC09-08SR22470 with the U.S. Department of Energy (DOE) Office of Environmental Management (EM).

**Disclaimer:**

This work was prepared under an agreement with and funded by the U.S. Government. Neither the U. S. Government or its employees, nor any of its contractors, subcontractors or their employees, makes any express or implied:

- 1 ) warranty or assumes any legal liability for the accuracy, completeness, or for the use or results of such use of any information, product, or process disclosed; or
- 2 ) representation that such use or results of such use would not infringe privately owned rights; or
- 3) endorsement or recommendation of any specifically identified commercial product, process, or service.

Any views and opinions of authors expressed in this work do not necessarily state or reflect those of the United States Government, or its contractors, or subcontractors.



# Impacts of Glycolate and Formate Radiolysis and Thermolysis on Hydrogen Generation Rate Calculations for the Savannah River Site Tank Farm

C. L. Crawford

W. D. King

August 2017

SRNL-STI-2017-00303, Revision 0



## **DISCLAIMER**

This work was prepared under an agreement with and funded by the U.S. Government. Neither the U.S. Government or its employees, nor any of its contractors, subcontractors or their employees, makes any express or implied:

1. warranty or assumes any legal liability for the accuracy, completeness, or for the use or results of such use of any information, product, or process disclosed; or
2. representation that such use or results of such use would not infringe privately owned rights; or
3. endorsement or recommendation of any specifically identified commercial product, process, or service.

Any views and opinions of authors expressed in this work do not necessarily state or reflect those of the United States Government, or its contractors, or subcontractors.

**Printed in the United States of America**

**Prepared for  
U.S. Department of Energy**

**Keywords:** *Flammability, Flammable Gas, Organic Decomposition*

**Retention:** *Permanent*

# Impacts of Glycolate and Formate Radiolysis and Thermolysis on Hydrogen Generation Rate Calculations for the Savannah River Site Tank Farm

C. L. Crawford  
W. D. King

August 2017

---

Prepared for the U.S. Department of Energy under contract number DE-AC09-08SR22470.



## REVIEWS AND APPROVALS

### AUTHORS:

---

C. L. Crawford, Advanced Characterization & Processing	Date
--	------

---

W. D. King, Advanced Characterization & Processing	Date
--	------

### TECHNICAL REVIEW:

---

W. H. Woodham, Process Technology Systems, Reviewed per E7 2.60	Date
---	------

### APPROVAL:

---

F. M. Pennebaker, Manager Chemical Processing Technologies	Date
---	------

---

D. E. Dooley, Director Chemical Processing Technologies	Date
--	------

---

E. J. Freed, Manager Defense Waste Processing Facility and Saltstone Facility Engineering	Date
--	------

---

J. P. Schwenker, Jr., Manager Tank Farm Facility Engineering	Date
---	------

---

R. E. Edwards, Manager Nuclear Safety & Engineering Integration	Date
--	------

## EXECUTIVE SUMMARY

Savannah River Remediation (SRR) personnel requested that the Savannah River National Laboratory (SRNL) evaluate available data and determine its applicability to defining the impact of planned glycolate anion additions to Savannah River Site (SRS) High Level Waste (HLW) on Tank Farm flammability (primarily with regard to  $H_2$  production). Flammability evaluations of formate anion, which is already present in SRS waste, were also needed. This report describes the impacts of glycolate and formate radiolysis and thermolysis on Hydrogen Generation Rate (HGR) calculations for the SRS Tank Farm.

Glycolate introduction into the SRS Tank Farm is anticipated in the future due to recycle stream returns from the Defense Waste Processing Facility (DWPF) nitric-glycolic acid alternative reductant flowsheet. Formic acid is currently utilized as a reductant in DWPF melter operations and soluble formate anion is present at levels of  $\sim 2,300$  mg/L within portions of the SRS Tank Farm caustic waste. Literature surveys were conducted pertaining to radiolysis and thermolysis of both glycolate and formate anions within the SRS Tank Farm. Based on the results, HGR calculations were conducted to predict the total hydrogen production from water and organic radiolysis and organic thermolysis. Potential impacts of formate and glycolate radiolytic and thermolytic terms on DWPF HGRs were also evaluated. Only glycolate and formate radiolysis and thermolysis were considered in this study, although various other organic compounds have been added to SRS waste.

Three different radiolysis HGR methodologies were identified that include both water radiolysis and the effects of organics on radiolytic hydrogen production. Organic radiolysis effects were considered as additive terms to the baseline water radiolysis HGR. The first set of radiolysis HGR equations include hydrogen gas produced from water radiolysis and from the reaction of organic compounds with the hydrogen atom produced from water radiolysis. The second methodology uses the same water radiolysis equations and employs an empirical relation for added organic compounds originally developed in the early 1990's for the prediction of Hanford Tank Farm waste hydrogen generation. A third radiolysis methodology is derived from the equations currently used at the Hanford Tank Farm which involve similar water radiolysis terms to those used at SRS, and organic radiolysis terms that are dependent on total organic carbon (TOC) levels. Comparison of these methods using a common set of inputs for SRS waste tank heat load (dose) and chemistry indicated that the first methodology appears to be the most conservative and bounding with regard to water and organic radiolysis.

The SRS baseline water radiolysis HGR equations, which have been previously shown to be conservative with respect to actual hydrogen measurements in the SRS Tank Farm, are also adequate to bound the sum of the formate radiolysis HGR at 10 g/L formate and actual measured HGR data. The reactivity of glycolate anion towards hydrogen atom abstraction to produce molecular hydrogen is only about 20% of the rate for formate. The case including 10 g/L glycolate with 10 g/L formate is also bounded by the current baseline HGR equations when considering radiolysis effects from these organics (formate and glycolate) alone.

Several techniques were used to develop the above conclusions regarding water and organic radiolysis including: analyses comparing all active SRS tanks; comparisons of additive terms to previous measured HGRs from five SRS tanks, and examination of the effects on the time to reach the hydrogen Lower Flammability Limit (TtLFL).

Literature survey results for the thermolysis of formate and glycolate anions in caustic nuclear waste solutions indicate that glycolate is susceptible to thermolytic degradation based on simulant testing at temperatures up to 120 °C. In contrast, several studies indicate that formate ion does not undergo thermolysis to produce hydrogen gas in caustic solutions at elevated temperatures. An empirical HGR

equation that predicts hydrogen production from thermolysis has been developed by Hanford that depends on aluminum and TOC concentrations and was formulated based on extensive testing of simulated and actual Hanford waste samples. This formulation estimates HGRs from thermolysis of Hanford organic waste constituents including various complexants, diluents, phthalate esters and remnants from the separation processes that were used historically at the Hanford site. Separate studies focused on the thermolysis of glycolate anion only in waste simulants was originally cited in a 2012 review of glycolate impacts to the SRS 2H Evaporator and the Effluent Treatment Facility (ETF) by SRNL. According to the glycolate thermolysis equation, hydrogen production is a function of the aluminate, nitrite, and hydroxide ion concentrations. Direct comparison of these two thermolysis equations using SRS Tank Farm input data indicates that the Hanford empirical equations generally give higher thermolysis HGRs than the glycolate-only thermolysis equations. The calculations using either thermolysis equations and a maximum 10 g/L glycolate also indicate that thermolysis HGRs are of similar order of magnitude to water radiolysis HGRs in the temperature range of 75°C (Hanford thermolysis equations) to 90°C (glycolate only thermolysis equations).

Combined water radiolysis, indirect organic radiolysis, and thermolysis (Ashby method) terms for SRS waste were examined in the temperature range of 50 to 100 °C. The results were compared to previous measurements within four high heat load SRS tanks from the late 1990s and also to current TtLFL values for all active SRS tanks. The following threshold upper bounding temperatures and associated formate and glycolate concentrations were identified for the SRS Tank Farm.

- 50°C for 10 g/L each of formate and glycolate
- 75°C for 5 g/L each of formate and glycolate
- 90°C for 3 g/L each of formate and glycolate

Identification of these thresholds consisted of 1) comparison of the additive terms to a 2002 established lower predicted bound of 25% uncertainty factor involving the chemical composition and heat loads of these tanks; 2) use of the additive terms to examine the change in HGR status of the tanks with respect to the TtLFL values. Using these criteria it is shown that at these levels the additive terms remain near or below the predicted HGRs for three of the four high heat load tanks minus a 25% uncertainty factor, and that only two of the existing rapid generation tanks have decreased TtLFL values below 7 days.

### Impacts to DWPF

Potential impacts of formate and glycolate radiolytic and thermolytic terms on DWPF HGRs were also performed building upon a recent position paper from DWPF and Saltstone Facility Engineering, as described below.<sup>a,b</sup>

### Radiolytic Terms:

- In Sections 2.1 and 2.2 of document X-ESR-S-00320 a conservative value for the fraction of hydrogen atoms reacting with an organic anion to produce molecular hydrogen,  $f_{\text{organic}}$ , is assigned a value of 1 due to the expected significant levels of formate present. Therefore, the DWPF

<sup>a</sup> A. T. Clare, "Inclusion of Organic Contribution to Radiolytic and Thermolytic Hydrogen Generation at DWPF", X-ESR-S-00320, Rev. 2, 2017.

<sup>b</sup> The impacts of added formate and glycolate from this report were assessed as a continuation of the above reference. Familiarization with the context, results and conclusions of that work are thus required to attain best perspective on the impacts of these organic levels to the DWPF process vessels presented and discussed in Section 4 of this report.

process vessels identified as the Sludge Receipt and Adjustment Tank (SRAT), Slurry Mix Evaporator (SME), Melter Feed Tank (MFT), Slurry Mix Evaporator Condensate Tank (SMECT), Recycle Collection Tank (RCT), Decontamination Waste Treatment Tank (DWTT), Strip Effluent Feed Tank (SEFT) and Precipitate Reactor Feed Tank (PRFT) would use the R value equations specified in X-ESR-S-00320 as equations for alpha heat loading (Eqn. 7) and for beta/gamma heat loading (Eqn. 8) without any adjustment for the formate and glycolate in the matrix considered in this report.

- In Section 2.3 for the DWPF Sludge Pump Tank (SPT), Precipitate Pump Tank (PPT), Late Wash Precipitate Tank (LWPT), and Late Wash Hold Tank (LWHT) process vessels that are associated with untreated sludge/salt from the Tank Farm, the calculated  $f_{\text{organic}}$  terms from X-ESR-S-00320 are significantly increased using the maximum formate and glycolate levels assumed for this report. The DWPF Sludge Batch 9 (SB9)  $f_{\text{organic}}$  term of 0.0053 was increased to 0.191 and the SB8  $f_{\text{organic}}$  term of 0.0051 was increased to 0.143 for the highest level of 10 g/L each for the formate and glycolate waste concentrations. However review of historic formate Tank 40 concentrations from WAPS reports indicates that the highest formate value reported is less than detectable < 585 mg/L. Substitution of this formate value into the SB8 and SB9 calculations results in  $f_{\text{organic}}$  of < 0.012. By analogy if glycolate concentrations in Tank 40 for the planned nitric/glycolic flowsheet are comparable to historic formate concentrations of < 585 mg/L, then the  $f_{\text{organic}}$  term is < 0.009. Thus these calculations along with the data presented in Section 2.3 of X-ESR-S-00320 support using a  $f_{\text{organic}}$  term of 0 for these vessels.
- In Section 2.4 the  $f_{\text{organic}}$  term was also increased for the DWPF Recycle Pump Tank (RPT) considering the formate and glycolate levels used in this report. The RPT  $f_{\text{organic}}$  term of 0.1442 was increased to 0.323 for the highest level of 10 g/L each for the formate and glycolate waste concentrations. However current nitric/formic flowsheet conditions indicate an upper limit of ~ 4,000 mg/L formate expected in the RPT with a  $f_{\text{organic}} = 0.1442$ . The calculated practical maximum limit for the planned nitric/glycolic flowsheet indicate 10,000 mg/L glycolate and 2,000 mg/L formate resulting in a  $f_{\text{organic}}$  of 0.143.

Thermolysis Impacts to the Nitric/Formic DWPF Flowsheet Using a Catalytic Limit of 0.15 lb/hr/6000 gal:

- Thermolysis rates using the Hanford correlation and its associated uncertainty and the adjusted TOC resulting from a SB9 SRAT heel blended with the adjusted TOC from DWPF incoming sludge give calculated thermolysis rate to formate catalysis rate ratios in the range of 0.003 to 0.011, or ~ 0.3% to 1.1%. Thus the same conclusion as was made in the DWPF position paper holds for the SB9 case scenario considered in this work. Thermolysis rates compared to catalysis rates at the ~ 105°C temperature of DWPF processing indicates that the catalytic rate is significantly bounding and remains bounding at lower temperatures.

Thermolysis Impacts to the Nitric/Glycolic DWPF Flowsheet Using a Catalytic Limit of 0.024 lb/hr/6000 gal:

- Thermolysis rates using outputs from the Hanford correlation for adjusted TOC and the glycolate thermolysis equations applied to the nitric/glycolic SRAT heel plus incoming sludge that could contain up to 10 g/L glycolate give calculated thermolysis rate to formate catalysis rate ratios in the range of 0.027 to 0.064, or ~ 3.7 to 6.4% for maximum antifoam and 0.020 to 0.041, or ~ 2 to 4.1% for a reduced antifoam addition. These values indicate that the predicted thermolysis rates



would be much lower than the potential 25% CLFL considered for the nitric/glycolic flowsheet for SRAT and SME flammability control.

Thermolysis HGRs for Nonheated Tanks Predicted at 50°C and Heated Tanks Predicted at 105°C Compared to Radiolytic HGRs:

- All of the predicted 50°C thermolysis rates determined for the nitric/formic or the nitric/glycolic flowsheets for nonheated tanks are shown to be lower than current conservative radiolytic HGRs from water radiolysis that are calculated without consideration for nitrate and nitrite scavengers. HGRs for heated tanks at a temperature of 105°C for these same scenarios are comparable to the radiolytic rates for sludge tanks and the LWPT salt tanks. The 105°C HGRs are an order of magnitude higher than the radiolytic rate for the LWHT salt tank.

## TABLE OF CONTENTS

LIST OF FIGURES .....	xi
LIST OF ABBREVIATIONS .....	xiii
1.0 Introduction .....	1
2.0 Literature Reviews .....	2
2.1 Radiolysis of Formate and Glycolate in the SRS Tank Farm and Evaporators.....	2
2.2 Thermolysis of Formate and Glycolate in the SRS Tank Farm and Evaporators .....	4
2.3 Quality Assurance .....	9
3.0 Hydrogen Generation Rate Calculations for the SRS Tank Farm .....	9
3.1 Comparison of Radiolytic HGR Methods .....	9
3.2 Comparison of Formate Levels for Radiolysis.....	13
3.3 Comparison of Formate and Glycolate Levels for Radiolysis .....	21
3.4 Glycolate Thermolysis .....	24
3.5 Comparison of Combined Radiolytic and Thermolytic HGRs .....	26
4.0 Evaluation of Potential Impacts to DWPF .....	46
4.1 Comparison of Radiolytic Additive Terms .....	46
4.2 Comparison of Thermolytic Additive Terms .....	49
4.2.1 Nitric/Formic Flowsheet for Heated Tanks in DWPF .....	49
4.2.2 Nitric/Glycolic Flowsheet for Heated Tanks in DWPF .....	50
4.3 Comparison of Thermolytic Additive Terms for Nonheated Tanks and Heated Tanks to Radiolytic Rates .....	54
5.0 Conclusions .....	55
6.0 Recommendations, Path Forward or Future Work .....	57
7.0 References .....	58
Appendix A Radiolysis HGR Equations for SRS Baseline Methodology Involving Water Radiolysis and Organic Radiolysis Via Competition Kinetics.....	A-1
Appendix B . Radiolysis HGR Equations for SRS Baseline Methodology Involving Water Radiolysis and Organic Radiolysis Via ANL Correlation.....	B-1
Appendix C . Radiolysis HGR Equations for Hanford .....	C-1
Appendix D . Fraction of Organics Reacting with Hydrogen Atom with Formate and Glycolate Equal to 10 g/L .....	D-1

## LIST OF TABLES

Table 3-1. Matrix of Glycolate and Formate Concentrations Evaluated .....	9
Table 3-2. Competition Kinetics Calculation Parameters for SRS Tank 39 .....	12
Table 3-3. Ratios of Baseline Plus Organic HGR (Competition Kinetics) to Baseline HGR from Various Formate Levels* .....	16
Table 3-4. Previous Measured and Predicted (Boley method) HGRs <sup>67</sup> .....	17
Table 3-5. Heat Loads and Waste Compositions for Previously Analyzed Tanks at the Time of Analysis .....	17
Table 3-6. Comparison of Time to Lower Flammability Limit for Baseline Water Radiolysis and Baseline + Maximum Organic Radiolysis Cases.....	23
Table 3-7. Ratio of Hanford to Ashby Thermolysis HGRs for 10 g/L Glycolate.....	26
Table 3-8. Comparison of Baseline TtLFL to 3 g/L Organics .....	43
Table 3-9. Comparison of Baseline TtLFL to 5 g/L Organics .....	44
Table 3-10. Comparison of Baseline TtLFL to 10 g/L Organics .....	45
Table 4-1. Calculation of $f_{\text{organic}}$ for SB9 Conditions and Glycolate and Formate .....	47
Table 4-2. Calculation of $f_{\text{organic}}$ for SB8 Conditions and Glycolate and Formate .....	47
Table 4-3. Calculation of $f_{\text{organic}}$ for RPT with Glycolate and Formate .....	48
Table 4-4. Scenario Considered for Thermolysis in Nitric/Formic Flowsheet with Heel .....	49
Table 4-5. Comparison of Thermolytic Rates to Catalytic Rates in Nitric/Formic DWPF Flowsheet .....	50
Table 4-6. Scenario Considered for Thermolysis in Nitric/Glycolic Flowsheet with Heel .....	51
Table 4-7. Comparison of Thermolytic Rates to Catalytic Rates in Nitric/Glycolic DWPF Flowsheet with Maximum Antifoam Addition .....	52
Table 4-8. Comparison of Thermolytic Rates to Catalytic Rates in Nitric/Glycolic DWPF Flowsheet with Reduced Antifoam Addition.....	53
Table 4-9. Comparison of Thermolysis Rates at 50°C and at 105°C to Radiolytic Rates in Temperature Range of 42.4°C to 50°C.....	54

## LIST OF FIGURES

Figure 2-1. Mechanism of Glycolate Thermal Decomposition in Simulated Waste Supernate (as reported by Ashby <sup>54</sup> ).....	7
Figure 3-1. Comparison of Radiolytic (water and organic) HGRs for Various Methods Using 10 g/L Glycolate and Formate at 25 °C. (SRS Baseline = Boley water radiolysis).....	11
Figure 3-2. Comparison of Radiolytic HGRs for SRS and Hanford Methods Using 10 g/L Glycolate and Formate at 25 °C. (SRS and Hanford Baseline involve water radiolysis only).....	13
Figure 3-3. Formate Radiolytic HGR by SRS Baseline Water Radiolysis + Competition Kinetics (w/Org.) vs. SRS Water Radiolysis Only (formate concentrations of 0.1 g/L (top) to 3 g/L (bottom)) at 25 °C.....	14
Figure 3-4. Formate Radiolytic HGR by SRS Baseline Water Radiolysis + Competition Kinetics (w/Org.) vs. SRS Water Radiolysis Only (formate concentrations of 5 g/L (top) to 10 g/L (bottom)) at 25 °C.....	15
Figure 3-5. Comparison of Measured and Measured + Calculated Formate (0.1 g/L to 3 g/L) Radiolysis (Competition Kinetics) HGRs Versus the Predicted HGR Using the Boley Method for Selected SRS Tanks Including 25% Uncertainties. “Linear” represents predicted vs predicted by Boley method. Measured tanks from left to right are SRS Tanks 38, 36, 33, 35, and 32.....	19
Figure 3-6. Comparison of Measured and Measured Plus Calculated Formate (5 g/L to 10 g/L) Radiolysis (Competition Kinetics) HGRs Versus the Predicted HGR Using the Boley Method for Selected SRS Tanks Including 25% Uncertainties. “Linear” represents predicted vs predicted by Boley method. Measured tanks from left to right are SRS Tanks 38, 36, 33, 35, and 32.....	20
Figure 3-7. Comparison of Measured and Measured Plus Calculated Formate plus Glycolate Radiolysis (Competition Kinetics) HGRs Versus the Predicted HGR Using the Boley Method for Selected SRS Tanks Including 25% Uncertainties (Glycolate = Formate = 10 g/L). “Linear represents predicted vs. predicted by Boley method. Measured tanks from left to right are SRS Tanks 38, 36, 33, 35, and 32.....	21
Figure 3-8. Comparison of Hanford (Hu) and Ashby Thermolysis HGRs at 120°C and 10 g/L Glycolate (no radiolysis contributions).....	24
Figure 3-9. Hanford Thermolysis HGR versus Temperature at 10 g/L Glycolate (no radiolysis contributions).....	25
Figure 3-10. Ashby Thermolysis HGRs versus Temperature at 10 g/L Glycolate (no radiolysis contributions).....	25
Figure 3-11. HGR Predictions for Organic Radiolysis and Organic Radiolysis plus Thermolysis Terms vs. SRS Baseline Water Radiolysis at 100 °C (top) and 90 °C (bottom) with 10 g/L Organics. Formate and Glycolate both at 10 g/L for Radiolysis and Glycolate at 10 g/L for Thermolysis.....	28
Figure 3-12. HGR Predictions for Organic Radiolysis and Organic Radiolysis plus Thermolysis Terms vs. SRS Baseline Water Radiolysis at 75°C (top) and 50°C (bottom) with 10 g/L Organics. Formate and Glycolate both at 10 g/L for Radiolysis and Glycolate at 10 g/L for Thermolysis.....	29

Figure 3-13. HGR Predictions for Organic Radiolysis and Organic Radiolysis plus Thermolysis Terms vs. SRS Baseline Water Radiolysis at 100°C (top) and 90°C (bottom) with 5 g/L Organics. Formate and Glycolate both at 5 g/L for Radiolysis and Glycolate at 5 g/L for Thermolysis. ....	30
Figure 3-14. HGR Predictions for Organic Radiolysis and Organic Radiolysis plus Thermolysis Terms vs. SRS Baseline Water Radiolysis at 75°C (top) and 50°C (bottom) with 5 g/L Organics. Formate and Glycolate both at 5 g/L for Radiolysis and Glycolate at 5 g/L for Thermolysis. ....	31
Figure 3-15. HGR Predictions for Organic Radiolysis and Organic Radiolysis plus Thermolysis Terms vs. SRS Baseline Water Radiolysis at 100°C (top) and 90°C (bottom) with 3 g/L Organics. Formate and Glycolate both at 3 g/L for Radiolysis and Glycolate at 3 g/L for Thermolysis. ....	32
Figure 3-16. HGR Predictions for Organic Radiolysis and Organic Radiolysis plus Thermolysis Terms vs. SRS Baseline Water Radiolysis at 75°C (top) and 50°C (bottom) with 3 g/L Organics. Formate and Glycolate both at 3 g/L for Radiolysis and Glycolate at 3 g/L for Thermolysis. ....	33
Figure 3-17. Comparison of Measured and Measured Plus Calculated Formate plus Glycolate Radiolysis (Competition Kinetics) and Thermolysis (Ashby) HGRs Versus the Predicted HGR Using the Boley Method for Selected SRS Tanks Including 25% Uncertainties (100 °C top, 90 °C bottom; glycolate = formate = 10 g/L). “Linear” represents predicted vs. predicted by Boley method. Measured tanks from left to right are SRS Tanks 38, 36, 33, 35, and 32. ....	35
Figure 3-18. Comparison of Measured and Measured Plus Calculated Formate plus Glycolate Radiolysis (Competition Kinetics) and Thermolysis (Ashby) HGRs Versus the Predicted HGR Using the Boley Method for Selected SRS Tanks Including 25% Uncertainties (75 °C top, 50 °C bottom; glycolate = formate = 10 g/L). “Linear” represents predicted vs. predicted by Boley method. Measured tanks from left to right are SRS Tanks 38, 36, 33, 35, and 32. ....	36
Figure 3-19. Comparison of Measured and Measured Plus Calculated Formate plus Glycolate Radiolysis (Competition Kinetics) and Thermolysis (Ashby) HGRs Versus the Predicted HGR Using the Boley Method for Selected SRS Tanks Including 25% Uncertainties (100 °C top, 90 °C bottom; glycolate = formate = 5 g/L). “Linear” represents predicted vs. predicted by Boley method. Measured tanks from left to right are SRS Tanks 38, 36, 33, 35, and 32. ....	37
Figure 3-20. Comparison of Measured and Measured Plus Calculated Formate plus Glycolate Radiolysis (Competition Kinetics) and Thermolysis (Ashby) HGRs Versus the Predicted HGR Using the Boley Method for Selected SRS Tanks Including 25% Uncertainties (75 °C top, 50 °C bottom; glycolate = formate = 5 g/L). “Linear” represents predicted vs. predicted by Boley method. Measured tanks from left to right are SRS Tanks 38, 36, 33, 35, and 32. ....	38
Figure 3-21. Comparison of Measured and Measured Plus Calculated Formate plus Glycolate Radiolysis (Competition Kinetics) and Thermolysis (Ashby) HGRs Versus the Predicted HGR Using the Boley Method for Selected SRS Tanks Including 25% Uncertainties (100 °C top, 90 °C bottom; glycolate = formate = 3 g/L). “Linear” represents predicted vs. predicted by Boley method. Measured tanks from left to right are SRS Tanks 38, 36, 33, 35, and 32. ....	39
Figure 3-22. Comparison of Measured and Measured Plus Calculated Formate plus Glycolate Radiolysis (Competition Kinetics) and Thermolysis (Ashby) HGRs Versus the Predicted HGR Using the Boley Method for Selected SRS Tanks Including 25% Uncertainties (75 °C top, 50 °C bottom; glycolate = formate = 3 g/L). “Linear” represents predicted vs. predicted by Boley method. Measured tanks from left to right are SRS Tanks 38, 36, 33, 35, and 32. ....	40

## LIST OF ABBREVIATIONS

ANL	Argonne National Laboratory
ARP	Actinide Removal Process
CLFL	Composite Lower Flammability Limit
CSTF	Concentration, Storage, and Transfer Facilities
DOE	Department of Energy
DWPF	Defense Waste Processing Facility
DWTT	Decontamination Waste Treatment Tank
EDTA	Ethylene Diamine Tetraacetic Acid
ETF	Effluent Treatment Facility
ft <sup>3</sup> /hr	Cubic feet per hour
ft <sup>3</sup> /hr/gal	Cubic feet per hour per gallon
HEDTA	(2-Hydroxyethyl)ethylenediaminetriacetic acid
HGR	Hydrogen Generation Rate
HHW	High Heat Waste
HLW	High-Level Waste
LFL	Lower Flammability Limit
LW	Liquid Waste
LWHT	Late Wash Hold Tank
LWPT	Late Wash Precipitate Tank
M	Molar
MCU	Modular Caustic Side Solvent Extraction Unit
MFT	Melter Feed Tank
PISA	Potential Inadequacy in the Safety Analysis
PPT	Precipitate Pump Tank
PRFT	Precipitate Reactor Feed Tank
RCT	Recycle Collection Tank
RPT	Recycle Pump Tank
s	second
SB8, SB9	(DWPF) Sludge Batch 8 or Sludge Batch 9
SEFT	Strip Effluent Feed Tank
SME	Slurry Mix Evaporator
SMECT	Slurry Mix Evaporator Condensate Tank
SPT	Sludge Pump Tank
SRAT	Sludge Receipt and Adjustment Tank
SRNL	Savannah River National Laboratory
SRR	Savannah River Remediation
SRS	Savannah River Site
SWPF	Salt Waste Processing Facility
TAR	Technical Assistance Request
TOC	Total Organic Carbon
TtLFL	Time to Lower Flammability Limit (days)
TTQAP	Task Technical and Quality Assurance Plan

TTR	Technical Task Request
WAPS	Waste Acceptance Product Specifications
WCS	Waste Characterization System
WTP	(Hanford) Waste Treatment and Immobilization Plant

## 1.0 Introduction

Savannah River Remediation (SRR) personnel requested that Savannah River National Laboratory (SRNL) evaluate available data and determine its applicability to defining the impact of glycolate on the Savannah River Site (SRS) Tank Farm flammability (primarily with regard to  $H_2$  production).<sup>1, 2</sup> Glycolate anion introduction into the SRS Tank Farm is anticipated in the future due to recycle stream returns from the Defense Waste Processing Facility (DWPF) nitric-glycolic acid alternative reductant flowsheet. The Chemical Processing Cell (CPC) portion of the DWPF alternative reductant flowsheet was recently demonstrated in the 2016 SRNL Shielded Cells qualification testing for Sludge Batch 9 (SB9).<sup>3</sup> In SRS caustic waste, glycolate will exist as the glycolate anion with the molecular formula,  $C_2H_3O_3^-$ . Formic acid is currently utilized as a reductant in DWPF to reduce mercury and to adjust the waste oxidation-reduction potential (REDOX) prior to feeding the melter, and formate ion ( $HCO_2^-$ ) is already present at significant levels (exceeding 2 g/L) within some SRS waste tanks.<sup>4, 5</sup> The presence of formate in SRS waste tanks is presumed to be derived from normal processing which can generate some formate in DWPF condensate streams, or from carryover events from DWPF Sludge Receipt and Adjustment Tank (SRAT) or Slurry Mix Evaporator (SME) operations over the past twenty years. A portion of the formate in SRS waste tanks also could derive from its formation from the decomposition of other key organics in SRS waste cited in Reference 4, such as tributylphosphate, siloxanes and siloxanols, ion exchange resins and alkyl-aryl sulfonates. Evaluations of the impacts of formate radiolysis and thermolysis on hydrogen generation rates (HGRs) are also needed. Potential Inadequacy in the Safety Analyses (PISAs) have recently been issued at SRS associated with the unaddressed impacts of hydrogen generation from organics in the SRS Tank Farm, DWPF, and Saltstone facilities.<sup>6, 7, 8</sup>

Literature reviews have been conducted to identify relevant data and equations for the prediction of HGRs from the radiolytic and thermal degradation of both glycolate and formate ions in SRS High Level Waste (HLW) slurries under Tank Farm operating conditions. Facilities of concern within the Tank Farm include waste storage tanks and evaporators. A 2011 SRNL assessment examined glycolic acid physical properties, impurities, and radiation effects pertaining to a nitric/formic/glycolic acid flowsheet for DWPF processing.<sup>9</sup> A 2012 SRNL literature review focused on the impacts of glycolate on the SRS 2H Evaporator and the Effluent Treatment Facility (ETF).<sup>10</sup> In order to evaluate the impacts of glycolate and formate radiolysis and thermolysis on HGRs, this report will address historical methods used at SRS for HGR calculations (which do not explicitly account for organic radiolysis/thermolysis, but conservatively estimate HGRs from water radiolysis) and how these calculations might be revised (as needed) to account for hydrogen production from organic radiolysis and thermolysis. Analogous methods currently utilized for predicting HGRs in the Hanford HLW Tank Farm and the planned Waste Treatment and Immobilization Plant (WTP), which include organic radiolysis and thermolysis terms, will be presented and discussed in relation to the SRS methods. A similar comparison of SRS and Hanford calculational methods using SRS Tank Farm data was performed in 2004, but that work only examined hydrogen produced from water radiolysis and did not include any organic terms.<sup>11</sup> An alternative method for predicting the HGR resulting from glycolate thermolysis only will also be discussed and compared to the Hanford methodology.

Total HGRs from the three primary hydrogen sources (water radiolysis, glycolate/formate radiolysis, and glycolate/formate thermolysis) using these calculational methods and the range of SRS Tank Farm conditions anticipated are presented and compared for most current SRS HLW compositions. Various combinations of organic concentrations up to 10 g/L glycolate and 10 g/L formate are considered. Temperatures up to 120 °C are considered. Since, it is expected that one of the various HGR calculational methods provided in this report will ultimately be applied toward SRS Tank Farm HGR predictions, recommendations are made regarding the most appropriate methodology to use and whether other supplemental data is needed.

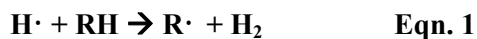


These reviews and evaluations were conducted following the Task Technical and Quality Assurance Plan (TTQAP) SRNL-RP-2017-00082 associated with this task.<sup>12</sup> Requirements for performing reviews of technical reports and the extent of review are established in Manual E7 Procedure 2.60.<sup>13</sup> SRNL documents the extent and type of review using the SRNL Technical Report Design Checklist contained in WSRC-IM-2002-00011, Rev. 2.<sup>14</sup> This report completes the Task 1 and Deliverable 2 items identified in the TTR<sup>2</sup> and the related request from the TAR.<sup>1</sup>

## 2.0 Literature Reviews

### 2.1 Radiolysis of Formate and Glycolate in the SRS Tank Farm and Evaporators

The baseline method utilized for SRS flammability calculations is well documented and has been used for several decades.<sup>15,16,17</sup> This method involves crediting the nitrate and nitrite scavenging of precursors to molecular hydrogen formed during water radiolysis by both beta/gamma and alpha radiation. Experimental SRNL studies involving Co-60 gamma radiolysis of DWPF and tetraphenylborate solutions and slurries cited other historical studies in the radiation chemistry literature supporting this approach.<sup>18, 19</sup> To date, the SRS Tank Farm flammability calculations have not involved any terms to address radiolytic hydrogen produced indirectly from the scavenging of hydrogen radicals (H·) by organics. Eqn. 1 shows this process for a generic water-soluble organic, RH, which generally leads to a reducing organic radical, R·, and molecular hydrogen.



Two different approaches to account for the radiolytic hydrogen production from Eqn. 1 have been examined. In the first approach, the first principles of water radiolysis are used involving competition kinetics of solute species that can react with the hydrogen radical. This method was used for formic acid in DWPF studies in 2007.<sup>20</sup> It was also addressed in a later report assessing glycolate in DWPF processing in 2011.<sup>9</sup> This method uses the solute concentrations and their respective published rate constants<sup>21</sup> for reaction with the hydrogen radical to derive a multiplier for the known yield of hydrogen radical from aqueous solutions from either beta/gamma or alpha irradiation. Since nitrate, nitrite and hydroxide anions are also reactive towards the hydrogen radical, but do not produce hydrogen gas,<sup>c</sup> these salts help to limit hydrogen production from Eqn. 1 in the presence of organics by competing for the hydrogen radical. Appendix A shows the relevant equations describing radiolytic hydrogen production from both water and soluble organics for either beta/gamma or alpha radiation. One detail to note in these equations is that while alpha radiation produces more molecular hydrogen than beta/gamma radiation, the effect is opposite for radiolytic hydrogen radical production. Alpha radiolysis only produces about one half the amount of H· as beta/gamma radiation. Equations in Appendix A as well as other method equations presented later in Appendices B and C are specified for the maximum organic concentration limits of glycolate (10 g/L) and formate (10 g/L).<sup>2</sup>

Another approach to predicting radiolytic hydrogen production from organics in the presence of nuclear waste solutions uses measured gas yields from simulant studies. This approach was originally used by Argonne National Laboratory (ANL) on Hanford simulants.<sup>22,23</sup> A correlation involving hydrogen production as a function of the organic species concentration was developed in 1991 using moderate concentrations of various soluble simple and complex organics believed to exist in Hanford waste tanks, including glycolate, but excluding formate.<sup>24</sup> This correlation involves both the number of R-H bonds of

<sup>c</sup> The product of the reaction  $\text{H}\cdot + \text{OH}^-$  is the hydrated electron,  $\text{e}_{\text{aq}}^-$ , which is a precursor to molecular hydrogen formation via  $\text{e}_{\text{aq}}^- + \text{e}_{\text{aq}}^- \rightarrow \text{H}_2 + 2\text{OH}^-$ . However this reaction is minimized in SRS Tank Waste by the scavengers nitrate and nitrite. See  $\text{G}(\text{H}_2)_{\text{Water Radiolysis}}$  equations in Appendix A.

the organic compound and its molar concentration. Appendix B shows the relevant equations describing radiolytic hydrogen production from both water and soluble organics using the Argonne correlation for beta/gamma irradiation. The ANL data set involved only Co-60 gamma irradiation. An assumption is made, based on the relative amounts of radiolytic hydrogen radical available, that alpha radiolysis would produce half of the amount computed by beta/gamma radiolysis. This approach has been used in the development of organic radiolysis equations to predict hydrogen production in Hanford waste as discussed in the next section. An assumption made in these equations is that the formate ion containing a single C-H bond is one half as proficient in radiolytic hydrogen production as glycolate ion which contains two C-H bonds. The relative reaction rates<sup>21</sup> for formate plus  $H\cdot$  ( $2.1E+08 M^{-1}s^{-1}$ ) and glycolate plus  $H\cdot$  ( $4.6E+07 M^{-1}s^{-1}$ ) are also used. The units for these rate constants are expressed as inverse Molar ( $M^{-1}$ ) and inverse second ( $s^{-1}$ ).

The approaches discussed above can be compared to hydrogen gas generation equations for the Hanford Tank Farm<sup>25, 26</sup> and the planned WTP.<sup>27</sup> These equations have evolved over time to include water radiolysis terms, soluble organic radiolysis terms and organic thermal decomposition terms. Appendix C shows the relevant equations describing radiolytic hydrogen production from both water and soluble organics using the Hanford Tank Farm equations.

A 2004 assessment of an earlier version set of the Hanford equations for water radiolysis (no organics) versus those used for the SRS Tank Farm concluded that predictions from the equations for total HGRs for the 47 active SRS waste tanks were, for the most part, similar.<sup>11</sup> The current set of Hanford equations have included an ‘excess sodium’ term for beta/gamma radiolysis that was not used in the previous SRNL comparison. This term serves to capture any additional scavengers (other than nitrate and nitrite) that might also reduce the hydrogen yield. It also corrects the effect that when the system reaches high ionic strength, insufficient free water exists to produce hydrogen through water radiolysis, e.g., a ‘salt cake’ tank. Another important factor in the Hanford water radiolysis equations is the use of the unitless  $L_f$  term representing liquid weight fraction in the waste. This term minimizes the hydrogen predicted from high solids waste such as that found in sludge and salt cake tanks. These two terms (excess sodium and liquid fraction) in the current Hanford Tank Farm equations serve to decrease HGR predictions relative to the previous Hanford method and the current baseline SRS method, given the same input parameters. The SRS water radiolysis equations are conservative in the sense that they only credit scavenging by nitrate and nitrite, and they treat all types of waste (sludge, salt cake and supernate) as capable of full radiolytic hydrogen production (as if all sludge and salt cake volume were supernate). The Hanford water radiolysis terms for both the beta/gamma and the alpha terms equate to the known hydrogen radiolysis G values in the absence of any scavengers, or  $G(H_2)_{b/g} \sim 0.45$  molecules/100 eV and  $G(H_2)_{alpha} \sim 1.4$  molecules/100 eV. It has been shown that using the full set of Hanford equations shown in Appendix C for water radiolysis, organic radiolysis and thermolysis provides calculated HGRs that are in the range of 0.5X to 3X compared to actual hydrogen measurements from 28 of the most active hydrogen generation tanks at Hanford.<sup>25</sup>

The organic radiolysis terms used in the Hanford equations are based on experimental studies as explained in References 25 and 27. The data suggests that the observed radiolysis rates are the result of thermal reactions of organic molecules (e.g., formaldehyde) formed in radiolytically induced reactions. Analysis indicates that the observed radiolysis rates are not only temperature dependent, but also follow Arrhenius behavior. These terms are dependent on the total organic carbon (TOC) content of the waste and the overall reactivity coefficient,  $r_f$ , of the organic species present. The TOC term and reactivity coefficients will be discussed in more detail below with regard to the thermolysis HGR terms in the Hanford equations. As explained in Reference 25, “the yield of hydrogen by radiolytically induced degradation of organics is expected to be lower from alpha radiolysis than from beta/gamma radiolysis. The reason for this is that alpha radiation deposits much higher energy per unit volume of matter than beta/gamma radiation. This causes higher yields of products from radical recombination and

consequently lower yields of radicals to diffuse from ionization tracks into the bulk solution.<sup>28</sup> The more that radical recombination occurs, the less that oxidizing radicals are available to degrade organic compounds to form hydrogen. It is estimated that the yield of radicals surviving intratrack reaction for alpha radiolysis is 50 percent of the yield by beta/gamma.” In the context quoted from Reference 25, the term ‘intratrack’ is used to mean ‘inside of the track’. This reasoning is the basis for suggesting that the total alpha organic radiolysis for tank waste is one half of the beta/gamma organic radiolysis. This same reasoning was applied in the development of the alpha organic radiolysis terms in the SRS equations shown in Appendices A and B.

## 2.2 Thermolysis of Formate and Glycolate in the SRS Tank Farm and Evaporators

A literature review was conducted focusing on the thermolytic degradation of glycolate and formate to produce H<sub>2</sub> gas under SRS Tank Farm and Evaporator conditions building upon the previous review conducted in 2012.<sup>10</sup> The most relevant research regarding the thermolysis of glycolate, formate, and various other organic compounds under caustic conditions and in radioactive waste solutions or simulated waste solutions was conducted primarily in the 1990’s by researchers at Pacific Northwest National Laboratory, Argonne National Laboratory, and Georgia Institute of Technology, and by personnel at the Department of Energy (DOE) site in Hanford, WA.

A global predictive equation shown in Eqn. 2 for organic thermolysis was developed by Hu based on simulated waste studies and measurements on actual Hanford waste samples.<sup>25,29</sup> The equation was developed based on empirical fitting of hydrogen generation data for various waste samples and simulants. A reactivity factor,  $r_f$ , was included to account for differences in the reactivity of the complexants, with different values used for Hanford double- and single-shell tanks. Concentration terms were included in the equation to account for the amounts of TOC, aluminum, and liquid fraction. A single pre-exponential factor,  $a$ , and a global activation energy,  $E$ , were recommended for hydrogen generation from all Hanford waste. The Hanford equation was based on sample temperatures  $\leq 120$  °C, and is applied to a maximum temperature near 75 °C in the Hanford Tank Farm. The uncertainty in Eqn. 2 is associated with the range in the activation energy shown.<sup>25</sup>.

$$\text{HGR} = a(r_f [\text{TOC}][\text{Al}]^{0.4} L_f \exp^{(-E/RT)}) \quad \text{Eqn. 2}$$

$a = 3.94 \times 10^9$  mol/kg waste·day

$r_f = 0.6$  for Hanford Double Shell Tanks;  $0.3$  for Single Shell Tanks

[TOC] = Total Organic Carbon wt. %

[Al] = aluminum wt. %

$L_f$  = liquid fraction

$E$  = activation energy for hydrogen generation (89.6 kJ/mol  $\pm$  1.94 kJ/mol used for Hanford tanks)

$R = 8.314$  J/K·mol, the gas constant

$T$  is the waste temperature in Kelvin

The application of the Hanford thermolysis equation to HGR calculations for SRS waste must be conducted with caution given the fact that the HGR equation terms are based on empirical fitting of HGR data for numerous Hanford waste samples. The Hanford equations are, however, partially based on actual tank waste samples and have been shown to predict HGRs reasonably well. The Hu equation has also been adapted for use under various waste processing conditions anticipated in the Hanford WTP as reported by Sherwood.<sup>27</sup>

Hanford waste contains a variety of organic complexants, e.g., glycolic acid, citric acid, HEDTA and EDTA, including numerous original complexants as well as organic fragments formed during waste aging.<sup>27,30,31,32</sup> Solvents used in Hanford chemical processes were mainly tributyl phosphate (TBP) and normal paraffin hydrocarbons (NPHs).<sup>32</sup> The primary organic compounds identified as having been introduced into SRS waste are TBP, siloxanes and siloxanols, ion exchange resins and alkyl-aryl sulfonates.<sup>4</sup> Sodium oxalate, which is not expected to impact HGRs, is common to both Hanford and SRS waste. The inorganic chemical composition of Hanford radioactive waste is also generally more diverse than SRS waste.<sup>33</sup>

SRS waste contains significant amounts of elemental mercury which was originally added as a catalyst to promote the dissolution of aluminum from various target and fuel materials.<sup>34,35</sup> All SRS fuel elements used aluminum cladding. It is estimated that >60 metric tons of mercury have been added to the SRS Tank Farm.<sup>34</sup> In contrast, the Hanford Tank Farm is estimated to contain <1 metric ton of mercury as indicated in Table A-1 of Reference 27. Hanford fuel elements consisted originally of aluminum and later zirconium, and Hanford N Reactor fuel elements were a more complex coextrusion of uranium and Zircaloy.<sup>27</sup> This use of multiple fuel cladding metals from Hanford versus the exclusive use of aluminum at SRS can explain the large difference in mercury levels in Hanford and SRS waste. Even at low concentrations, mercury is known to serve as a catalyst poison for Platinum Group metals in petrochemical processing.<sup>36</sup> Mercury has been shown to reduce, but not eliminate, hydrogen gas generation from formic acid under acidic to slightly caustic (pH 10) conditions catalyzed by the Platinum Group metals ruthenium and rhodium.<sup>37</sup> Mercuric oxide, which is known to be present in SRS waste, is known to react with H<sub>2</sub> and has been used in alkaline batteries (electrolyte solution: ~5-10 M KOH) to inhibit the formation of H<sub>2</sub> gas. Based on this information, it is believed that the presence of elemental mercury and mercuric oxide in SRS waste will not result in increased hydrogen generation rates. SRS waste is also known to contain soluble organomercury (di- and mono-methyl) compounds at low concentrations.<sup>35</sup> Organomercury compounds are utilized as catalysts in some organic reactions including polyurethane production,<sup>38</sup> but no specific references have been located associated with hydrogen production from reactions of these compounds with organic compounds. Specific tests evaluating catalytic effects of soluble organomercury species on HGRs resulting from organic thermolysis in either SRS Tank Farm simulants or actual radioactive samples have not been conducted.

In addition to the work conducted at Hanford, a group of researchers conducted tests in the 1990's focused on hydrogen generation from simulated caustic waste supernate containing various individual complexants, including glycolate and formate.<sup>22,23,39,40,41,42,43,44,45,46,47,48,49,50,51,52,53</sup> Limited testing was also completed in these solutions evaluating catalytic effects on the thermolysis of EDTA (Ethylene Diamine Tetraacetic Acid), HEDTA ((2-Hydroxyethyl)EthylenediamineTriacetic acid), and citrate ion from selected transition and noble metals (Cr<sup>3+</sup>, Fe<sup>3+</sup>, Pd<sup>4+</sup>, and Pt<sup>4+</sup>).<sup>22</sup> No catalytic enhancement of the thermolytic HGRs of these complexants was observed by these metals.

In simplified caustic salt solutions with no metals present, the concentration of formate ion was reported to be unchanged based on ion chromatography analyses after being held at 120 °C for 1000 h in air.<sup>54</sup> Similar results were reported for the anions acetate and oxalate under the same experimental conditions.<sup>54</sup> Under inert and oxygen atmospheres in these solutions, the H<sub>2</sub> concentration detected in the off-gas was the same as was observed for control samples containing no formate ion. It was concluded that sodium formate does not react to form gaseous products under these conditions. Meisel et al. also reported that no H<sub>2</sub> was detected from simple caustic sodium salt solutions containing formate at 60 °C.<sup>22</sup> More recent studies focused on hydrogen production from liquors resulting from the Bayer Process are generally consistent with the references discussed above, even though they consisted of only caustic and organic and did not include aluminum or any other waste components. In caustic solutions at elevated temperatures (3.8 M NaOH at 250 °C for 15 minutes) under anaerobic conditions no hydrogen production or organic degradation was observed for the formate ion, whereas significant hydrogen gas was observed

with the glycolate ion ( $\sim 0.1$  moles  $H_2$ /mole glycolate) under these conditions.<sup>55</sup> A second study by the same research group under alkaline conditions at  $275^\circ C$  for up to 300 minutes finds that while the formate anion is a stable product, glycolate anion reacts to produce hydrogen and oxalate per Scheme I of Reference 56. Consistent with these observations, formate ion is one of the end products of gas forming reactions of Hanford waste solutions containing various other complexants.<sup>29</sup>

In a separate study focused on technetium reduction reactions, Chamberlin and Arterburn reported that various complexants (including formate and glycolate) promote the reduction of both pertechnetate and the unsaturated organic compound, cinnamate, in the presence of selected noble metals ( $Ru^{3+}$ ,  $Rh^{3+}$ , and  $Pd^{2+}$ ) in 2-5 M NaOH solutions (no other salts present) via a transfer hydrogenation reaction.<sup>57, 58</sup> Although the molar ratio of complexant:pertechnetate was high in the initial experiments, the ratio of complexant:cinnamate of 4:1 used in subsequent tests was much lower and hydrogenation of cinnamate was quantitative, indicating that significant degradation of the complexant occurred. The authors state that radioactive tank waste aging models that do not take catalytic reactivity into account may significantly underestimate processes such as the generation of hydrogen gas. Formate ion was the most reactive of the various organics studied towards catalytic transfer hydrogenation, with glycolate being intermediate in reactivity. It was stated that the noble metals in these experiments may not have been completely soluble and heterogeneous catalysis may have been involved. Ruthenium, rhodium, and palladium are present in SRS tank waste at low levels.<sup>59</sup> It should be emphasized that no direct  $H_2$  gas analysis was conducted in these tests, rather transfer of hydrogen atoms mediated by the metals was observed. Based on a recent review of flammable gas generation mechanisms for SRS HLW facilities,<sup>60</sup> nitrite ion (even at low levels) is an effective inhibitor of  $H_2$  generation from HLW sludge under caustic conditions. As a result, the applicability of the above-mentioned results to SRS waste HGRs may be limited.

In contrast to formate, glycolate decomposes at elevated temperatures in the range of  $60^\circ C$  to  $120^\circ C$  producing various gases. Meisel reported that the HGR from caustic salt solutions containing glycolate was slow at  $60^\circ C$ .<sup>22</sup> Ashby reported a proposed chemical mechanism for glycolate thermal degradation in simulated waste solutions and reported a rate equation for glycolate decomposition.<sup>54</sup> The rate equation derivation from Ashby is provided in Eqns. 3 through 5. The rate of glycolate decomposition is directly dependent upon the aluminum tetrahydroxide and nitrite anion concentrations and the inverse of the hydroxide ion concentration. Based on the proposed chemical mechanism (shown in Figure 2-1) from Ashby,<sup>54</sup> aluminate is not consumed in the reaction sequence, but catalytically promotes the formation of a nitrite ester of glycolate which subsequently decomposes by one of two chemical pathways leading to either the production of formate and  $H_2$  gas or oxalate and  $H_2$  gas. Other gaseous products formed include carbon dioxide ( $CO_2$ ), nitrous oxide ( $N_2O$ ), and methane ( $CH_4$ ). Formaldehyde is also formed as an intermediate species in Eqn. 1.3 of Figure 2-1 as part of the decomposition path that leads to hydrogen and formate (Eqns. 1.9 to 1.11 in Figure 2-1). Based on the chemical mechanism, the theoretical molar ratio of glycolate: $H_2$ : $N_2O$  should be 1.0:1.0:0.5. At  $120^\circ C$ , under an inert atmosphere, the observed molar ratio for these gases was 1:<1:>0.5. When the tests were conducted in air, nitrous oxide production was suppressed, hydrogen production was greater than observed under inert conditions, and the rate of glycolate decomposition decreased significantly. Tests were conducted at both  $120^\circ C$  and  $90^\circ C$  to determine the activation energy for hydrogen formation of 30 kcal/mol, or 113 kJ/mol.

$$\text{Rate} = k[\text{Gly}] [\text{Al}(\text{OH})_4^-] [\text{NO}_2^-]/[\text{OH}^-] \quad \text{Eqn. 3}$$

$$\ln[\text{Gly}]_t - \ln[\text{Gly}]_{t=0} = k' * t \quad \text{Eqn. 4}$$

$$k' = k[\text{Al}(\text{OH})_4^-][\text{NO}_2^-]/[\text{OH}^-] \quad \text{Eqn. 5}$$

where, the concentrations are expressed in moles/liter (M), and  $k/[\text{OH}^-]$  is calculated to be a maximum of  $2.39\text{E-}4 \text{ hr}^{-1}\text{M}^{-2}$  in four different tests conducted at  $120^\circ\text{C}$  in air at a fixed hydroxide concentration of 2M.

It should be noted that testing in Reference 54 included various concentrations for  $\text{Al}(\text{OH})_4^-$  and  $\text{NO}_2^-$  to determine their reaction order of one. Since the  $\text{OH}^-$  concentration was fixed at 2M, no indication was given as to the actual reaction order of hydroxide in the rate equation. An assumed value of one is used for this work and further testing using the conditions of the Ashby study would be required to determine the hydroxide reaction order.

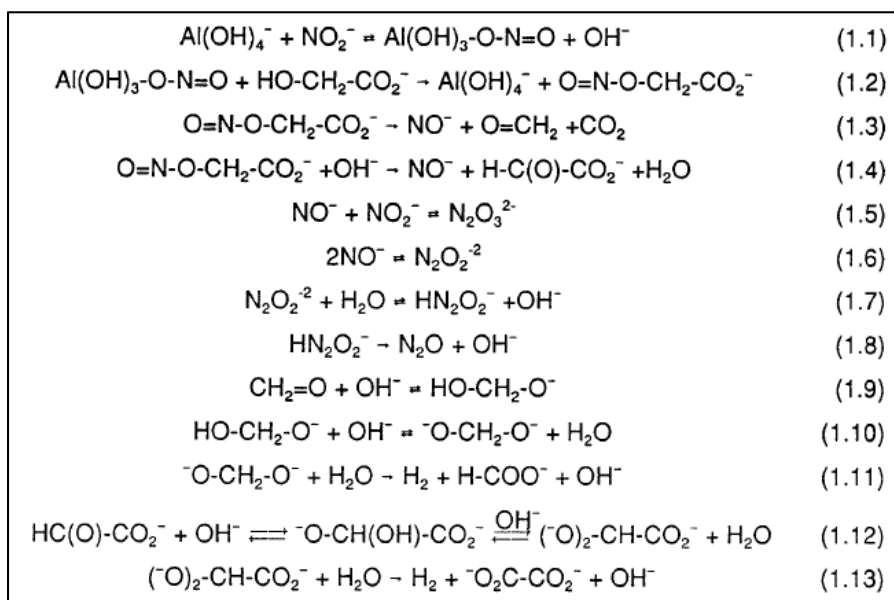


**Figure 2-1. Mechanism of Glycolate Thermal Decomposition in Simulated Waste Supernate (as reported by Ashby<sup>54</sup>).**

Differences in the ratios of gaseous products from glycolate thermolysis as a function of temperature were attributed to a “solvent cage” effect at lower temperatures and higher viscosities. This effect was hypothesized to result in a different chemical mechanism than that shown in Figure 2-1, which leads to the formation of increasingly larger amounts of  $\text{N}_2$  gas rather than  $\text{N}_2\text{O}$  as the temperature is decreased below  $90^\circ\text{C}$ . At  $60^\circ\text{C}$ , very little  $\text{H}_2$  gas was formed as a result of this effect. Many of these tests were conducted in concentrated solutions near 9 M total  $\text{Na}^+$ , so this effect may not be observed in more dilute solutions.

Equations 3 through 5 were used with a starting glycolate concentration of 10 g/L to calculate the molar amount of glycolate decomposed at a short duration time of ten hours at  $120^\circ\text{C}$ . This molar concentration was then equated to the maximum amount of molecular hydrogen (1:1 glycolate: $\text{H}_2$  molar stoichiometry)

produced under SRS Waste Characterization System (WCS) tank conditions. A sample calculation for an SRS High Heat Waste (HHW) sample, Tank 39, is given below.

$$k' * t = (k/[OH^-] * ([2M]/[OH^-]_{Tk39}) * [Al(OH)_4^-]_{Tk39}[NO_2^-]_{Tk39} \times 10hr)$$

$$k' * t = - (2.39E-4 \text{ hr}^{-1}M^{-2}) * ([2M]/[1.5617]_{Tk39}) * [0.1787]_{Tk39}[0.2979]_{Tk39} \times 10hr)$$

$$k' * t = -0.0001629$$

$$\ln[Gly]_t = k' * t + \ln[Gly]_{t=0} = -0.0001629 + \ln(0.133255) = -0.0001629 - 2.01549$$

where  $[Gly]_{t=0}$  is calculated from 10 g/L / formula weight of glycolate = 75.04402 g/mol

$$\ln[Gly]_t = -2.0156529$$

$$[Gly]_t = \exp(-2.0156529) = 0.133233$$

$$[H_2]_t = [Gly]_{t=0} - [Gly]_t = 0.133255 - 0.133233 = 2.17E-05 \text{ M}$$

Hydrogen production values for lower temperatures were calculated using the activation energy for hydrogen formation via Eqn. 6 below. The Arrhenius equation was used to solve for HGRs at lower temperatures ( $T_1$ ) than the temperature ( $T_2 = 120 \text{ }^\circ\text{C}$ ) used in the Ashby studies where the activation energy,  $E_a$ , is known.

$$\log k = \log A - E_a/(2.3*RT) \quad \text{Eqn. 6}$$

where,

$k$  = rate constant

$A$  = a constant

$E_a$  = activation energy = 113 kJ/mol for  $H_2$  from glycolate thermolysis

$R$  = 8.314 J/K-mol, the gas constant

$T$  is the waste temperature in Kelvin

with  $k_1$ ,  $T_1$  and  $k_2$ ,  $T_2$ ,

$$\log k_1 - \log k_2 = (\log A - E_a/(2.3*RT_1)) - (\log A - E_a/(2.3*RT_2))$$

$$\text{or, } \log (k_1/k_2) = E_a/(2.3*RT) * (1/T_2 - 1/T_1)$$

It should be noted that the unit order dependence of the Ashby equations for the hydroxide ion concentration was assumed since testing only used a fixed concentration of 2 M hydroxide. Other limitations for the application of the Ashby glycolate equations to SRS Tank Farm conditions are that Ashby studied nitrite and aluminate concentration ranges of 1.12 – 2.24 M and 1 – 1.54 M, respectively, whereas the SRS tanks vary in nitrite and aluminate in the range of 0.16 – 3.2 M and 0.01 - 1.6 M.

Other references on glycolate thermolysis were identified which were consistent with the references discussed above. Stock reported that although glycolate was the most abundant original complexant in Hanford waste, it is largely absent in the tanks and is much less abundant than oxalate.<sup>30</sup> Barefield

estimated that the half-life of glycolate is less than 1 year at 60 °C.<sup>61</sup> Camaioni et al. reported that glycolate is the most reactive of the primary original Hanford complexants.<sup>62</sup>

### 2.3 Quality Assurance

Requirements for performing reviews of technical reports and the extent of review are established in Manual E7 Procedure 2.60.<sup>13</sup> SRNL documents the extent and type of review using the SRNL Technical Report Design Checklist contained in WSRC-IM-2002-00011, Rev. 2.<sup>14</sup>

## 3.0 Hydrogen Generation Rate Calculations for the SRS Tank Farm

### 3.1 Comparison of Radiolytic HGR Methods

WCS data was obtained from February 2017 and used as input to the various HGR calculations.<sup>63</sup> The organic concentrations specified for evaluation with regard to HGRs in the TTQAP are provided in Table 3-1. Maximum concentrations of 10 g/L for both glycolate and formate were evaluated as well as various combinations of organic concentrations from the maximum value down to 0 g/L. High formate concentrations on the order of 2 g/L have been observed in the SRS 2H Evaporator tanks.<sup>64</sup>

**Table 3-1. Matrix of Glycolate and Formate Concentrations Evaluated**

	<b>g/L</b>	<b>g/L</b>	<b>wt% TOC*</b>	<b>wt% TOC*</b>	<b>Molar</b>	<b>Molar</b>
	<b>glycolate</b>	<b>formate</b>	<b>glycolate</b>	<b>formate</b>	<b>glycolate</b>	<b>formate</b>
1	10	10	0.26	0.22	0.133	0.222
2	10	5	0.26	0.11	0.133	0.111
3	10	3	0.26	0.07	0.133	0.067
4	10	0.1	0.26	0.00	0.133	0.002
5	5	10	0.13	0.22	0.067	0.222
6	5	5	0.13	0.11	0.067	0.111
7	5	3	0.13	0.07	0.067	0.067
8	5	0.1	0.13	0.00	0.067	0.002
9	3	10	0.08	0.22	0.040	0.222
10	3	5	0.08	0.11	0.040	0.111
11	3	3	0.08	0.07	0.040	0.067
12	3	0.1	0.08	0.00	0.040	0.002
13	0	10	0.00	0.22	0.000	0.222
14	0	5	0.00	0.11	0.000	0.111
15	0	3	0.00	0.07	0.000	0.067
16	0	0.1	0.00	0.00	0.000	0.002

\*Assumes a nominal waste supernate density of 1.23 g/mL.

To compare the different radiolytic HGR methods involving both water radiolysis and organic radiolysis, the highest levels of organics with both 10 g/L glycolate and formate were used along with the chemical concentration data from WCS. The HGR rates in units of ft<sup>3</sup>/hr are shown in Figure 3-1 as calculated from the different methods. These results represent the sum of existing HGR values in WCS from water radiolysis and the organic radiolysis terms calculated from the various methods. The total radiolysis HGR results are compared in each plot to the baseline water radiolysis HGR. All HGR calculations throughout this report assume that the vapor space temperature within the tanks is the same as that of the supernate and the hydrogen gas volumes are determined based on this assumed temperature. All data shown in Figure 3-1 is calculated for a temperature of 25°C.



The top plot in Figure 3-1 shows the current SRS baseline water radiolysis HGR (Boley method) and the total HGR from the sum of water radiolysis (Boley) plus organic radiolysis calculated using the SRS competition kinetics methodology (equations in Appendix A). The plots shown in Figure 3-1 display the HGRs on a logarithmic scale and the results indicate that the range of HGRs from SRS tanks is broadly distributed over the range of  $\sim 0.001$  up to near  $6 \text{ ft}^3/\text{hr}$ . A sample calculation of the competition kinetics values using the tank having the highest HGR, SRS Tank 39, is shown in Table 3-2 where it is indicated that a  $f_{\text{org.}}$  value of 0.17 was utilized for the combined contribution from glycolate ( $f_{\text{gly.}} = 0.02$ ) and formate ( $f_{\text{form.}} = 0.15$ ). The  $f_{\text{gly.}}$  and  $f_{\text{form.}}$  and resulting  $f_{\text{organic}}$  values are shown in Appendix D for all SRS active (non-closed) tanks along with the pertinent nitrite, nitrate and hydroxide concentrations from WCS and hypothetical formate and glycolate concentrations of  $10 \text{ g/L}$ . That data shows a minimum  $f_{\text{organic}}$  value of 0.022 and a maximum  $f_{\text{organic}}$  value of 0.273 for Tanks 2 and 11, respectively. The hydroxide anion is present in all SRS Tank Farm waste and it is a minor contributor as a scavenger in the competition kinetics. As shown in Appendix D the  $f_{\text{organic}}$  terms increase slightly by leaving the hydroxide term out of the competition kinetics giving a minimum  $f_{\text{organic}}$  value of 0.023 and a maximum  $f_{\text{organic}}$  value of 0.311 for Tanks 9 and 11, respectively. Overall the  $f_{\text{organic}}$  term only increases  $\sim 8\%$  on average for all SRS tanks by neglecting the hydroxide term in the competition kinetics. The hydroxide term was used in all the competition kinetics treatment throughout Section 3 of this report. Conclusions determined from the calculations in Section 3 of this report would not be changed by ignoring the hydroxide term since it is a minor contributor to the scavenging of the hydrogen radical. In Section 4 of this report the hydroxide term was not included in the  $f_{\text{organic}}$  competition kinetics calculations as was noted in the original analysis of organics impacts to the DWPF.<sup>65</sup> Similar treatment of competition kinetics used in the analysis of organics impacts to the SRS Concentration, Storage, and Transfer Facilities does consider the hydroxide anion.<sup>66</sup>

The middle plot of Figure 3-1 shows a similar comparison (water radiolysis only vs. water plus organic radiolysis) using the ANL empirical data equations (equations shown in Appendix B). Comparison of the additive contributions from organic radiolysis using the ANL methodology and the SRS calculations (upper plot) indicates that these two methodologies give similar results. The average ratio of SRS water radiolysis plus competition kinetics organics to SRS water radiolysis for all tanks is  $1.45 \pm 0.24$ , whereas the average ratio of SRS water radiolysis plus ANL organics to SRS water radiolysis is  $1.51 \pm 0.34$ . Some potential limitations to the ANL organic radiolysis equations should be pointed out. Firstly, the ANL empirical relationship does not include formate from the original data source,<sup>24</sup> so an assumption based on the reactivities of formate and glycolate with the hydrogen atom was used. Secondly, the empirical correlation for  $G(\text{H}_2)$  from various organics was developed using a single simulant waste composition containing  $\sim 75\%$  of the major inorganic components originally fed into Hanford Tank 101-SY (composition:  $2.3 \text{ M NaOH}$ ,  $0.9 \text{ M NaAlO}_2$ ,  $2.2 \text{ M NaNO}_2$ ,  $2.8 \text{ M NaNO}_3$ ).<sup>24</sup> Thus, as cautioned by the authors of that work, the correlation developed for  $G(\text{H}_2)$  applied for only that single simulant waste composition. The correlation involving the  $R_x$  term in Appendix B could increase or decrease across the various salt compositions existing in the SRS tanks.

The bottom plot of Figure 3-1 provides HGR results using the SRS baseline water radiolysis method (Appendix A) and the Hanford organic radiolysis terms calculated using a reactivity factor of  $r_f = 0.6$  (Appendix C). Comparison of the additive contributions from organic radiolysis using the Hanford methodology and the SRS calculations (upper plot) indicates that the SRS competition kinetics approach is more conservative giving higher values for organic radiolysis contributions across all tanks.

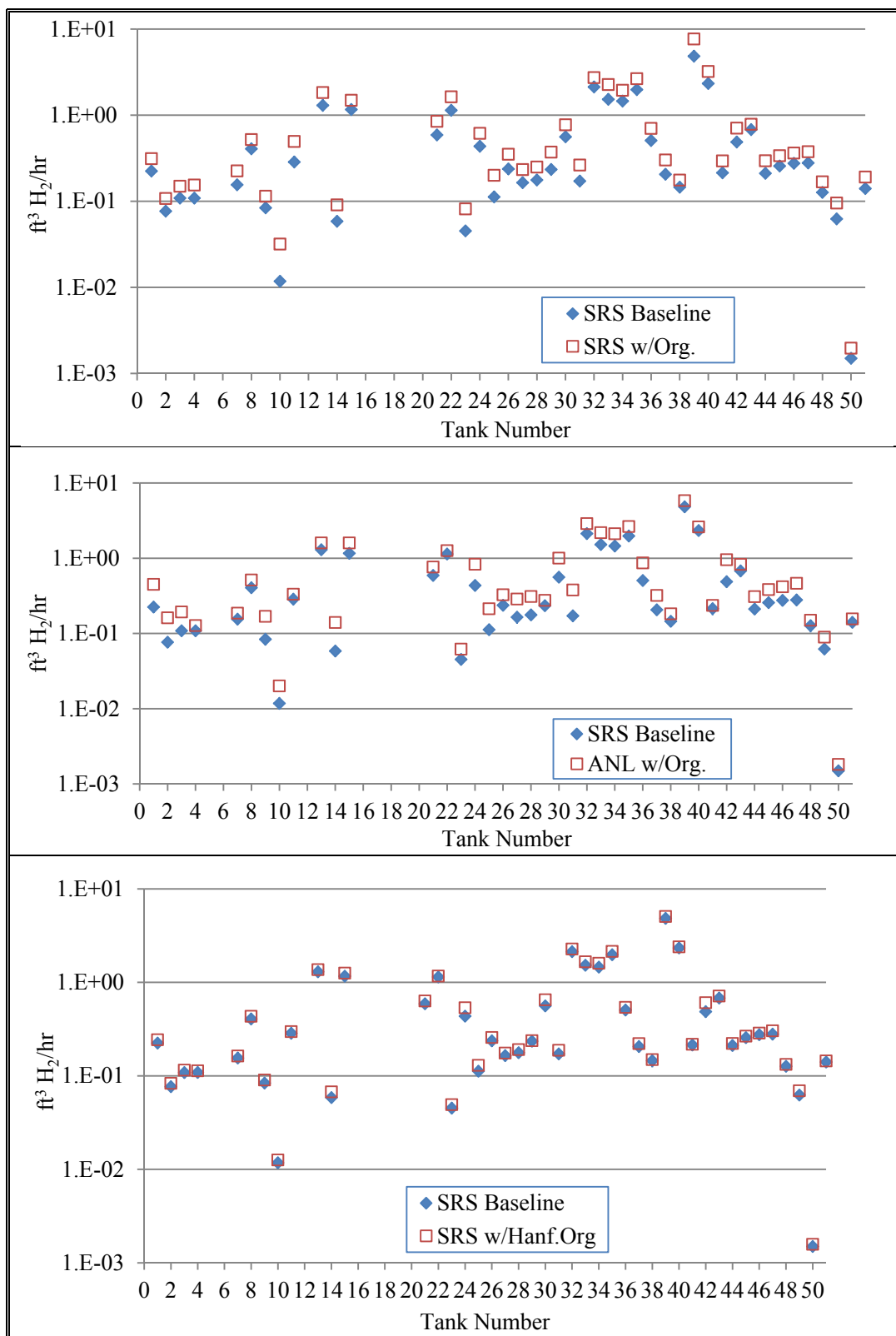


**Figure 3-1. Comparison of Radiolytic (water and organic) HGRs for Various Methods Using 10 g/L Glycolate and Formate at 25 °C. (SRS Baseline = Boley water radiolysis)**

**Table 3-2. Competition Kinetics Calculation Parameters for SRS Tank 39**

Tank 39	Rate, $M^{-1}s^{-1}$ *	Conc., M	Reactivity Factor, $s^{-1}$ **	Fraction Reacting w/ $H\cdot$ , $f_x$
$NO_2^-$	7.1E+08	0.30	2.1E+08	0.70
$NO_3^-$	1.4E+06	1.66	2.3E+06	0.01
glycolate	4.6E+07	0.13	6.1E+06	0.02
formate	2.1E+08	0.22	4.7E+07	0.15
$OH^-$	2.2E+07	1.56	3.4E+07	0.11

\*Rate constants from Reference 21

\*\*Reactivity Factor calculated from Rate x Concentration

Figure 3-2 provides HGR results calculated at 25°C using the SRS baseline water radiolysis method (Boley) from Appendix A, the Hanford water radiolysis method, and the Hanford baseline water radiolysis plus the Hanford organic radiolysis terms of Appendix C. Both the Hanford baseline water radiolysis and the Hanford organic radiolysis terms used the liquid fraction multiplier calculated for the SRS Tank conditions that ranged from 0.3 up to 1.0. Comparison of the SRS baseline water radiolysis data (solid diamonds) to the Hanford baseline water radiolysis data (solid triangles) shows less conservative and lower values for the Hanford water radiolysis terms in most cases. This result was expected due to the extra sodium term used in the denominator of the Hanford equations and the liquid fraction values invoked in the Hanford equations which serve to decrease the calculated HGRs. The additive contribution from organic radiolysis to the Hanford baseline water radiolysis is shown in Figure 3-2 by the (X) symbols. An ambient temperature of 25°C was used in these calculations since the Hanford organic radiolysis terms are temperature dependent. Calculated HGRs for Hanford baseline water plus Hanford organic radiolysis are also lower than the values calculated by the SRS baseline method in most cases.

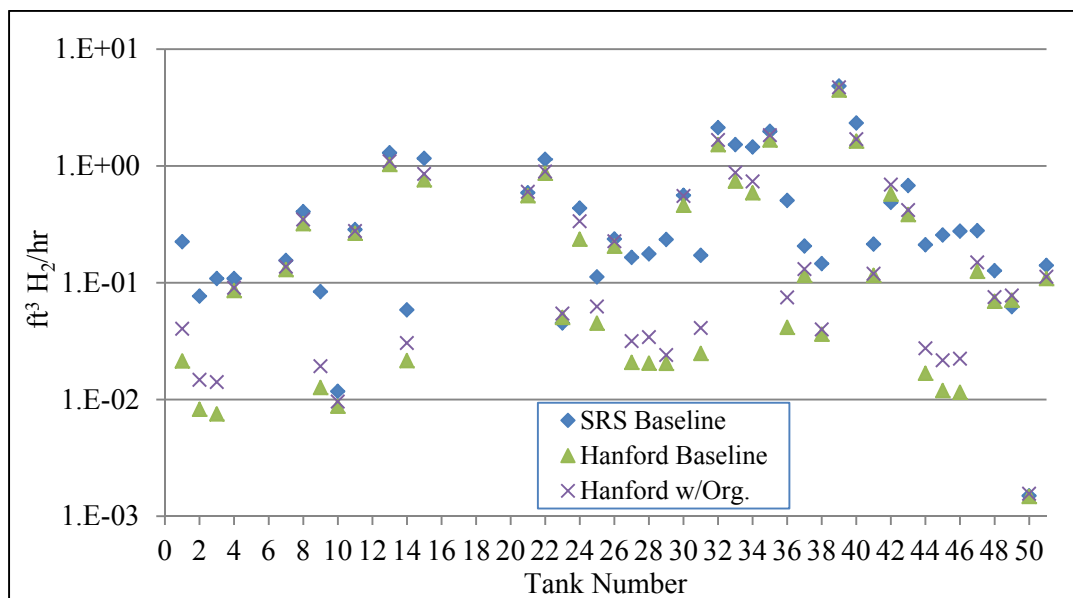


**Figure 3-2. Comparison of Radiolytic HGRs for SRS and Hanford Methods Using 10 g/L Glycolate and Formate at 25 °C. (SRS and Hanford Baseline involve water radiolysis only)**

### 3.2 Comparison of Formate Levels for Radiolysis

The SRS HGR method was also applied to the formate only cases to show how the sequential increase in formate ion concentrations could affect the total HGR (including water radiolysis and organic radiolysis by competition kinetics) relative to the SRS baseline for water radiolysis. This analysis would pertain to the current SRS Tank Farm conditions before potential introduction of glycolate ion from planned alternative reductant flowsheet activities in DWPF.

Figure 3-3 shows the results considering formate-only at levels of 0.1 g/L and 3 g/L and Figure 3-4 shows results at formate concentrations of 5 g/L and 10 g/L. These calculations were conducted at 25°C. Results for a formate concentration of 0.1 g/L show insignificant contributions from organic radiolysis relative to water radiolysis. Increasing the formate level up to 3 g/L, 5 g/L and 10 g/L increases the average HGR across all SRS tanks by 13, 21, and 40%, respectively, relative to baseline water radiolysis. For the tank with the highest HGR by water radiolysis, SRS Tank 39, these adds are 18, 29, and 53%, respectively. These data are shown for all active SRS tanks excluding Tank 48 in Table 3-3. Tank 48 is not considered for any of the detailed analyses in this report as it is not considered linked to any of the other tanks and should not ever contain the elevated concentrations of either formate or glycolate used for these analyses. Reference 67 uses the term HHW for tanks that are in the heat load range of 136,287 to 448,543 Btu/hr for SRS Tank Farm data from 2002. Table 3-3 shows HHW SRS tanks with BTU/hr values above 136,000 Btu/hr in greyscale to differentiate these tanks from the other lower heat load tanks.

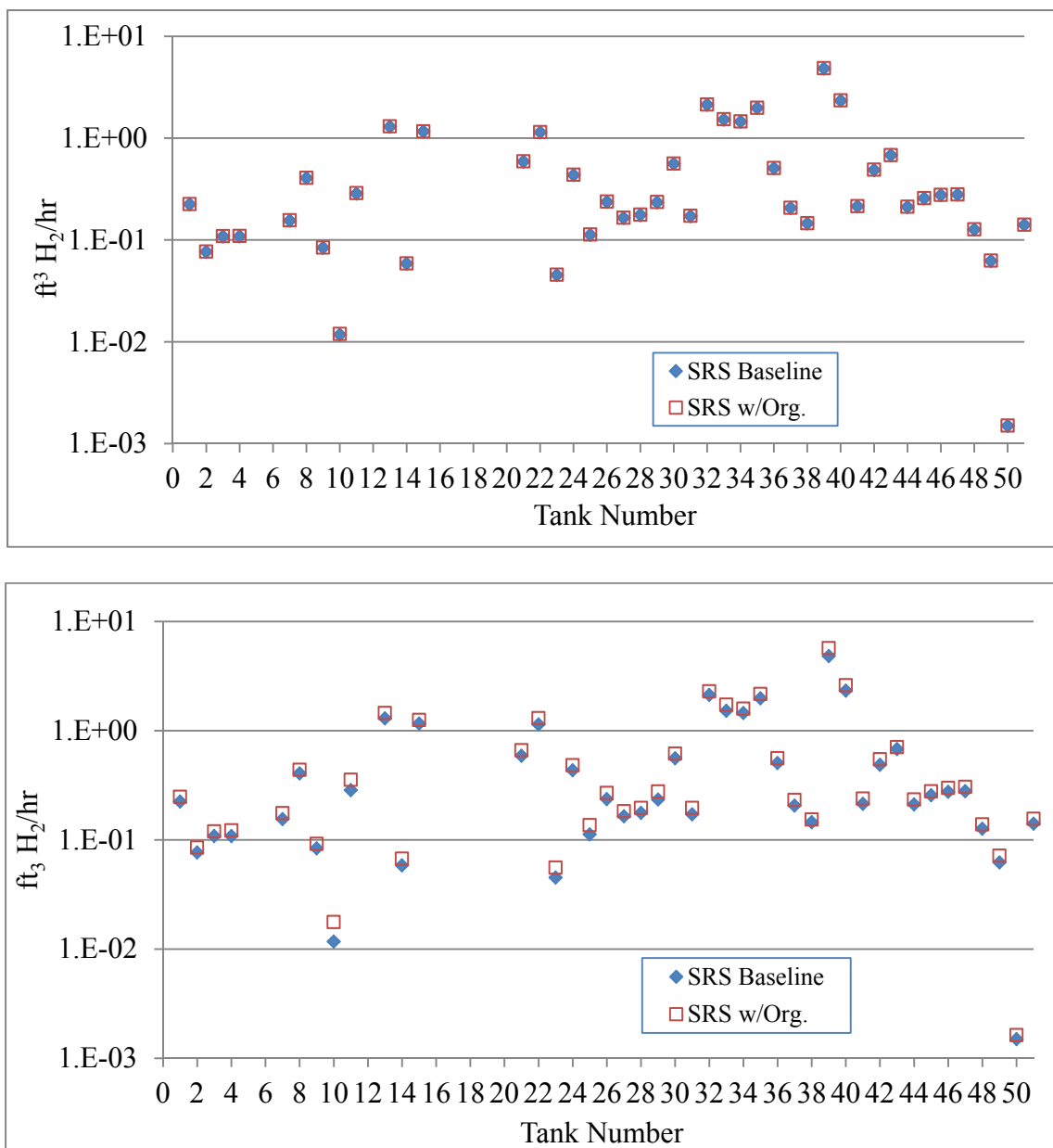


**Figure 3-3. Formate Radiolytic HGR by SRS Baseline Water Radiolysis + Competition Kinetics (w/Org.) vs. SRS Water Radiolysis Only (formate concentrations of 0.1 g/L (top) to 3 g/L (bottom)) at 25 °C.**

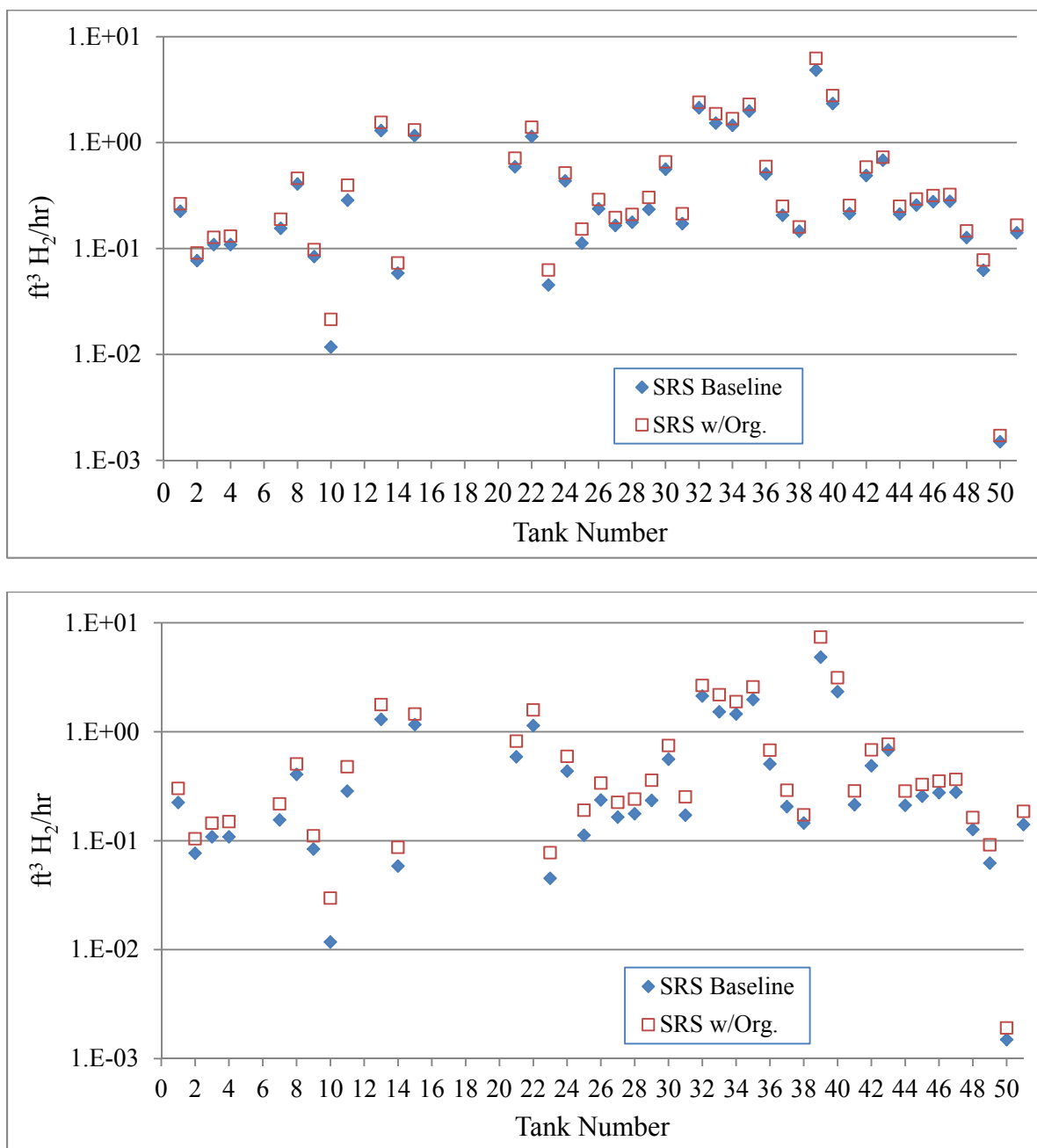


**Figure 3-4. Formate Radiolytic HGR by SRS Baseline Water Radiolysis + Competition Kinetics (w/Org.) vs. SRS Water Radiolysis Only (formate concentrations of 5 g/L (top) to 10 g/L (bottom)) at 25 °C.**

**Table 3-3. Ratios of Baseline Plus Organic HGR (Competition Kinetics) to Baseline HGR from Various Formate Levels\***

Tank	Overall Total Heat (Btu/hr)	Formate, 0.1 g/L, Ratio to Baseline	Formate, 3 g/L, Ratio to Baseline	Formate, 5 g/L, Ratio to Baseline	Formate, 10 g/L, Ratio to Baseline
1	67,817	1.00	1.11	1.18	1.35
2	25,618	1.00	1.11	1.18	1.36
3	25,759	1.00	1.10	1.17	1.33
4	5,755	1.00	1.12	1.20	1.38
7	9,452	1.00	1.13	1.22	1.41
8	34,107	1.00	1.08	1.13	1.25
9	25,743	1.00	1.10	1.16	1.32
10	2,571	1.02	1.51	1.82	2.53
11	15,305	1.01	1.24	1.38	1.67
13	92,873	1.00	1.12	1.19	1.37
14	24,672	1.00	1.15	1.25	1.49
15	135,097	1.00	1.08	1.13	1.25
21	54,857	1.00	1.12	1.20	1.39
22	37,721	1.01	1.14	1.22	1.39
23	5,169	1.01	1.23	1.38	1.72
24	119,680	1.00	1.11	1.19	1.37
25	30,876	1.01	1.22	1.36	1.70
26	28,651	1.00	1.14	1.22	1.43
27	37,465	1.00	1.11	1.19	1.37
28	40,427	1.00	1.11	1.18	1.36
29	12,558	1.01	1.18	1.29	1.53
30	134,807	1.00	1.10	1.17	1.33
31	62,882	1.00	1.14	1.24	1.47
32	252,560	1.00	1.08	1.13	1.25
33	202,111	1.00	1.14	1.22	1.43
34	207,304	1.00	1.09	1.15	1.30
35	221,469	1.00	1.10	1.16	1.30
36	108,727	1.00	1.10	1.17	1.34
37	34,733	1.00	1.13	1.21	1.41
38	11,761	1.00	1.06	1.10	1.19
39	343,882	1.01	1.18	1.29	1.53
40	86,330	1.00	1.12	1.19	1.34
41	7,020	1.00	1.12	1.19	1.34
42	141,794	1.00	1.12	1.20	1.40
43	49,580	1.00	1.04	1.07	1.13
44	29,959	1.00	1.11	1.18	1.35
45	38,606	1.00	1.09	1.14	1.28
46	43,005	1.00	1.09	1.14	1.28
47	57,355	1.00	1.09	1.16	1.31
49	8,591	1.01	1.15	1.25	1.47
50	113	1.00	1.09	1.14	1.28
51	5,072	1.00	1.11	1.18	1.32
Min.	113	1.00	1.04	1.07	1.13
Max.	343,882	1.02	1.51	1.82	2.53
Avg.	67,139	1.00	1.13	1.21	1.40

\*greyscale indicates HHW tanks exceeding 136,000 Btu/hr

One of the goals of Task 1 in the TTQAP<sup>12</sup> is to identify threshold limits for the organic levels based on the modified HGR equations including the additive contribution from organic radiolysis. One measure of a threshold limit would be to consider the previous overall uncertainty value in the SRS baseline water radiolysis equations of ~ 25% as discussed by Hester.<sup>67</sup> In that analysis it is postulated that reducing the baseline predictive equations by 25% would still provide HGR predictions that are conservative relative to measured values from certain tanks. Table 3-4 shows measured SRS tank sampling data from 5 selected tanks during the period from 1998 - 2000 and the predicted HGR for those tanks based on water radiolysis (SRS Boley method) at the time of sampling. At the time of these tests there could have been formate present in all of these waste tanks. For instance Reference 68 indicates measured formate concentration of ~ 1,300 mg/L in Tank 33 in 1999. However the predicted HGRs only used water radiolysis equations and did not include any contributions from formate radiolysis. For the HHW tanks, the large ratios of the predicted HGRs using only water radiolysis to the measured HGRs from tanks that could have contained formate are shown in the final column of Table 3-4. For the HHW tanks these ratios in the range of 3.0 to 6.6 are an indication that the water radiolysis predictions are conservative for the HHW tanks even considering presence of formate in them at the time of these measurements. Table 3-5 contains the corresponding heat loads and chemical compositions for these tanks during the time of sampling. This data is derived from the references within the Hester report.<sup>67</sup>

**Table 3-4. Previous Measured and Predicted (Boley method) HGRs<sup>67</sup>**

SRS Tank	Waste Type	Waste Form	Measured HGR (ft <sup>3</sup> H <sub>2</sub> /hr)	Predicted HGR During Sampling (ft <sup>3</sup> H <sub>2</sub> /hr)	Ratio of Predicted HGR to Measured HGR
32	HHW	Sludge	0.444	2.55	4.3
33	HHW	Mixed	0.166	1.47	6.6
35	HHW	Sludge	0.292	1.84	4.7
36	HHW	Salt	0.178	0.71	3.0
38	LHW	Salt	0.066	0.06	0.7

**Table 3-5. Heat Loads and Waste Compositions for Previously Analyzed Tanks at the Time of Analysis**

SRS Tank	Total Beta/Gamma Heat Load (Btu/hr)	Total Alpha Heat Load (Btu/hr)	NO <sub>2</sub> <sup>-</sup> (M)	NO <sub>3</sub> <sup>-</sup> (M)	OH <sup>-</sup> (M)	Al(OH) <sub>4</sub> <sup>-</sup> (M)
32	353104	62164	1.18	2.39	1.58	0.42
33	150750	1813	0.037	1.13	1.35	0.03
35	322393	45449	1.08	2.85	1.83	0.54
36	141696	725	1.75	1.57	9.68	0.4
38	16102	841	2.15	2.32	6.91	0.26



These data are used along with the formate competition kinetics to construct the plots shown in Figure 3-5 for 0.1 to 3 g/L formate and Figure 3-6 for 5 to 10 g/L formate. In each of these plots the measured HGR values (solid diamonds) are plotted on the y-axis vs. the predicted HGR values on the x-axis. The predicted HGRs are also plotted on the y-axis as (X) data points vs. the predicted HGR values on the x-axis. Dashed lines are also shown representing the  $\pm 25\%$  uncertainty for the predicted values as discussed in Reference 67. The contribution from formate radiolysis in the concentration range of 0.1 to 10 g/L is added onto the measured value and represented by the solid squares on the plots, referred to in the figure caption as 'Measured + OrgRad'. At the lowest formate concentration of 0.1 g/L the solid square HGR values are overlapped with the measured HGRs indicating insignificant contribution from formate radiolysis at this level. The Measured + OrgRad solid square values fall below or near the conservative baseline predicted HGR minus an estimated 25% uncertainty for all the formate concentration levels except for SRS Tank 33 when formate is at or above 3 g/L. SRS Tank 33 shows high additive terms from formate radiolysis due to the relatively low nitrite concentration (0.037 M) compared to the other tanks with nitrite concentrations in the range of 1.08 to 2.15 M. Data in these figures are plotted from left to right in the following SRS tank order: 38, 36, 33, 35, and 32.

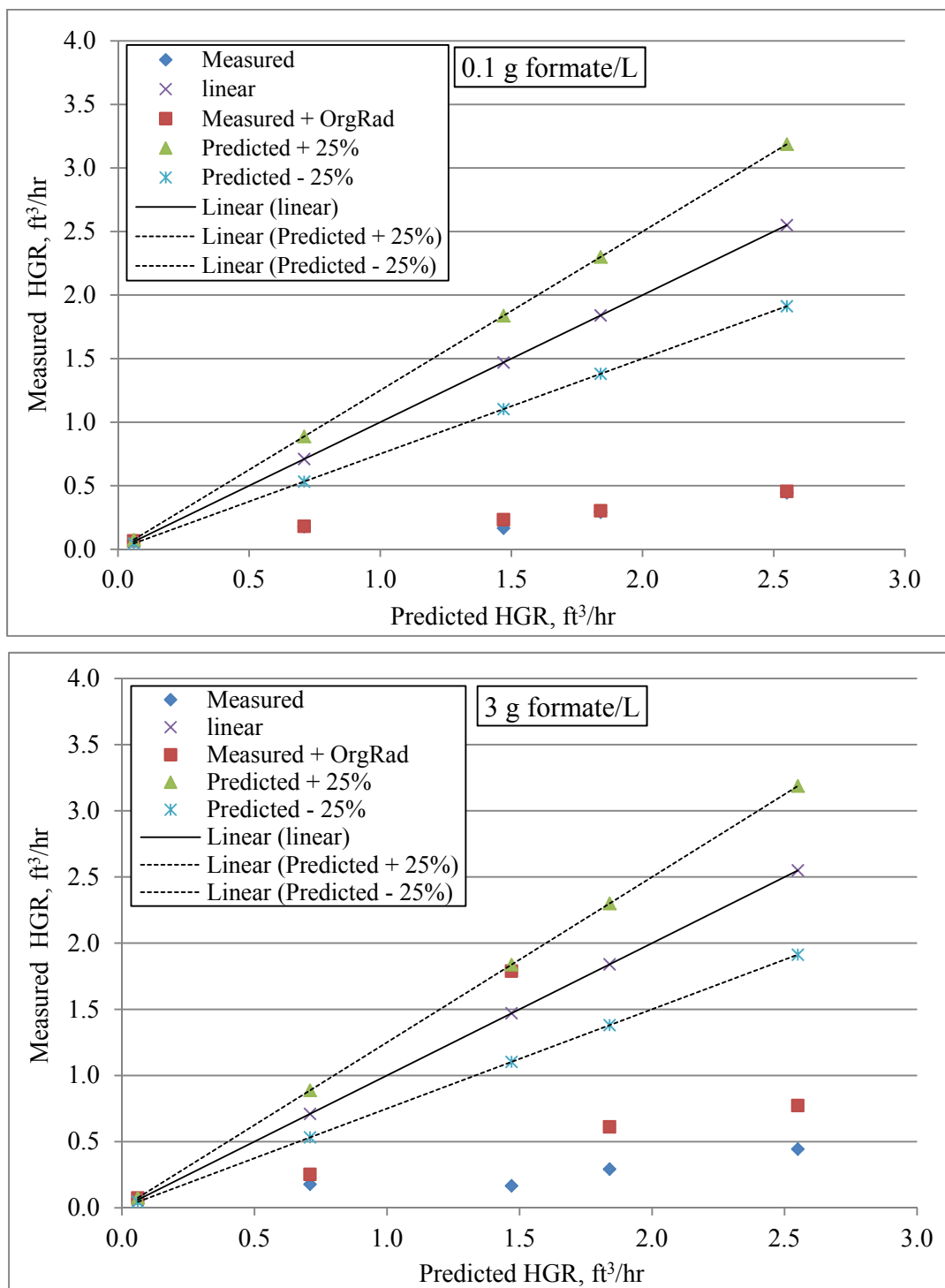


**Figure 3-5. Comparison of Measured and Measured + Calculated Formate (0.1 g/L to 3 g/L) Radiolysis (Competition Kinetics) HGRs Versus the Predicted HGR Using the Boley Method for Selected SRS Tanks Including 25% Uncertainties. “Linear” represents predicted vs predicted by Boley method. Measured tanks from left to right are SRS Tanks 38, 36, 33, 35, and 32.**

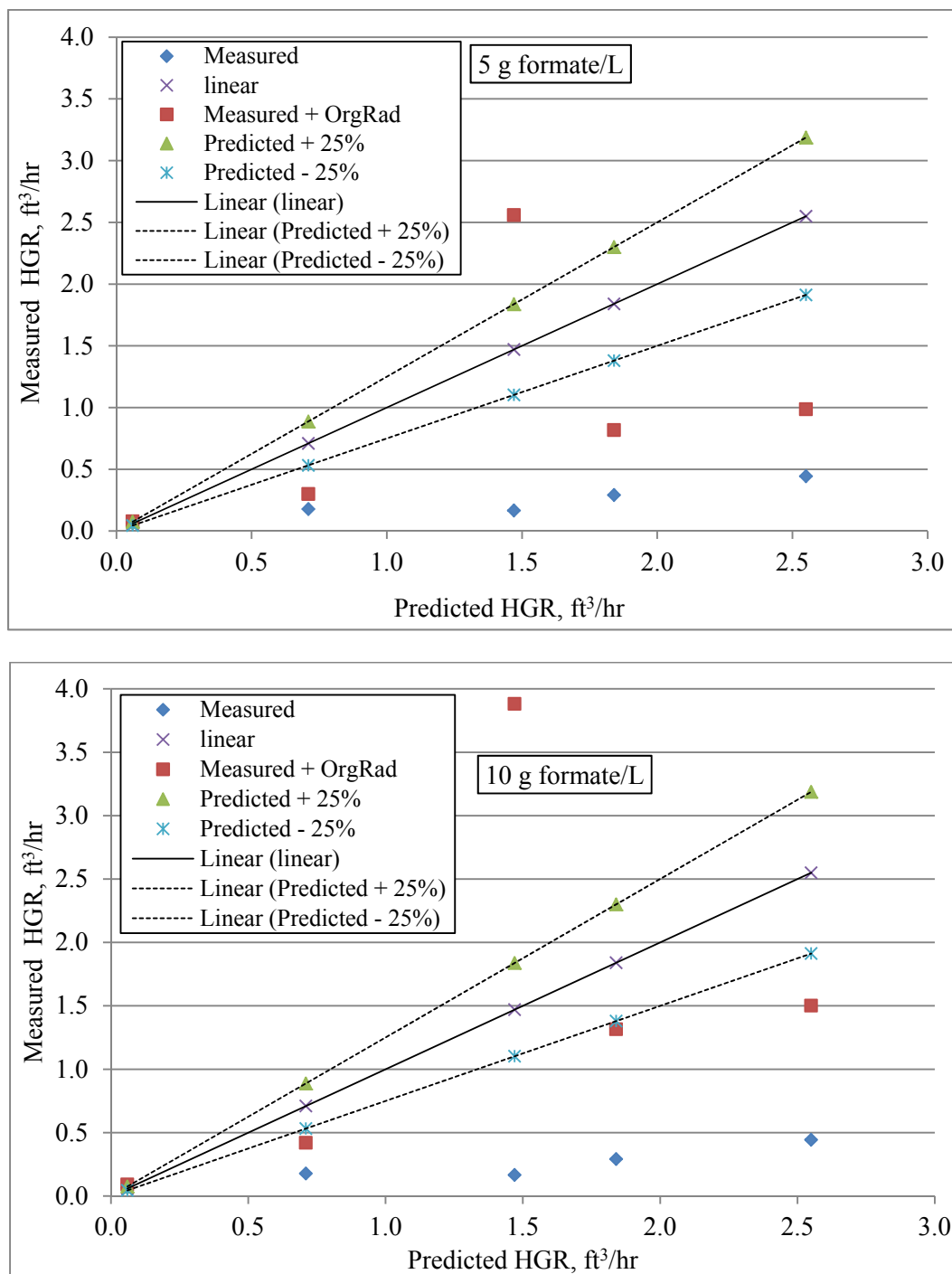


**Figure 3-6. Comparison of Measured and Measured Plus Calculated Formate (5 g/L to 10 g/L) Radiolysis (Competition Kinetics) HGRs Versus the Predicted HGR Using the Boley Method for Selected SRS Tanks Including 25% Uncertainties. “Linear” represents predicted vs predicted by Boley method. Measured tanks from left to right are SRS Tanks 38, 36, 33, 35, and 32.**

### 3.3 Comparison of Formate and Glycolate Levels for Radiolysis

The previous analysis (Section 3.2) on radiolysis of formate-only can be extended to include glycolate using the equations presented in Appendix A. The relative contribution from glycolate radiolysis compared to that of formate is very low due to its low rate of reaction with the hydrogen atom ( $H\cdot$ ) compared to formate. The ratio of  $(\text{glycolate} + H\cdot \text{ rate}) / (\text{formate} + H\cdot \text{ rate}) = 4.6E7 \text{ M}^{-1}\text{s}^{-1} / 2.1E8 \text{ M}^{-1}\text{s}^{-1}$  is only 0.22. When the molar concentrations of glycolate and formate at the 10 g/L level of 0.13 M and 0.22 M, respectively, are taken into consideration, the overall reactivity ratio of glycolate to formate towards  $H\cdot$  is only 0.13 (13%). Figure 3-7 shows that considering both glycolate and formate at the 10 g/L level results in a slight increase in the values for the 'Measured + OrgRad' radiolysis terms vs. the 10 g/L formate-only case (lower plot of Figure 3-6). The solid squares are at or near the 'Predicted - 25%' values except for SRS Tank 33. With the exception of the very low nitrite SRS Tank 33, these data indicate that the threshold level for ambient temperature radiolysis is near the maximum considered levels of glycolate and formate (both at 10 g/L). These maximum levels for both organic compounds bound any of the combinations listed in Table 3-1.

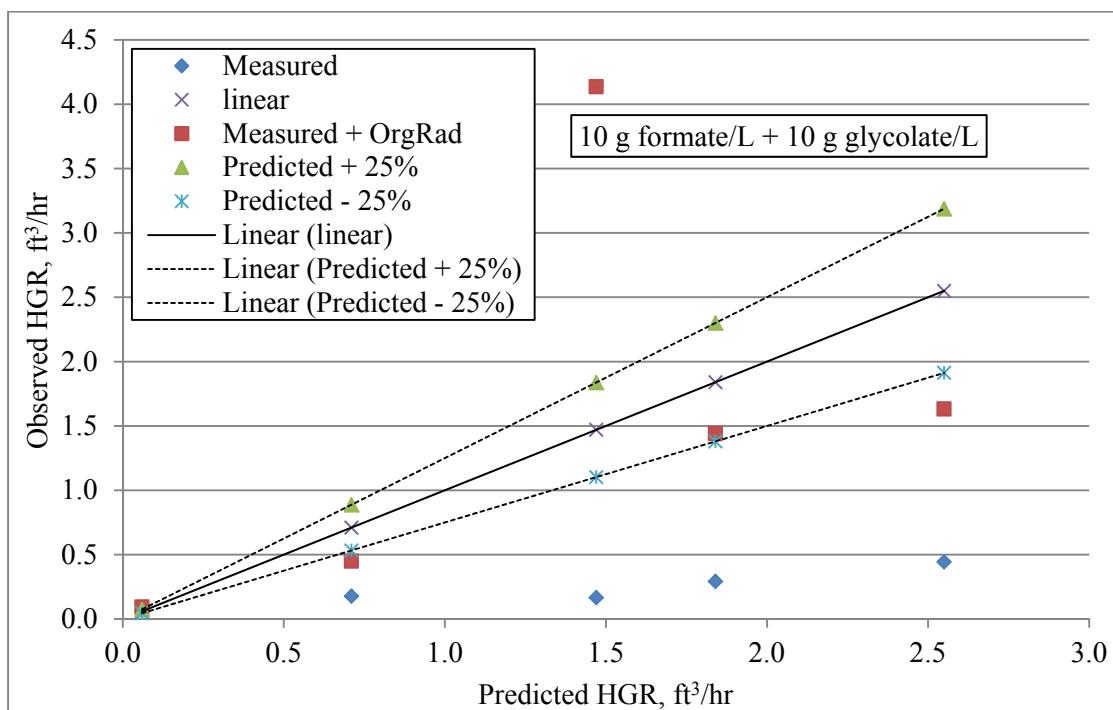


**Figure 3-7. Comparison of Measured and Measured Plus Calculated Formate plus Glycolate Radiolysis (Competition Kinetics) HGRs Versus the Predicted HGR Using the Boley Method for Selected SRS Tanks Including 25% Uncertainties (Glycolate = Formate = 10 g/L). “Linear represents predicted vs. predicted by Boley method. Measured tanks from left to right are SRS Tanks 38, 36, 33, 35, and 32.**

A critical parameter calculated from the baseline radiolytic HGR values in the WCS database is the time to reach the (hydrogen) lower flammability limit (TtLFL) in each active SRS tank. This parameter can be used as an additional measure for estimating threshold limits of either radiolytic or radiolytic plus thermolytic additive terms for formate and glycolate throughout this report. This parameter was used to assess the effects of maximum organic levels in the waste as shown in Table 3-6 considering radiolysis (water and organic). This table shows the heat loading and supernate flammability maximum temperatures used to calculate the TtLFL for each SRS tank based on the information in WCS.<sup>63</sup> Tanks with heat loads in excess of 136,287 Btu/hr, or HHW tanks according to Reference 67, are shown in grey-scale. All HGRs shown in Table 3-6 are the temperature adjusted values using the existing supernate temperatures shown in column three from WCS.<sup>63</sup> The TtLFL values are listed as 'NEVER' when the HGR is sufficiently low that considering atmospheric tank breathing the vapor space hydrogen concentration will never reach the LFL for hydrogen, corrected for temperature and organic.<sup>69</sup> These tanks are referred to as 'very slow generation tanks'. Other designations of tanks include those that have TtLFL values of  $\geq 28$  days as 'slow generation tanks', and TtLFL values of  $\geq 7$  days and  $< 28$  days as 'rapid generation tanks'. The first five data columns in the table are from the WCS, where the baseline HGR and the TtLFL are calculated using the Boley method.<sup>63</sup> It is noted in Table 3-6 that several of the SRS tanks are essentially salt tanks that include mostly saltcake with nominally 30% interstitial liquid supernate per the WCS.<sup>63</sup> These tanks are included for calculational purposes throughout this report, but the interstitial liquid associated with these saltcake tanks could probably not be increased in either formate or formate-plus-glycolate without introduction of water to dissolve the saltcake. The salt volumes expressed as a percentage of the total tank waste volumes and noted at the bottom of Table 3-6 were calculated using the 'adjusted salt volume' and the 'total waste volume' from the Formula 04 tab of WCS.<sup>63</sup>

These data show that currently only two SRS tanks (33 and 39) are close to challenging the nominal 7-day minimum for TtLFL. This duration is the time associated with reestablishing ventilation in a tank if the ventilation system were to fail. The effects of adding in the formate and the formate-plus-glycolate radiolytic terms at the maximum levels of organic (10 g/L) on the HGR and TtLFL are also shown (last four columns). Comparing the 10 g/L formate and the 10 g/L formate/glycolate TtLFL values to the baseline indicates that both SRS Tanks 33 and 39 fall below the 7-day threshold, giving values (TtLFL  $\leq 6$  days). The other HHW tanks shown in Table 3-6 have TtLFL values that remain in the range of 7 to 28 days with the addition of organic. Out of the fourteen tanks designated as 'NEVER' in the current WCS spreadsheet based on the Boley method, four of the tanks transition from the 'NEVER' designation to actual TtLFL values (SRS Tanks 7, 11, 41, and 49) of  $> 100$  days.<sup>63</sup> The ten tanks that remain as TtLFL designations as 'NEVER' consist of either salt tanks (SRS Tanks 2, 3, 9, 10 and 14) or tanks with overall heat loads below 8,000 Btu/hr (SRS Tanks 4, 23, 48, 50 and 51).<sup>63</sup>

**Table 3-6. Comparison of Time to Lower Flammability Limit for Baseline Water Radiolysis and Baseline + Maximum Organic Radiolysis Cases**

SRS Tank	Overall Total Heat (Btu/hr)	Supernatant Temp. °C	Temp. Adj. Baseline HGR (ft <sup>3</sup> /hr) <sup>1</sup>	Radiolytic Time to LFL (Days)	Temp. Adj. Baseline + Max. Formate (ft <sup>3</sup> /hr) <sup>2</sup>	Radiolytic Time to LFL (Days)	Temp. Adj. Baseline + Max. Formate/Glycolate (ft <sup>3</sup> /hr) <sup>3</sup>	Radiolytic Time to LFL (Days)
1*	67,817	75	0.26	253.1	0.35	138.4	0.36	131.0
2*	25,618	75	0.09	NEVER	0.12	NEVER	0.13	NEVER
3*	25,759	75	0.13	NEVER	0.17	NEVER	0.17	NEVER
4	5,755	60	0.12	NEVER	0.17	NEVER	0.17	NEVER
7	9,452	55	0.17	NEVER	0.24	630.7	0.25	424.1
8	34,107	60	0.45	59.1	0.57	45.0	0.58	43.7
9*	25,743	75	0.10	NEVER	0.13	NEVER	0.13	NEVER
10**	2,571	75	0.01	NEVER	0.03	NEVER	0.04	NEVER
11	15,305	100	0.36	NEVER	0.60	153.5	0.62	143.2
13	92,873	75	1.52	12.5	2.07	8.8	2.14	8.5
14**	24,672	75	0.07	NEVER	0.10	NEVER	0.11	NEVER
15	135,097	75	1.36	49.4	1.70	35.5	1.74	34.3
21	54,857	100	0.74	52.6	1.03	32.4	1.06	31.0
22	37,721	40	1.20	113.6	1.67	59.7	1.72	57.0
23	5,169	70	0.05	NEVER	0.09	NEVER	0.09	NEVER
24	119,680	100	0.54	152.5	0.74	92.8	0.77	88.4
25	30,876	70	0.13	76.9	0.22	33.4	0.23	31.2
26	28,651	100	0.30	39.6	0.42	26.3	0.44	25.3
27***	37,465	100	0.21	84.4	0.28	55.9	0.29	53.6
28	40,427	100	0.22	56.2	0.30	38.6	0.31	37.1
29***	12,558	100	0.29	41.4	0.45	25.4	0.47	24.4
30	134,807	100	0.70	15.6	0.94	11.5	0.97	11.1
31	62,882	75	0.20	68.5	0.30	42.3	0.31	40.4
32****	252,560	100	2.67	17.5	3.33	13.8	3.42	13.5
33	202,111	50	1.65	8.5	2.37	5.9#	2.46	5.7#
34	207,304	60	1.63	10.4	2.12	7.9	2.18	7.7
35	221,469	50	2.15	10.4	2.80	7.9	2.88	7.6
36***	108,727	100	0.63	16.8	0.85	12.3	0.88	11.9
37	34,733	100	0.26	48.1	0.36	32.1	0.38	30.8
38	11,761	100	0.18	72.3	0.22	57.9	0.22	56.5
39	343,882	70	5.57	9.4	8.51	6.0#	8.83	5.8#
40	86,330	75	2.73	31.7	3.66	22.6	3.76	22.0
41	7,020	60	0.24	NEVER	0.32	451.6	0.33	366.7
42	141,794	60	0.54	27.7	0.76	19.1	0.79	18.4
43	49,580	100	0.85	19.2	0.97	16.7	0.98	16.5
44	29,959	60	0.24	55.1	0.32	38.3	0.33	36.9
45***	38,606	75	0.30	40.5	0.38	30.5	0.39	29.5
46***	43,005	75	0.32	37.2	0.41	28.1	0.42	27.3
47	57,355	100	0.35	17.0	0.46	12.4	0.47	12.0
48	7,143	35	0.13	NEVER	0.17	NEVER	0.17	NEVER
49	8,591	70	0.07	NEVER	0.11	186.0	0.11	171.9
50	113	43	0.00	NEVER	<0.01	NEVER	<0.01	NEVER
51	5,072	75	0.16	NEVER	0.22	NEVER	0.22	NEVER

#Tanks below 7 day TtLFL

<sup>1</sup> Baseline radiolytic HGR (water radiolysis only using Boley method, temp. corrected)

<sup>2</sup> Baseline + Organic Radiolysis HGR using 10 g/L formate-only, temp. corrected

<sup>3</sup> Baseline + Organic Radiolysis HGR using 10 g/L each formate and glycolate, temp. corrected

\* Tanks 1, 2, 3 and 9 of ~ 500,000 gallons waste volume with 95-99% salt volume

\*\* Tanks 10 and 14 of ~ 200,000 gallons waste volume with 74-86% salt volume

\*\*\* Tanks 27, 29, 36, 45 and 46 with > 1E+06 gallons waste volume with 91-100% salt volume

\*\*\*\* Greyscale indicates HHW tanks exceeding 136,000 Btu/hr

### 3.4 Glycolate Thermolysis

Since formate thermolysis contributions to HGRs are believed to be negligible under the caustic conditions of the SRS Tank Farm, only glycolate thermolysis impacts were considered. A comparison of the two thermolysis HGRs (Hanford Hu<sup>29</sup> and Ashby<sup>54</sup>) can be made by applying Eqn. 2 and the Ashby Equations 3-5 presented in Section 2.2 to the WCS Tank Farm data for all SRS tanks using a glycolate concentration of 10 g/L.<sup>63</sup> Since the Ashby equations are based on 120 °C data, a comparison of thermolytic HGRs at this temperature by the two methods is shown in Figure 3-8. The Ashby data used a short 10 hr duration as in the sample calculation in Section 2.2 to derive these HGRs. All data in units of ft<sup>3</sup>/hr have been temperature adjusted to account for the molar volume of gas at 120°C. Figure 3-8 indicates that the Hanford thermolysis rates are generally higher than those calculated by Ashby.

These same calculations are used to compare the different thermolysis HGR predictions as a function of temperature in Figure 3-9 for Hanford and Figure 3-10 for Ashby. These figures further show the generally higher or more conservative HGR for the Hanford equation vs. the Ashby equation. These data also show the exponential nature of the HGR trend as a function of temperature for both calculations. There is a steep decrease in the predicted HGR values using the Hanford equations going from 120°C down to 90°C, with average HGRs below 1 ft<sup>3</sup>/hr levels at 75°C and below. For the Ashby equations, the thermolysis average HGRs approach levels below 1 ft<sup>3</sup>/hr at or below 90 °C. For comparison to water radiolysis HGRs, the temperature adjusted average HGRs for SRS Tanks are in the range of 0.65 ft<sup>3</sup>/hr to 0.75 ft<sup>3</sup>/hr for 50°C to 100°C, respectively. Table 3-7 shows the ratios of the temperature adjusted HGRs by the two methods in the temperature range of 120°C to 50°C. These data indicate that with few exceptions, indicated in grey-scale, that the Hanford equations predict higher average thermolysis HGRs for glycolate than the Ashby equations. This effect is higher at the lowest 50°C temperature (~ 24X) and decreases to ~5X at the upper temperature of 120°C.

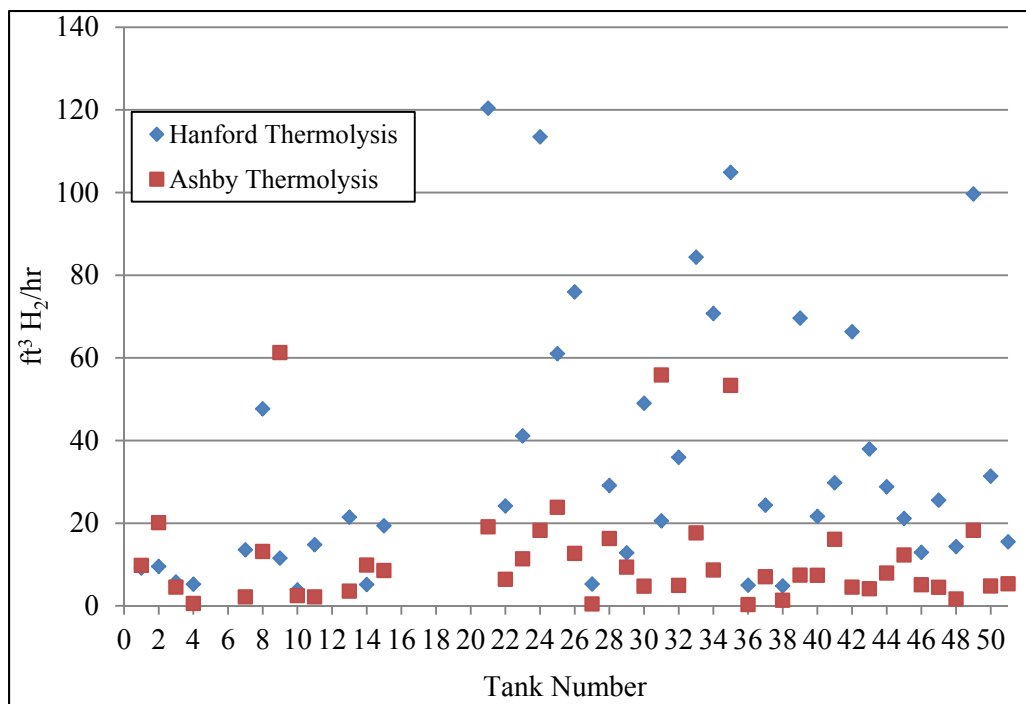


**Figure 3-8. Comparison of Hanford (Hu) and Ashby Thermolysis HGRs at 120°C and 10 g/L Glycolate (no radiolysis contributions).**

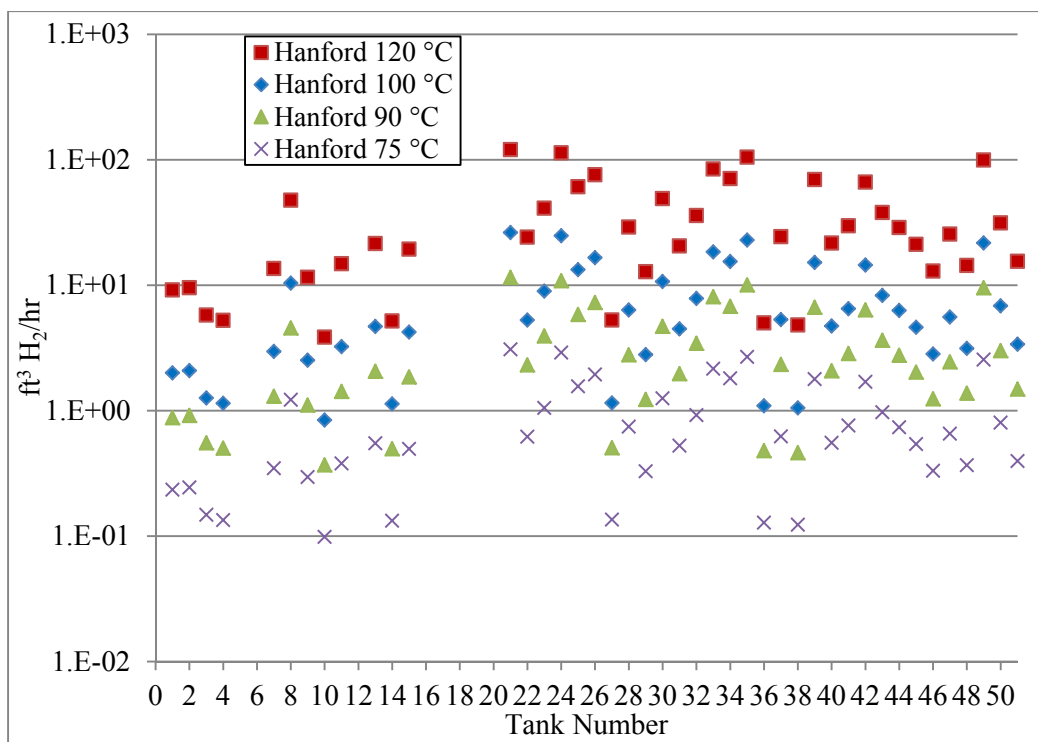


**Figure 3-9. Hanford Thermolysis HGR versus Temperature at 10 g/L Glycolate (no radiolysis contributions).**

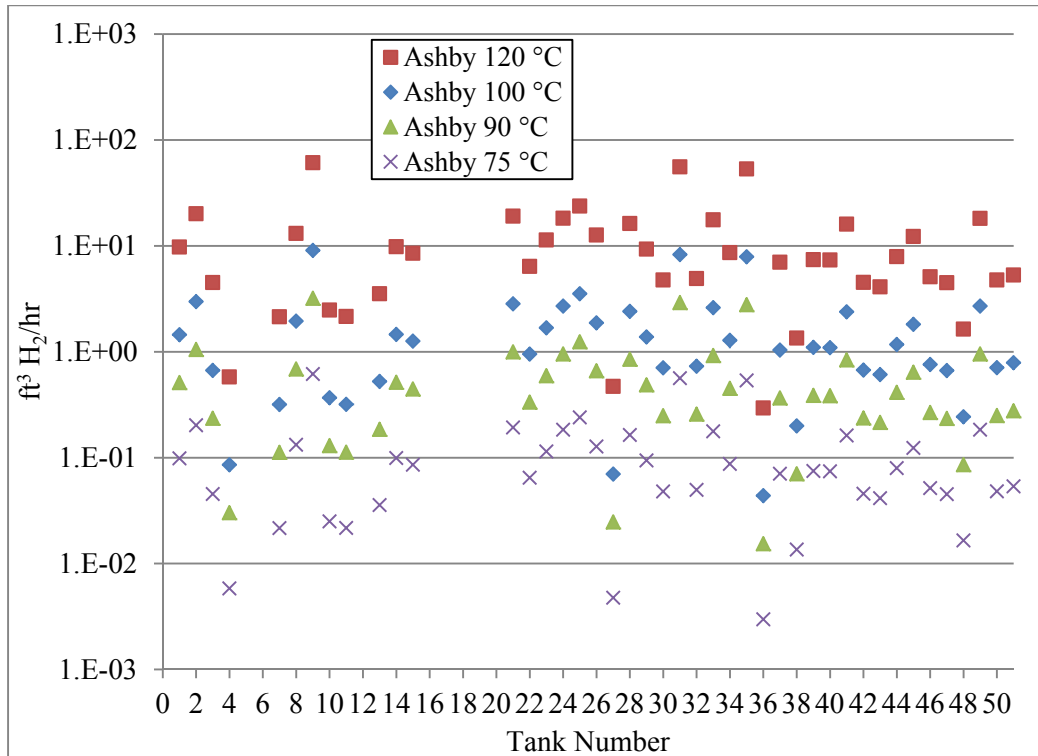


**Figure 3-10. Ashby Thermolysis HGRs versus Temperature at 10 g/L Glycolate (no radiolysis contributions).**



**Table 3-7. Ratio of Hanford to Ashby Thermolysis HGRs for 10 g/L Glycolate**

Tank	120°C	100°C	90°C	75°C	50°C
1	0.9*	1.4	1.7	2.4	4.5
2	0.5	0.7	0.9	1.2	2.3
3	1.3	1.9	2.3	3.3	6.1
4	9.1	13.3	16.6	23.0	43.2
7	6.3	9.3	11.6	16.1	30.2
8	3.6	5.3	6.6	9.2	17.3
9	0.2	0.3	0.3	0.5	0.9
10	1.5	2.3	2.8	3.9	7.4
11	6.9	10.1	12.6	17.5	32.8
13	6.1	8.9	11.1	15.4	28.9
14	0.5	0.8	1.0	1.3	2.5
15	2.3	3.3	4.2	5.8	10.8
21	6.3	9.3	11.5	16.0	30.0
22	3.8	5.6	6.9	9.6	18.0
23	3.6	5.3	6.6	9.2	17.3
24	6.2	9.1	11.4	15.8	29.6
25	2.6	3.8	4.7	6.5	12.2
26	6.0	8.8	11.0	15.2	28.6
27	11.2	16.5	20.5	28.4	53.4
28	1.8	2.6	3.3	4.5	8.5
29	1.4	2.0	2.5	3.5	6.6
30	10.3	15.1	18.8	26.1	49.1
31	0.4	0.5	0.7	0.9	1.8
32	7.3	10.7	13.4	18.5	34.8
33	4.8	7.0	8.8	12.2	22.8
34	8.2	12.0	15.0	20.8	39.0
35	2.0	2.9	3.6	5.0	9.4
36	16.9	24.9	31.0	43.1	80.9
37	3.5	5.1	6.4	8.8	16.6
38	3.6	5.3	6.5	9.1	17.0
39	9.4	13.8	17.2	23.8	44.7
40	2.9	4.3	5.4	7.5	14.0
41	1.9	2.7	3.4	4.7	8.8
42	14.6	21.5	26.8	37.1	69.8
43	9.2	13.6	16.9	23.4	44.0
44	3.6	5.4	6.7	9.2	17.4
45	1.7	2.5	3.2	4.4	8.2
46	2.5	3.7	4.6	6.4	12.1
47	5.7	8.4	10.4	14.5	27.2
49	5.5	8.0	10.0	13.9	26.1
50	6.6	9.7	12.0	16.7	31.3
51	2.9	4.3	5.3	7.4	13.9
Min.	0.2	0.3	0.3	0.5	0.9
Avg.	5.0	7.3	9.1	12.7	23.8
Max.	16.9	24.9	31.0	43.1	80.9

\*greyscale indicates cases where the Ashby HGR exceeds the Hanford HGR (ratio below 1)

### 3.5 Comparison of Combined Radiolytic and Thermolytic HGRs

Calculated HGRs from radiolysis and thermolysis can be combined to examine the overall expected additive terms in the HGR equations relative to the SRS baseline equations for water radiolysis. The highest levels of 10 g/L for both formate and glycolate radiolysis and glycolate thermolysis were used as input along with the SRS Tank Farm WCS data to generate figures showing the effect of adding in both radiolytic and thermolytic contributions to the baseline water radiolytic HGR.<sup>63</sup> Equations from Appendix A were used to calculate the organic radiolysis terms. The Ashby equation was used for glycolate thermolysis based on the expectation that calculations based on glycolate-only data are more representative than the Hanford HGR equation based on numerous organic compounds. Figure 3-11 provides the combined HGRs at 100°C and 90°C, and Figure 3-12 provides the combined HGRs at 75°C

and 50°C at the maximum levels (10 g/L) of both formate and glycolate for radiolysis with glycolate at 10 g/L for thermolysis. All the HGR data in these graphs have been temperature corrected for the molar volume of gas at the specified temperature.

Similar plots are provided in Figure 3-13 and Figure 3-14 for 5 g/L formate and glycolate levels and in Figure 3-15 and Figure 3-16 for 3 g/L formate and glycolate.

These data suggest that there is little contribution from the thermolysis terms relative to the baseline plus organic radiolysis terms at ~ 50°C for all the organic concentrations. This is evident from the near overlap of all the solid triangles (representing baseline plus organic radiolysis plus thermolysis terms) to the open squares (representing baseline plus organic radiolysis terms) for the 50°C plots. At temperatures of 75°C and above, the solid green triangles show increasing separation from the open squares indicating the increasing predicted overall HGRs due to thermolysis. This effect is more evident for the highest concentration of 10 g/L of both formate and glycolate. All three of the organic concentration levels show visible separation between the thermolysis terms and the organic radiolysis terms on a logarithmic scale for the 100°C data.

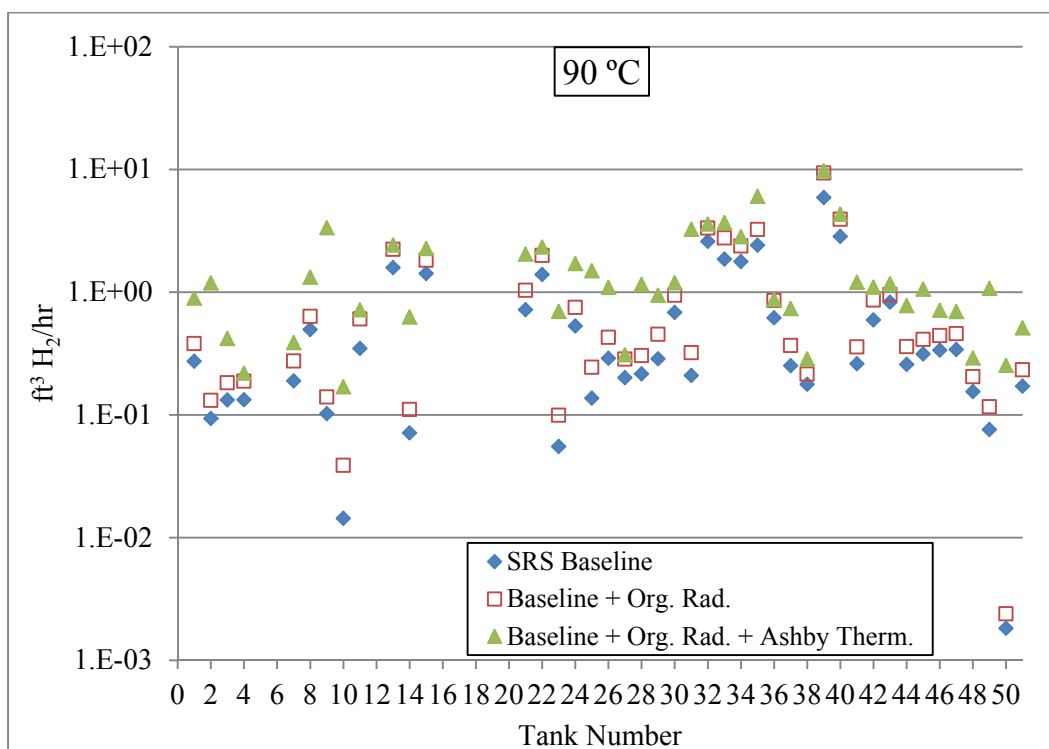
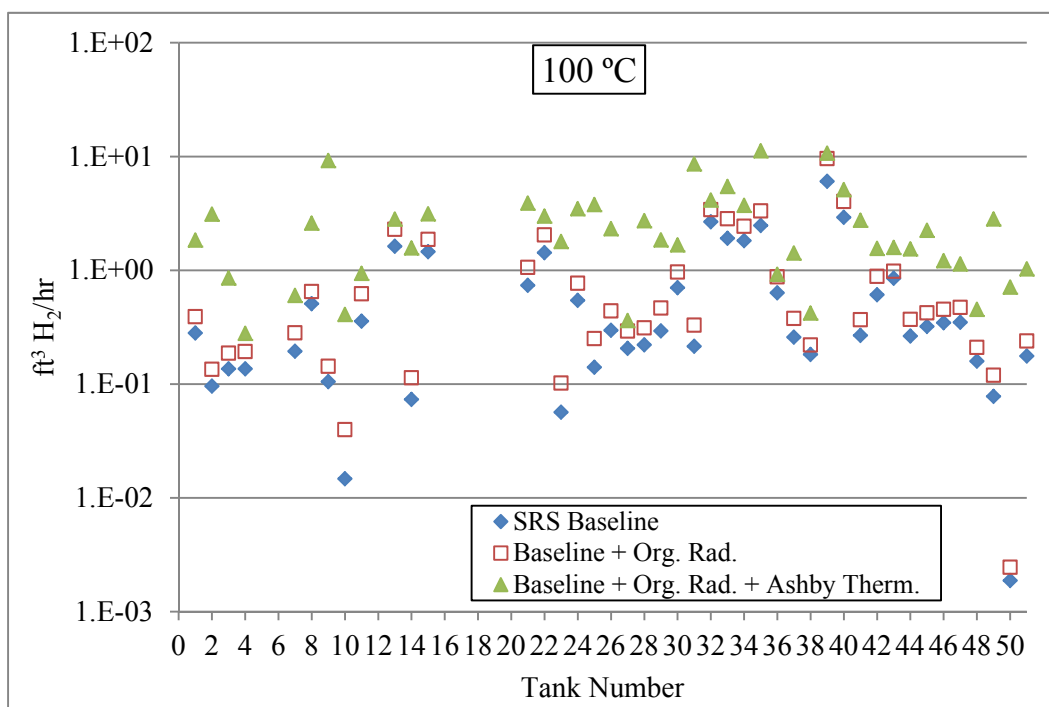


**Figure 3-11. HGR Predictions for Organic Radiolysis and Organic Radiolysis plus Thermolysis Terms vs. SRS Baseline Water Radiolysis at 100 °C (top) and 90 °C (bottom) with 10 g/L Organics. Formate and Glycolate both at 10 g/L for Radiolysis and Glycolate at 10 g/L for Thermolysis.**

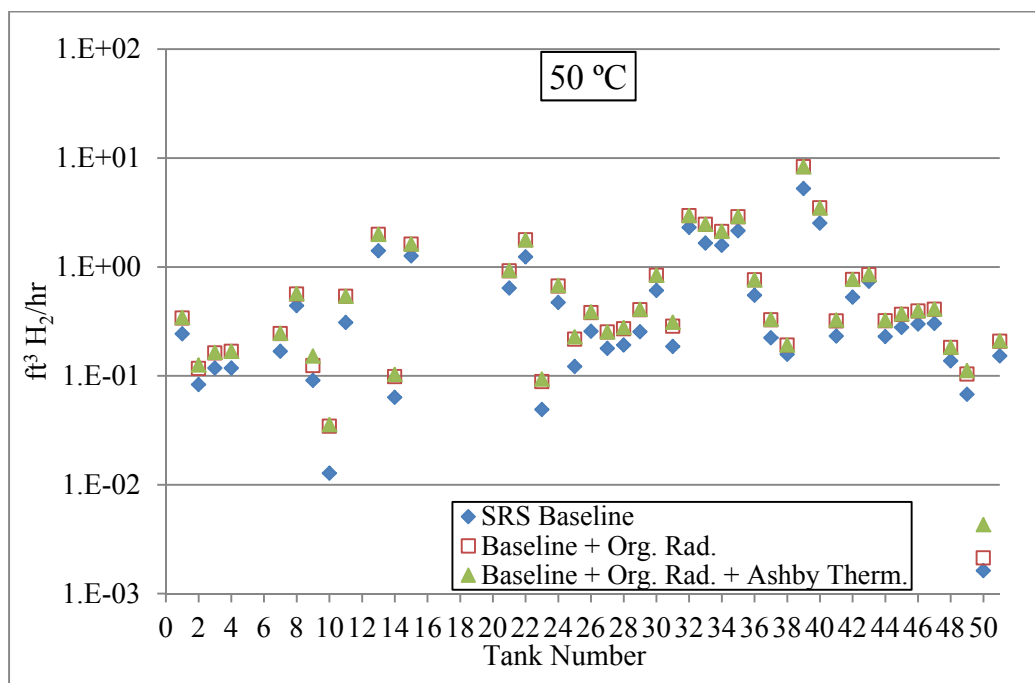
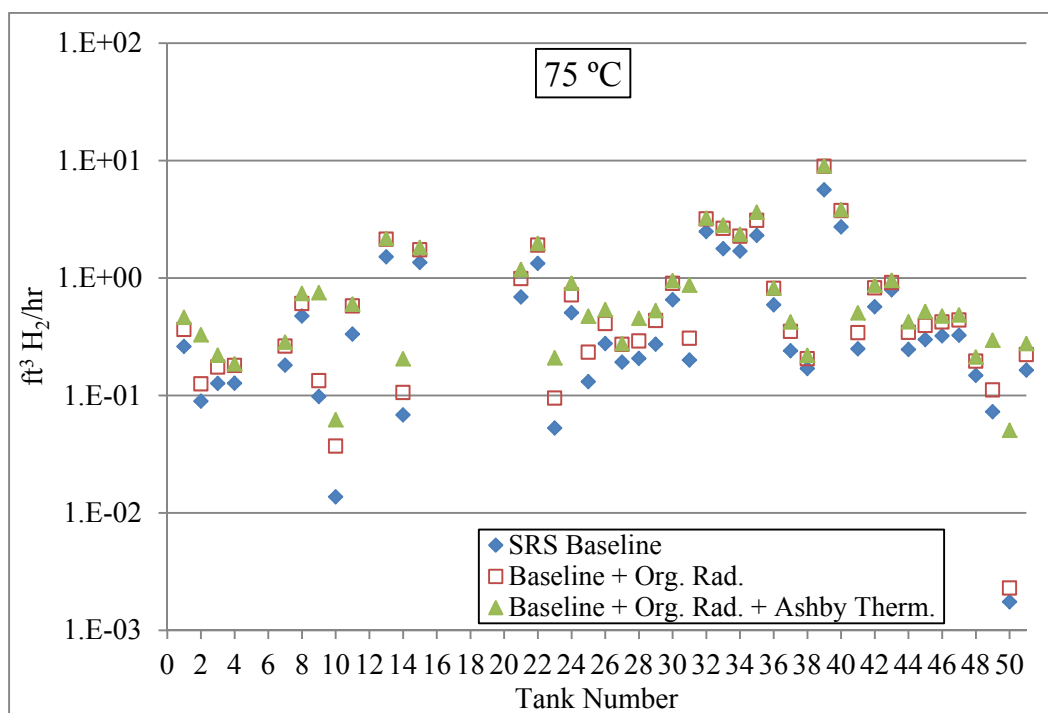


**Figure 3-12. HGR Predictions for Organic Radiolysis and Organic Radiolysis plus Thermolysis Terms vs. SRS Baseline Water Radiolysis at 75°C (top) and 50°C (bottom) with 10 g/L Organics. Formate and Glycolate both at 10 g/L for Radiolysis and Glycolate at 10 g/L for Thermolysis.**

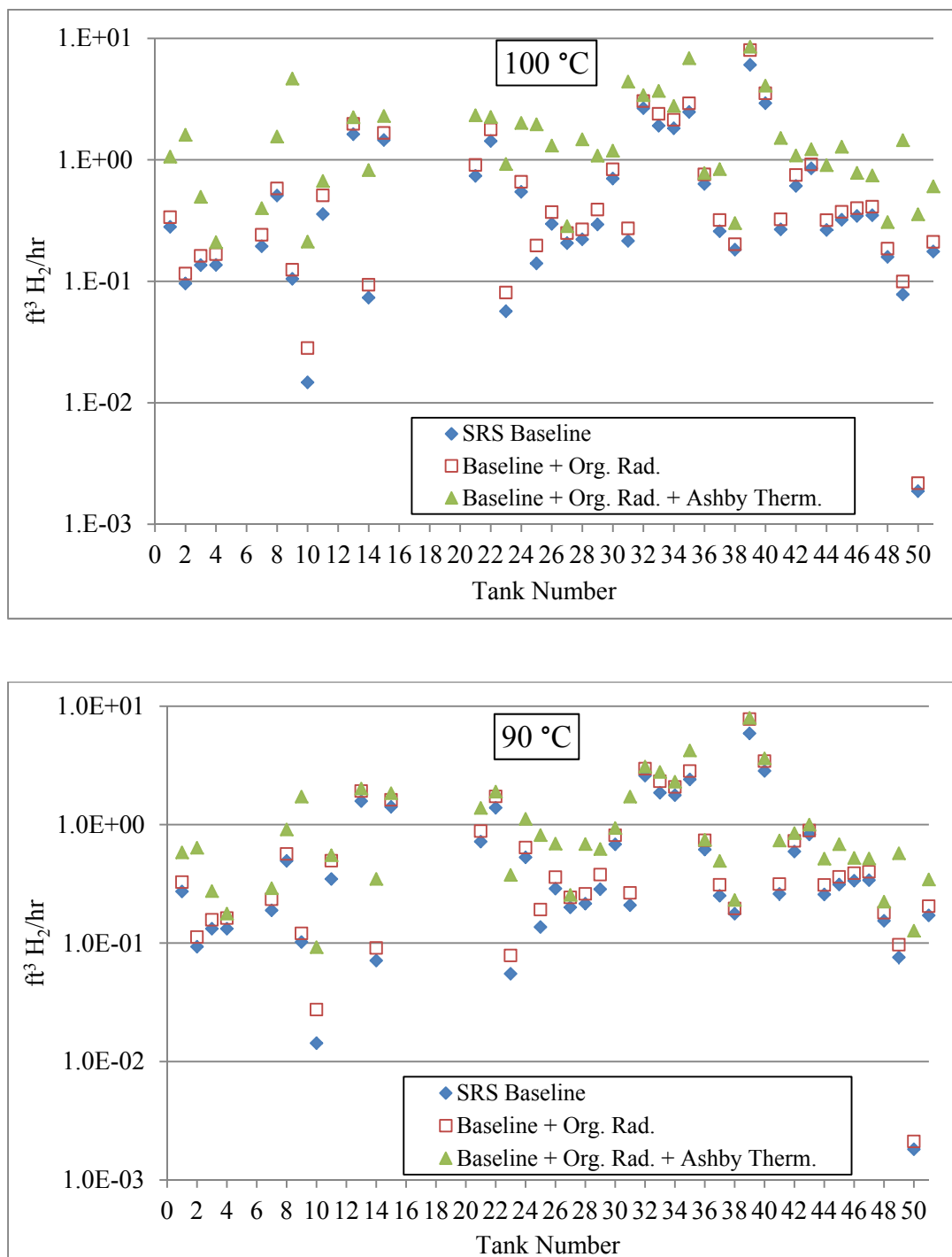


**Figure 3-13. HGR Predictions for Organic Radiolysis and Organic Radiolysis plus Thermolysis Terms vs. SRS Baseline Water Radiolysis at  $100^\circ\text{C}$  (top) and  $90^\circ\text{C}$  (bottom) with 5 g/L Organics. Formate and Glycolate both at 5 g/L for Radiolysis and Glycolate at 5 g/L for Thermolysis.**

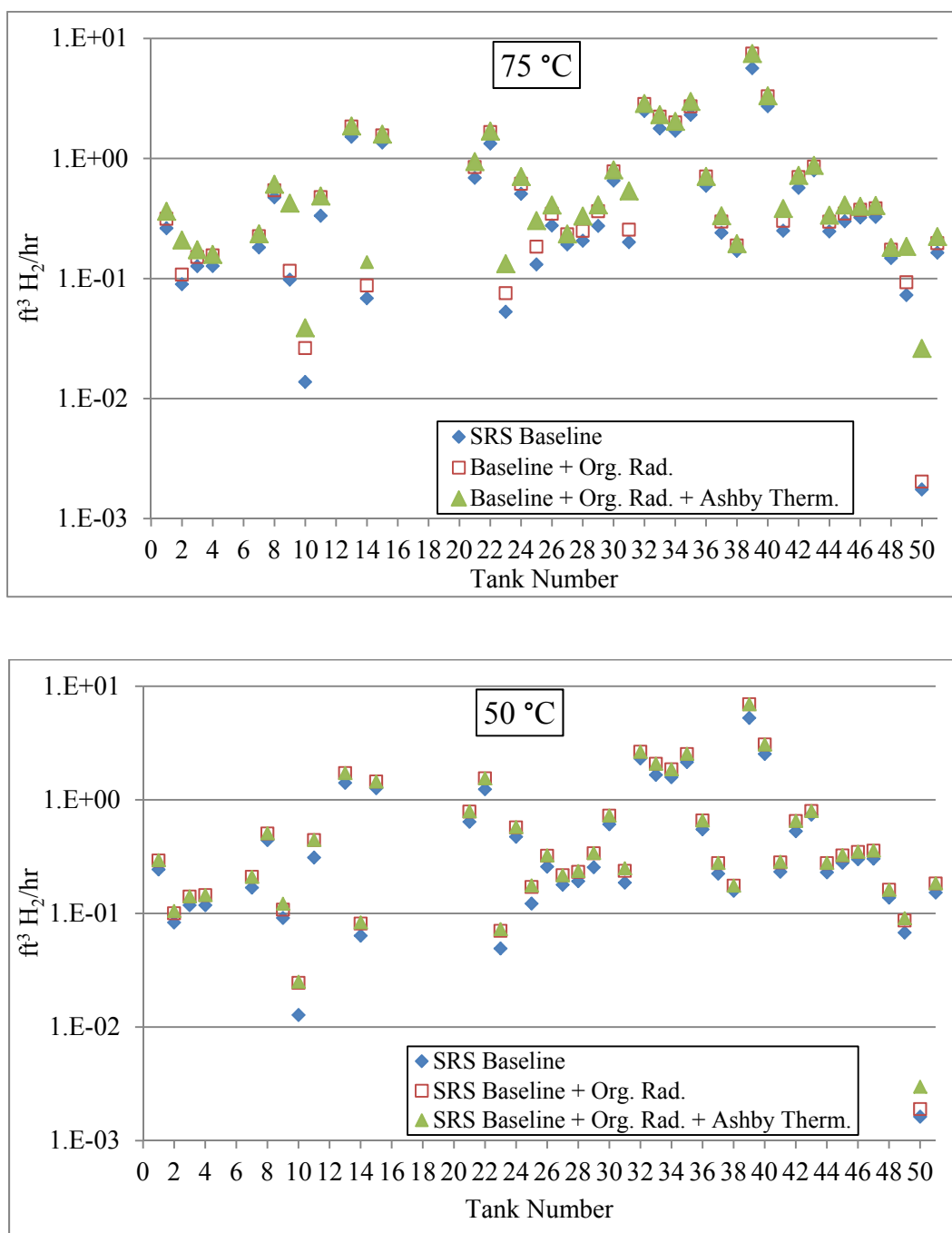


**Figure 3-14. HGR Predictions for Organic Radiolysis and Organic Radiolysis plus Thermolysis Terms vs. SRS Baseline Water Radiolysis at  $75^\circ\text{C}$  (top) and  $50^\circ\text{C}$  (bottom) with 5 g/L Organics. Formate and Glycolate both at 5 g/L for Radiolysis and Glycolate at 5 g/L for Thermolysis.**

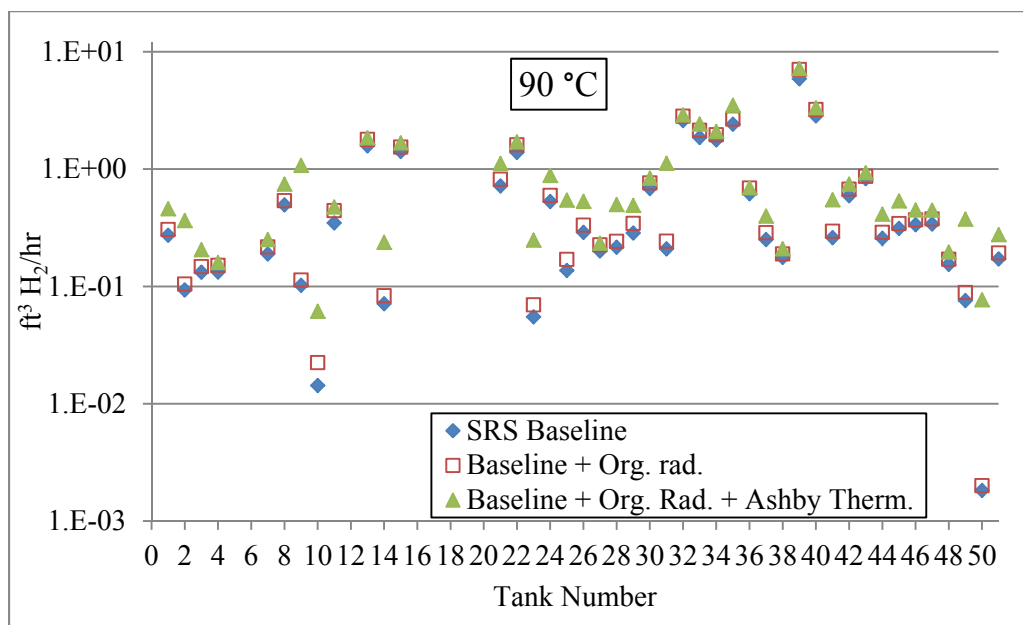
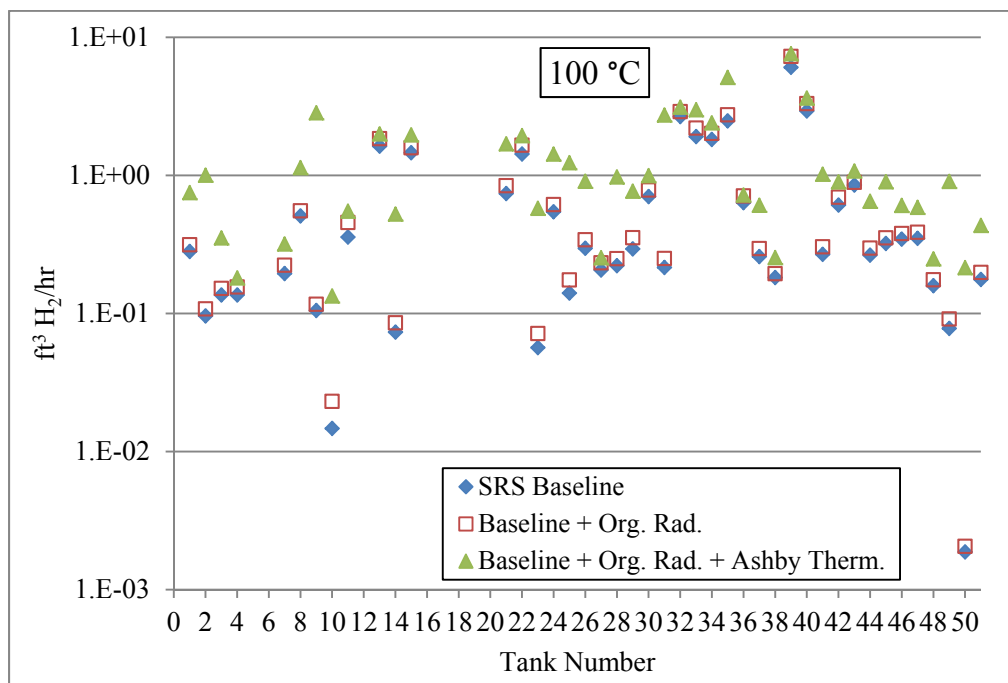


**Figure 3-15. HGR Predictions for Organic Radiolysis and Organic Radiolysis plus Thermolysis Terms vs. SRS Baseline Water Radiolysis at 100°C (top) and 90°C (bottom) with 3 g/L Organics. Formate and Glycolate both at 3 g/L for Radiolysis and Glycolate at 3 g/L for Thermolysis.**

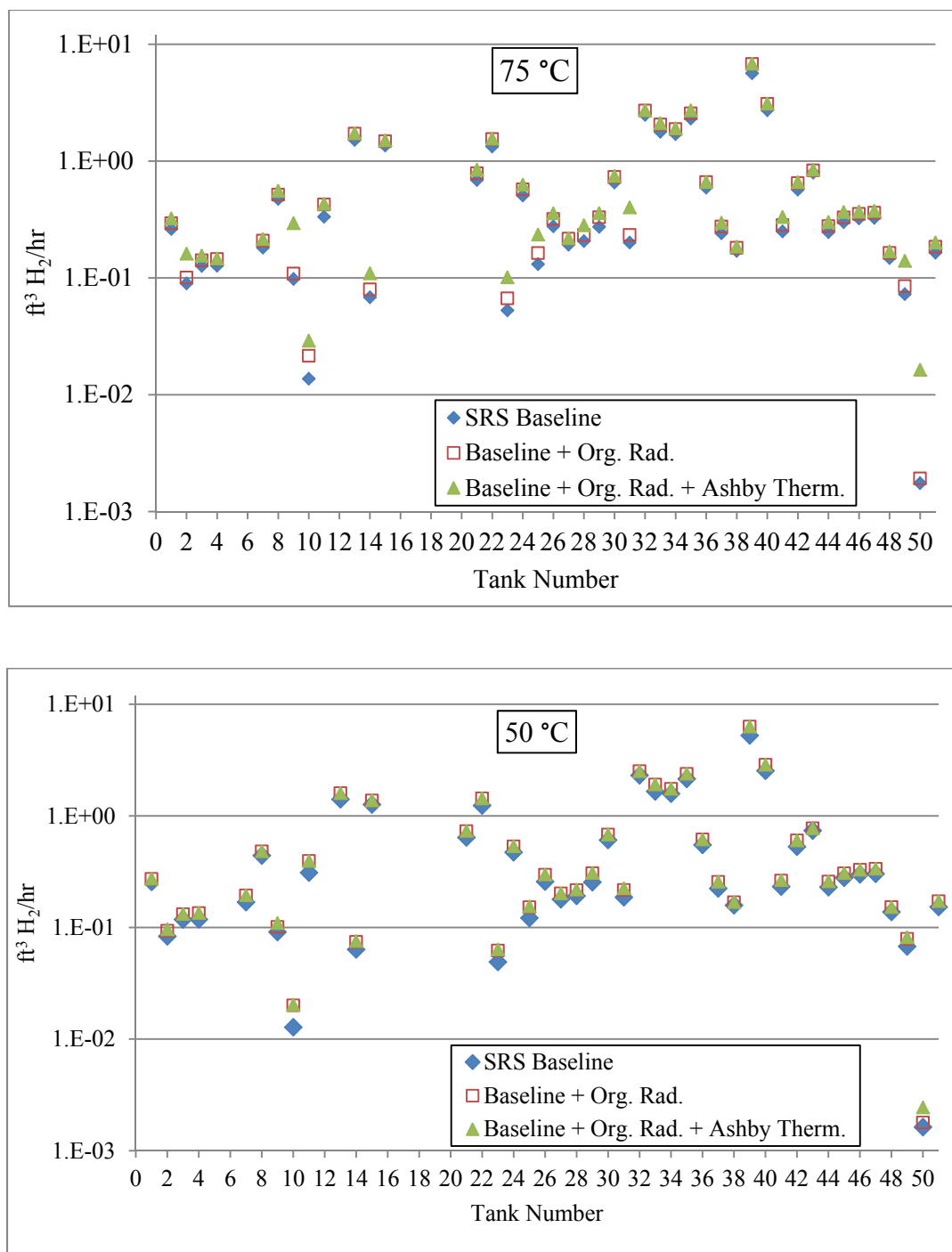


**Figure 3-16. HGR Predictions for Organic Radiolysis and Organic Radiolysis plus Thermolysis Terms vs. SRS Baseline Water Radiolysis at 75°C (top) and 50°C (bottom) with 3 g/L Organics. Formate and Glycolate both at 3 g/L for Radiolysis and Glycolate at 3 g/L for Thermolysis.**



The additive organic radiolysis and thermolysis terms can be compared to the previously measured tanks reported by Hester<sup>67</sup>, as was done in Sections 3.2 and 3.3 for radiolysis alone. The total HGR predictions and data including water radiolysis (Boley), organic radiolysis (Competition Kinetics), and glycolate thermolysis (Ashby) for various temperatures are plotted in Figure 3-17 and Figure 3-18 for 10 g/L formate and glycolate (assuming no formate contributions to thermolytic hydrogen). The total HGR predictions and data including water radiolysis, organic radiolysis, and glycolate thermolysis for 5 g/L formate and glycolate are provided in Figure 3-19 and Figure 3-20. The total HGR predictions and data including water radiolysis, organic radiolysis, and glycolate thermolysis for 3 g/L formate and glycolate are provided in Figure 3-21 and Figure 3-22. All of the HGR data in these graphs has been temperature corrected for the molar volume of gas at the specified temperature. The tanks involved in previous sampling that are shown in these figures from left to right are SRS Tanks 38, 36, 33, 35, and 32.

Comparison of the measured values plus the additive terms from radiolysis and thermolysis against the baseline predicted HGRs minus 25% uncertainty allows for the determination of threshold temperatures for each concentration above which HGRs would be unacceptably large. Figure 3-17 and Figure 3-18 for the 10 g/L of both formate and glycolate show that the overall baseline plus organic radiolysis plus thermolysis terms (represented by the '+OrgTherm' data '+' data points) are above the 'Linear - 25%' dashed lines for 100°C, 90°C, and 75°C. At 50°C the '+' data points are below or near the 'Linear - 25%' dashed lines indicating acceptable levels. A similar analysis of the 5 g/L formate and glycolate in Figure 3-19 and Figure 3-20 indicates a similar threshold temperature of ~ 75°C. The threshold temperature for the 3 g/L case appears to be between 75°C and 90°C.

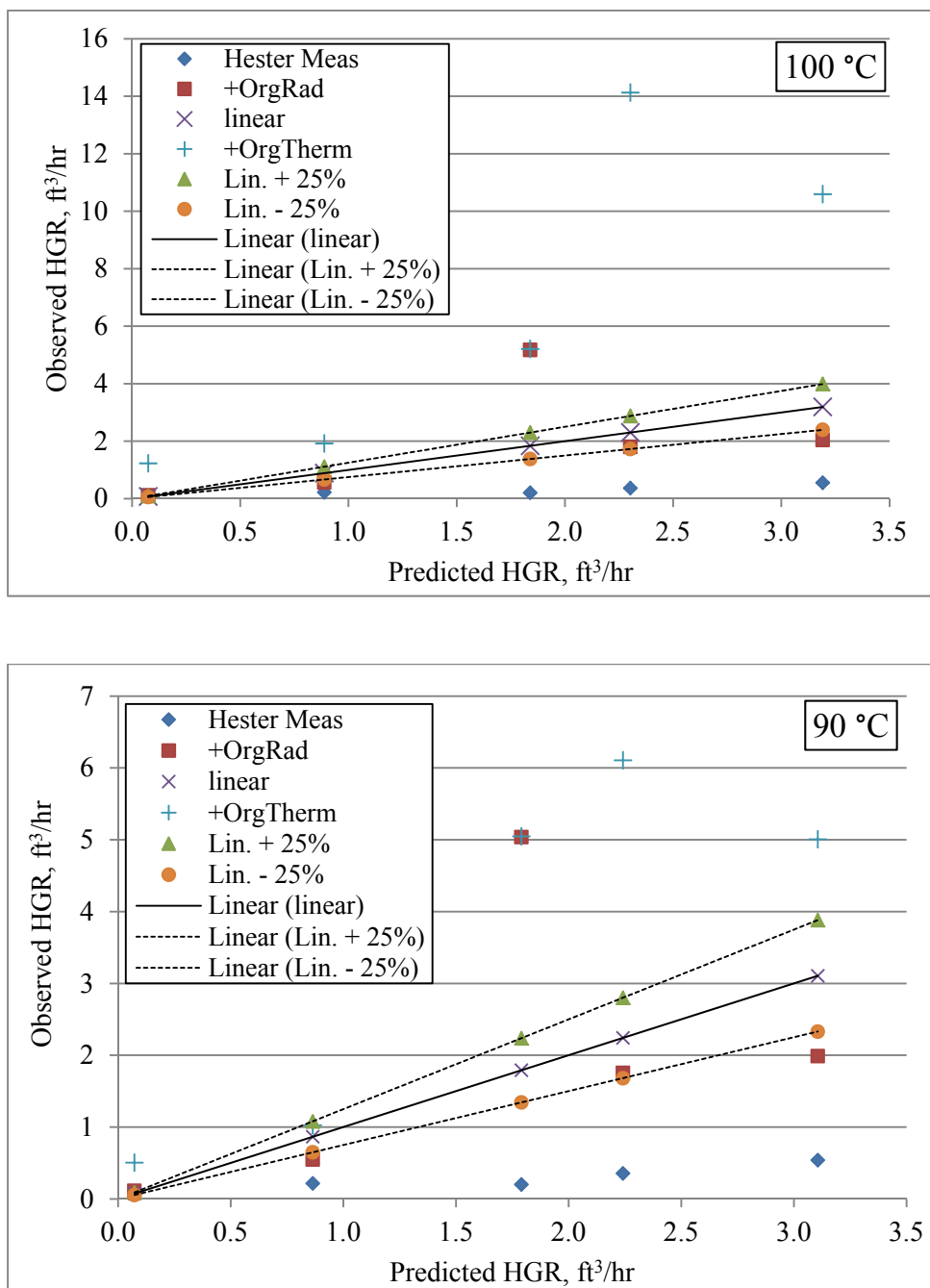


**Figure 3-17. Comparison of Measured and Measured Plus Calculated Formate plus Glycolate Radiolysis (Competition Kinetics) and Thermolysis (Ashby) HGRs Versus the Predicted HGR Using the Boley Method for Selected SRS Tanks Including 25% Uncertainties (100 °C top, 90 °C bottom; glycolate = formate = 10 g/L). “Linear” represents predicted vs. predicted by Boley method. Measured tanks from left to right are SRS Tanks 38, 36, 33, 35, and 32.**

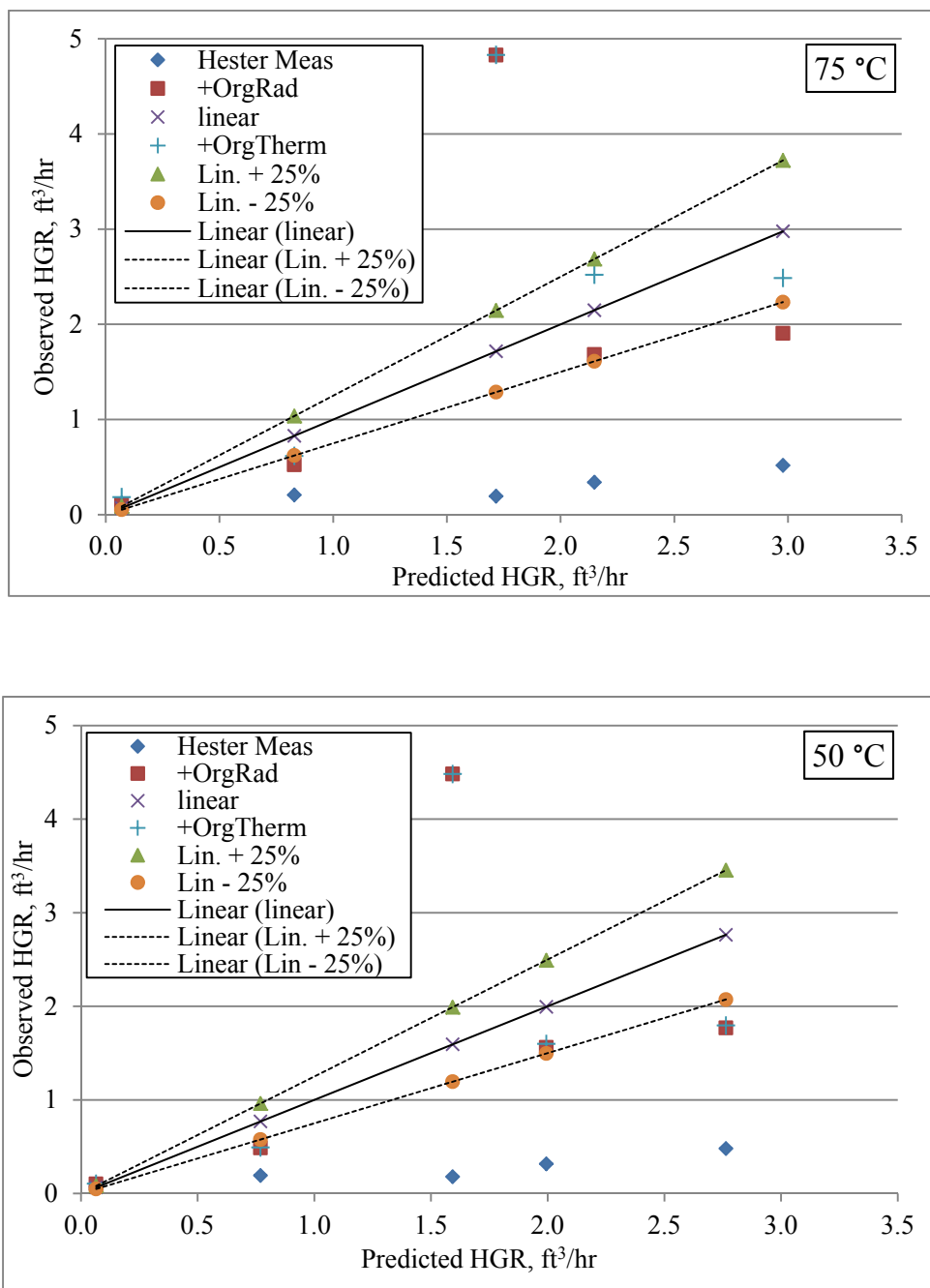


**Figure 3-18. Comparison of Measured and Measured Plus Calculated Formate plus Glycolate Radiolysis (Competition Kinetics) and Thermolysis (Ashby) HGRs Versus the Predicted HGR Using the Boley Method for Selected SRS Tanks Including 25% Uncertainties (75 °C top, 50 °C bottom; glycolate = formate = 10 g/L). “Linear” represents predicted vs. predicted by Boley method. Measured tanks from left to right are SRS Tanks 38, 36, 33, 35, and 32.**

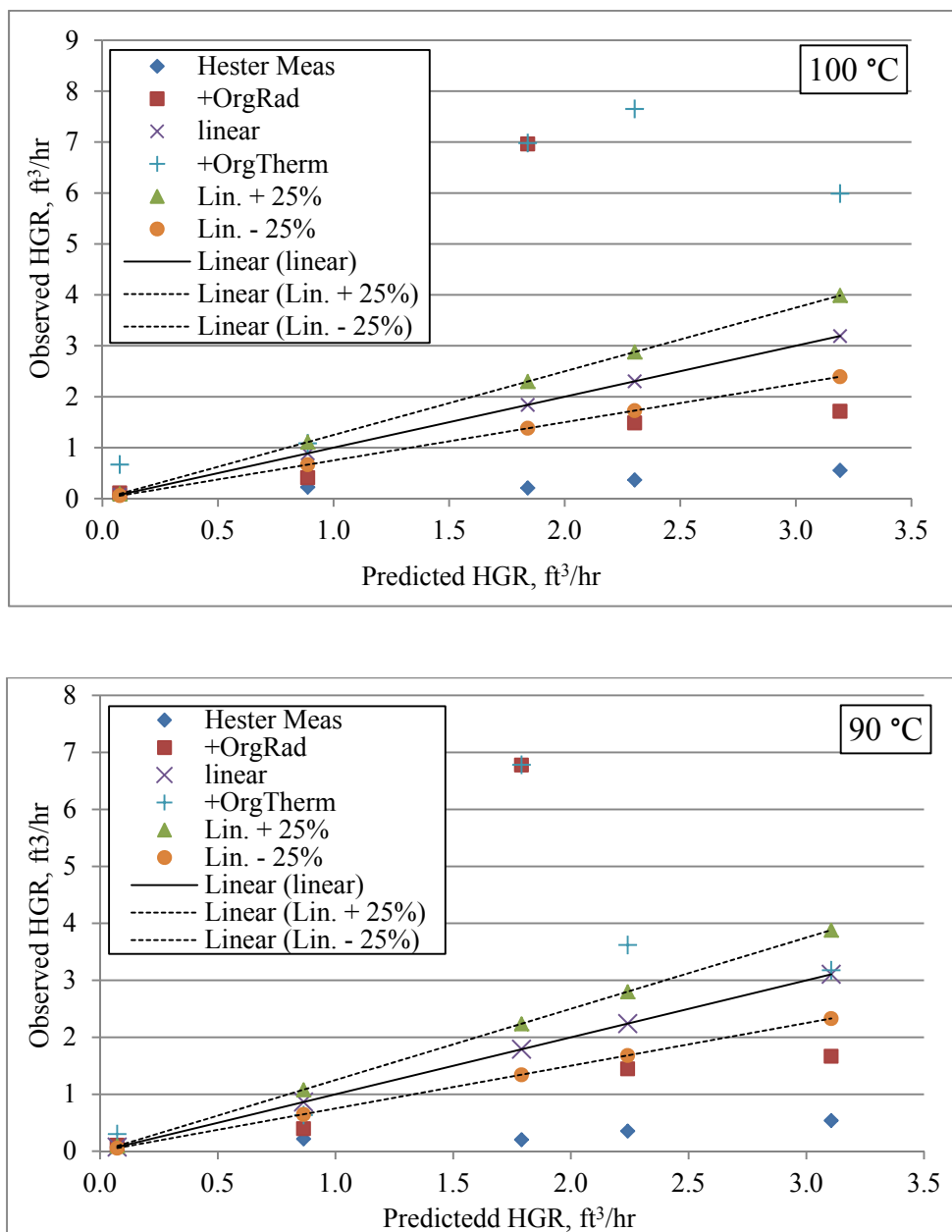


**Figure 3-19. Comparison of Measured and Measured Plus Calculated Formate plus Glycolate Radiolysis (Competition Kinetics) and Thermolysis (Ashby) HGRs Versus the Predicted HGR Using the Boley Method for Selected SRS Tanks Including 25% Uncertainties (100 °C top, 90 °C bottom; glycolate = formate = 5 g/L). “Linear” represents predicted vs. predicted by Boley method. Measured tanks from left to right are SRS Tanks 38, 36, 33, 35, and 32.**

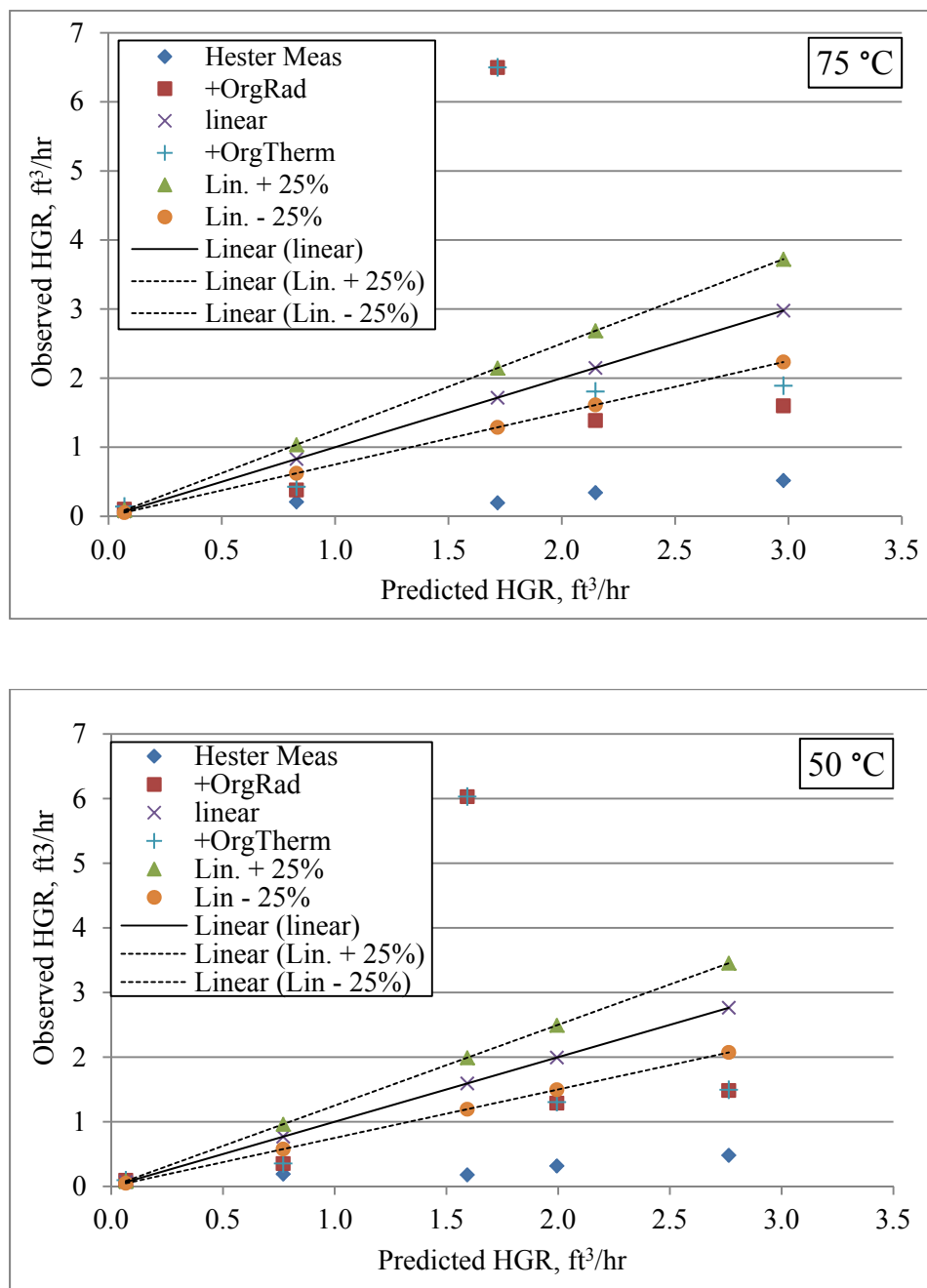


**Figure 3-20. Comparison of Measured and Measured Plus Calculated Formate plus Glycolate Radiolysis (Competition Kinetics) and Thermolysis (Ashby) HGRs Versus the Predicted HGR Using the Boley Method for Selected SRS Tanks Including 25% Uncertainties (75 °C top, 50 °C bottom; glycolate = formate = 5 g/L). “Linear” represents predicted vs. predicted by Boley method. Measured tanks from left to right are SRS Tanks 38, 36, 33, 35, and 32.**

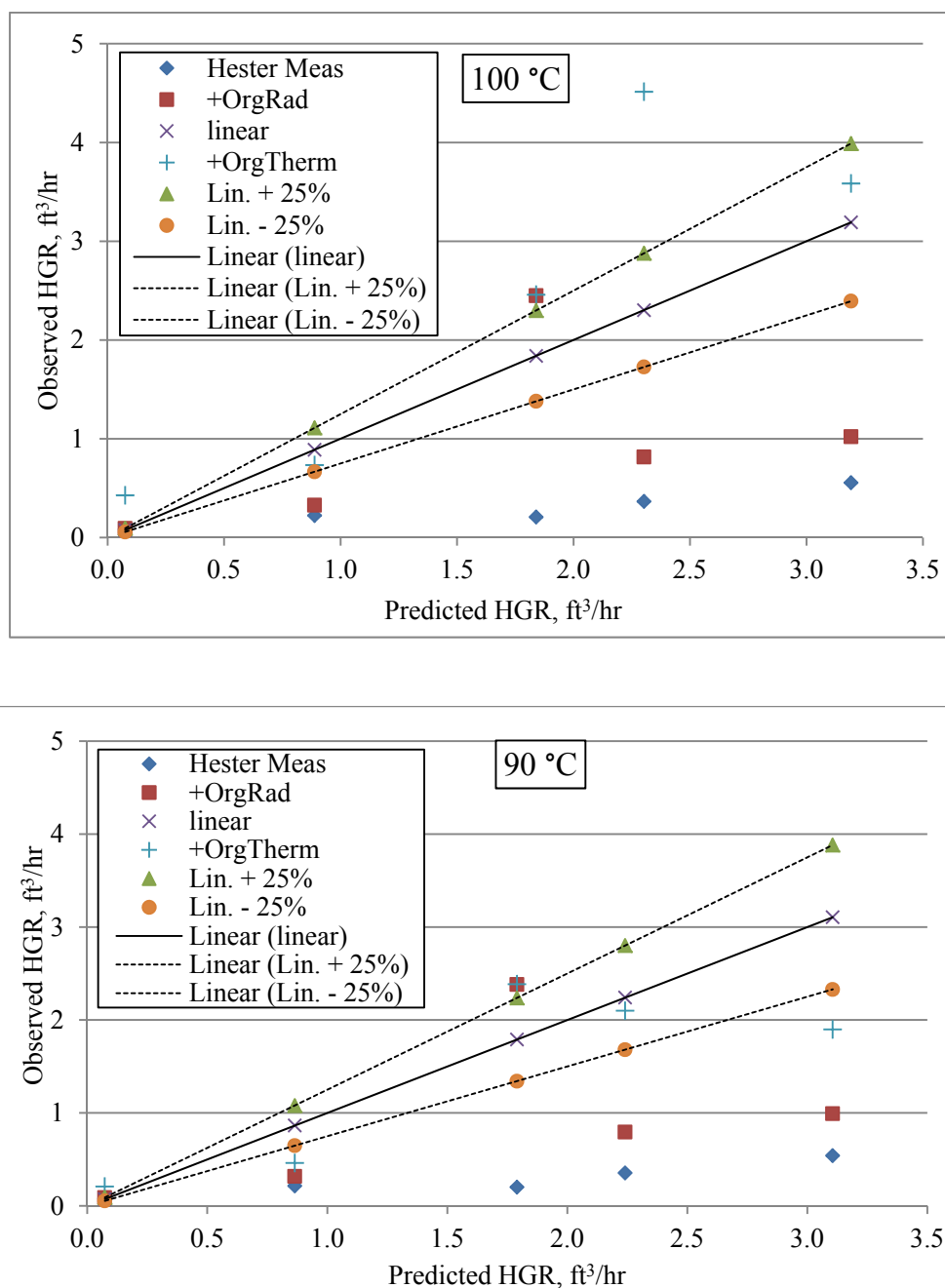


**Figure 3-21. Comparison of Measured and Measured Plus Calculated Formate plus Glycolate Radiolysis (Competition Kinetics) and Thermolysis (Ashby) HGRs Versus the Predicted HGR Using the Boley Method for Selected SRS Tanks Including 25% Uncertainties (100 °C top, 90 °C bottom; glycolate = formate = 3 g/L). “Linear” represents predicted vs. predicted by Boley method. Measured tanks from left to right are SRS Tanks 38, 36, 33, 35, and 32.**

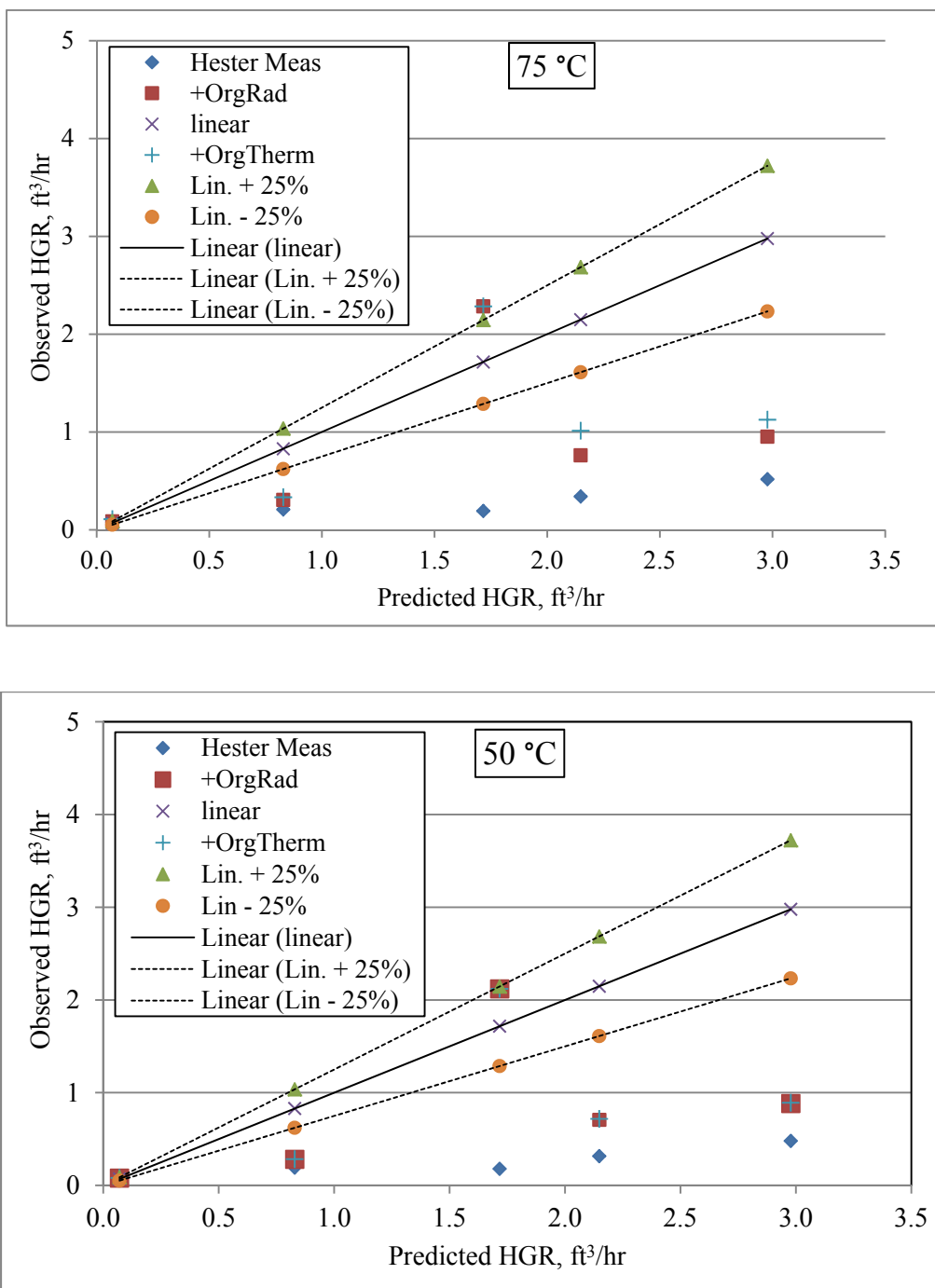


**Figure 3-22. Comparison of Measured and Measured Plus Calculated Formate plus Glycolate Radiolysis (Competition Kinetics) and Thermolysis (Ashby) HGRs Versus the Predicted HGR Using the Boley Method for Selected SRS Tanks Including 25% Uncertainties (75 °C top, 50 °C bottom; glycolate = formate = 3 g/L). “Linear” represents predicted vs. predicted by Boley method. Measured tanks from left to right are SRS Tanks 38, 36, 33, 35, and 32.**

The approximate threshold temperature limits above determined from the limited number of tanks associated with Reference 67 were applied to all the current active SRS tanks excluding Tank 48 per reasons stated above and Tank 50 which is temperature controlled to a maximum of 43°C and is not considered in TtLFL calculations evaluated above 43°C.<sup>69</sup> A higher temperature was also included for comparison. An analysis of how these threshold levels would affect the baseline TtLFL values is shown as follows: Table 3-8 for 3 g/L each of formate and glycolate at the limit of 90°C and a higher temperature of 100°C, Table 3-9 for 5 g/L each of formate and glycolate at the limit of 75°C and a higher temperature of 90°C, and



Table 3-10 for 10 g/L each of formate and glycolate at the limit of 50°C and a higher temperature of 75°C. In each of these tables, the comparative baseline water radiolysis TtLFL values are shown for active SRS tanks (Column 4) using the listed WCS tank temperatures (Column 3).<sup>63</sup> Grey-scale rows indicate the HHW tanks. Each of the tables shows the suggested limiting or threshold temperature (Column 5) for each organic concentration along with the calculated TtLFL values (Column 6) and the percent reduction vs. the baseline TtLFL (Column 7). These columns are then repeated for the increased temperature values (Columns 8 through 10).

There are only a few tanks for each set of initial temperature conditions that show calculated TtLFL of less than 7 day minimum associated with rapid generation tanks (HHW SRS Tanks 33 and 35 for 3 g/L at 90°C and HHW SRS Tanks 33 and 39 for the higher levels of organics (5 g/L at 75°C and 10 g/L at 50°C)), as indicated by the number sign (#).

Table 3-8 for the 3 g/L formate and glycolate at a temperature of 90°C shows that 8 of the very slow generating tanks would transition to shorter TtLFL designations (7 to slow generation and 1 to rapid generation) and 6 of the very slow generation tanks remain unaffected. As the temperature is increased to 100°C, 9 of the very slow generating tanks transition to shorter TtLFL designations (7 to slow generation and 2 to rapid generation) and 5 of the very slow generation tanks remain unaffected. Also at this higher temperature there are 6 tanks that fall below the 7 day TtLFL as indicated by the number (#) sign.

Table 3-9 for the 5 g/L formate and glycolate at a temperature of 75°C shows that 6 of the ‘very slow generating tanks’ would transition to shorter TtLFL designations (6 to slow generation) and 8 of the ‘very slow generation tanks’ would remain unaffected. As the temperature is increased to 90°C, 9 of the very slow generating tanks transition to shorter TtLFL designations (8 to slow generation and 1 to rapid generation) and 5 of the very slow generation tanks remain unaffected. Also at this higher temperature there are 5 tanks that fall below the 7 day TtLFL as indicated by the number (#) sign.

for the 10 g/L formate and glycolate at a temperature of 50°C shows that only 4 of the ‘very slow generating tanks’ would transition to ‘slow generation tanks’ and 10 of the ‘very slow generation tanks’ would remain unaffected. At 10 g/L organic levels and 50°C, three SRS tanks actually show a slight increase in TtLFL relative to the WCS calculation, primarily due to the lower temperature of 50°C used vs. the baseline WCS temperature which ranged from 75 -100°C.<sup>63</sup> As the temperature is increased to 75°C, 8 of the very slow generating tanks transition to slow generation tanks and 6 of the very slow generation tanks remain unaffected. Also at this higher temperature there are 4 tanks that fall below the 7 day TtLFL.

**Table 3-8. Comparison of Baseline TtLFL to 3 g/L Organics  
(Formate and Glycolate) at 90°C and 100°C**

Tank	Overall Total Heat (Btu/hr)	Baseline TtLFL Temp. (°C)	Baseline Radiolytic TtLFL (Days)	Temp. (°C)	Rad. & Therm. TtLFL (Days)	TtLFL Percent Reduced	Temp. (°C)	Rad. & Therm. TtLFL (Days)	TtLFL Percent Reduced
1*	67817	75	253.1	90	85.4	66	100	43.5	83
2*	25618	75	NEVER	90	94.2	--	100	30.7	--
3*	25759	75	NEVER	90	415.1	--	100	124.7	--
4	5755	60	NEVER	90	NEVER	--	100	NEVER	--
7	9452	55	NEVER	90	271.7	--	100	114.9	--
8	34107	60	59.1	90	30.3	49	100	18.2	69
9*	25743	75	NEVER	90	28.7	--	100	9.9	--
10**	2571	75	NEVER	90	NEVER	--	100	NEVER	--
11	15305	100	NEVER	90	256.2	--	100	173.7	--
13	92873	75	12.5	90	9.8	22	100	8.8	30
14**	24672	75	NEVER	90	NEVER	--	100	NEVER	--
15	135097	75	49.4	90	34.9	29	100	27.2	45
21	54857	100	52.6	90	28.4	46	100	16.2	69
22	37721	40	113.6	90	51.1	55	100	40.8	64
23	5169	70	NEVER	90	NEVER	--	100	121.8	--
24	119680	100	152.5	90	71.3	53	100	37.7	75
25	30876	70	76.9	90	9.9	87	100	4.0#	95
26	28651	100	39.6	90	20.0	50	100	10.9	72
27***	37465	100	84.4	90	72.2	15	100	63.3	25
28	40427	100	56.2	90	21.1	63	100	9.9	82
29***	12558	100	41.4	90	22.6	45	100	13.4	68
30	134807	100	15.6	90	13.0	17	100	10.6	32
31	62882	75	68.5	90	8.9	87	100	3.5#	95
32****	252560	100	17.5	90	16.2	8	100	14.7	16
33	202111	50	8.5	90	5.4#	37	100	4.2#	50
34	207304	60	10.4	90	7.6	27	100	6.5#	38
35	221469	50	10.4	90	5.8#	44	100	3.8#	63
36***	108727	100	16.8	90	15.5	8	100	14.6	13
37	34733	100	48.1	90	28.6	41	100	17.2	64
38	11761	100	72.3	90	60.3	17	100	46.1	36
39	343882	70	9.4	90	7.0	25	100	6.5#	31
40	86330	75	31.7	90	24.5	23	100	21.8	31
41	7020	60	NEVER	90	65.9	--	100	25.2	--
42	141794	60	27.7	90	18.6	33	100	14.9	46
43	49580	100	19.2	90	17.5	9	100	14.7	23
44	29959	60	55.1	90	26.4	52	100	15.5	72
45***	38606	75	40.5	90	19.8	51	100	11.0	73
46***	43005	75	37.2	90	24.5	34	100	17.1	54
47	57355	100	17.0	90	12.7	25	100	9.1	47
49	8591	70	NEVER	90	27.4	--	100	10.3	--
51	5072	75	NEVER	90	NEVER	--	100	NEVER	--

#TtLFL values that are below 7 days

\*Tanks 1,2,3 and 9 of ~ 500,000 gallons waste volume with 95-99% salt volume

\*\*Tanks 10 and 14 of ~ 200,000 gallons waste volume with 74-86% salt volume

\*\*\* Tanks 27, 29, 36, 45 and 46 with > 1E+06 gallons waste volume with 91-100% salt volume

\*\*\*\* Greyscale indicates HHW tanks exceeding 136,000 Btu/hr

**Table 3-9. Comparison of Baseline TtLFL to 5 g/L Organics  
(Formate and Glycolate) at 75°C and 90°C**

Tank	Overall Total Heat (Btu/hr)	Baseline TtLFL Temp. (°C)	Baseline Radiolytic TtLFL (Days)	Temp. (°C)	Rad. & Therm. TtLFL (Days)	TtLFL Percent Reduced	Temp. (°C)	Rad. & Therm. TtLFL (Days)	TtLFL Percent Reduced
1*	67817	75	253.1	75	132.0	48	90	64.7	74
2*	25618	75	NEVER	75	960.3	--	90	59.1	--
3*	25759	75	NEVER	75	NEVER	--	90	225.6	--
4	5755	60	NEVER	75	NEVER	--	90	NEVER	--
7	9452	55	NEVER	75	553.7	--	90	164.0	--
8	34107	60	59.1	75	40.3	32	90	24.9	58
9*	25743	75	NEVER	75	106.0	--	90	18.8	--
10**	2571	75	NEVER	75	NEVER	--	90	NEVER	--
11	15305	100	NEVER	75	260.5	--	90	183.8	--
13	92873	75	12.5	75	10.0	21	90	8.9	29
14**	24672	75	NEVER	75	NEVER	--	90	NEVER	--
15	135097	75	49.4	75	38.8	21	90	30.9	37
21	54857	100	52.6	75	38.3	27	90	22.4	57
22	37721	40	113.6	75	54.1	52	90	43.8	61
23	5169	70	NEVER	75	NEVER	--	90	407.7	--
24	119680	100	152.5	75	105.1	31	90	54.8	64
25	30876	70	76.9	75	21.7	72	90	6.9#	91
26	28651	100	39.6	75	28.3	28	90	15.6	61
27***	37465	100	84.4	75	73.6	13	90	64.5	24
28	40427	100	56.2	75	35.9	36	90	15.7	72
29***	12558	100	41.4	75	29.2	29	90	18.0	56
30	134807	100	15.6	75	14.0	10	90	11.7	25
31	62882	75	68.5	75	21.5	69	90	6.1#	91
32****	252560	100	17.5	75	16.8	4	90	15.2	14
33	202111	50	8.5	75	5.8#	32	90	4.7#	45
34	207304	60	10.4	75	8.1	22	90	7.0	33
35	221469	50	10.4	75	7.1	31	90	4.9#	53
36***	108727	100	16.8	75	15.5	8	90	14.4	15
37	34733	100	48.1	75	36.9	23	90	23.1	52
38	11761	100	72.3	75	68.9	5	90	53.9	25
39	343882	70	9.4	75	6.8#	27	90	6.3#	33
40	86330	75	31.7	75	25.1	21	90	22.3	30
41	7020	60	NEVER	75	170.2	--	90	44.0	--
42	141794	60	27.7	75	19.9	28	90	16.4	41
43	49580	100	19.2	75	19.2	0	90	16.3	15
44	29959	60	55.1	75	35.2	36	90	21.3	61
45***	38606	75	40.5	75	28.3	30	90	15.8	61
46***	43005	75	37.2	75	29.1	22	90	21.1	43
47	57355	100	17.0	75	14.8	13	90	11.0	35
49	8591	70	NEVER	75	73.5	--	90	18.5	--
51	5072	75	NEVER	75	NEVER	--	90	NEVER	--

#TtLFL values that are below 7 days

\*Tanks 1,2,3 and 9 of ~ 500,000 gallons waste volume with 95-99% salt volume

\*\*Tanks 10 and 14 of ~ 200,000 gallons waste volume with 74-86% salt volume

\*\*\* Tanks 27, 29, 36, 45 and 46 with > 1E+06 gallons waste volume with 91-100% salt volume

\*\*\*\* Greyscale indicates HHW tanks exceeding 136,000 Btu/hr

**Table 3-10. Comparison of Baseline TtLFL to 10 g/L Organics  
(Formate and Glycolate) at 50°C and 75°C**

Tank	Overall Total Heat (Btu/hr)	Baseline TtLFL Temp. (°C)	Baseline Radiolytic TtLFL (Days)	Temp. (°C)	Rad. & Therm. TtLFL (Days)	TtLFL Percent Reduced	Temp. (°C)	Rad. & Therm. TtLFL (Days)	TtLFL Percent Reduced
1*	67817	75	253.1	50	153.7	39	75	90.9	64
2*	25618	75	NEVER	50	NEVER	--	75	163.2	--
3*	25759	75	NEVER	50	NEVER	--	75	524.6	--
4	5755	60	NEVER	50	NEVER	--	75	NEVER	--
7	9452	55	NEVER	50	507.5	--	75	187.4	--
8	34107	60	59.1	50	45.4	23	75	32.2	45
9*	25743	75	NEVER	50	NEVER	--	75	49.4	--
10**	2571	75	NEVER	50	NEVER	--	75	NEVER	--
11	15305	100	NEVER	50	218.1	--	75	161.6	--
13	92873	75	12.5	50	9.6	23	75	8.4	33
14**	24672	75	NEVER	50	NEVER	--	75	NEVER	--
15	135097	75	49.4	50	39.8	19	75	32.1	35
21	54857	100	52.6	50	41.1	22	75	28.1	47
22	37721	40	113.6	50	53.0	53	75	42.8	62
23	5169	70	NEVER	50	NEVER	--	75	NEVER	--
24	119680	100	152.5	50	118.3	22	75	74.3	51
25	30876	70	76.9	50	32.9	57	75	12.8	83
26	28651	100	39.6	50	31.4	21	75	21.0	47
27***	37465	100	84.4	50	69.8	17	75	59.6	29
28	40427	100	56.2	50	46.0	18	75	25.1	55
29***	12558	100	41.4	50	30.5	26	75	22.0	47
30	134807	100	15.6	50	13.8	11	75	11.7	25
31	62882	75	68.5	50	41.4	40	75	12.8	81
32****	252560	70	15.6	50	16.8	-7	75	14.8	6
33	202111	50	8.7	50	5.6*	35	75	4.8#	45
34	207304	60	10.4	50	8.0	23	75	6.9#	33
35	221469	50	11.0	50	7.6	31	75	5.8#	47
36***	108727	100	13.0	50	14.9	-14	75	13.2	-2
37	34733	100	48.1	50	38.7	19	75	28.1	42
38	11761	100	295.9	50	73.6	75	75	59.2	80
39	343882	70	9.4	50	6.3*	32	75	5.6#	40
40	86330	75	31.7	50	24.8	22	75	21.5	32
41	7020	60	NEVER	50	430.6	--	75	86.7	--
42	141794	60	27.7	50	19.2	31	75	16.2	41
43	49580	100	19.2	50	20.6	-7	75	17.5	9
44	29959	60	55.1	50	38.3	31	75	27.1	51
45***	38606	75	40.5	50	32.8	19	75	21.8	46
46***	43005	75	37.2	50	30.5	18	75	24.0	35
47	57355	100	17.0	50	15.3	10	75	12.1	29
49	8591	70	NEVER	50	174.7	--	75	40.4	--
51	5072	75	NEVER	50	NEVER	--	75	NEVER	--

#TtLFL values that are below 7 days

\*Tanks 1,2,3 and 9 of ~ 500,000 gallons waste volume with 95-99% salt volume

\*\*Tanks 10 and 14 of ~ 200,000 gallons waste volume with 74-86% salt volume

\*\*\* Tanks 27, 29, 36, 45 and 46 with > 1E+06 gallons waste volume with 91-100% salt volume

\*\*\*\* Greyscale indicates HHW tanks exceeding 136,000 Btu/hr

## 4.0 Evaluation of Potential Impacts to DWPF

### 4.1 Comparison of Radiolytic Additive Terms

The matrix of glycolate and formate concentrations shown previously in Table 3-1 were considered relative to the various process tanks presented in the position paper<sup>65</sup> responding to the DWPF PISA.<sup>8</sup> In Sections 2.1 and 2.2 of Reference 65 a conservative value for  $f_{\text{organic}}$  is taken as 1 due to the expected significant levels of formate present. Therefore the DWPF process vessels identified as Sludge Receipt and Adjustment Tank (SRAT), Slurry Mix Evaporator (SME), Melter Feed Tank (MFT), Slurry Mix Evaporator Condensate Tank (SMECT), Recycle Collection Tank (RCT), Decontamination Waste Treatment Tank (DWTT), Strip Effluent Feed Tank (SEFT) and Precipitate Reactor Feed Tank (PRFT) would use the R value equations specified in Reference 65 as Equation (7) for alpha heat loading and Equation (8) for beta/gamma heat loading. It should be noted that the assignment of  $f_{\text{organic}} = 1$  is the most conservative case and provides the highest possible radiolytic HGR and is independent of the organic and scavenger concentrations.

Section 2.3 of Reference 65 calculates a  $f_{\text{organic}}$  term for untreated sludge from the Tank Farm using recent data sets from qualification processing of SB9<sup>70</sup> and SB8<sup>71</sup> in the SRNL Shielded Cells Facility. These solutions apply to the DWPF Sludge Pump Tank (SPT)/Precipitate Pump Tank (PPT)/Late Wash Precipitate Tank (LWPT)/Late Wash Hold Tank (LWHT). Since the washed sludge/salt from the SRS Tank Farm Concentration, Storage and Transfer Facilities (CSTF) via Tank 40 is high in nitrite and low in formate, very low values are calculated for  $f_{\text{organic}}$  for SB9 ( $f_{\text{organic}} = 0.0053$ ) from Table 1 of Reference 65 and SB8 ( $f_{\text{organic}} = 0.0051$ ) from Table 2 of Reference 65. These calculations were repeated using the glycolate and formate matrix as shown in Table 4-1 for SB9 and Table 4-2 for SB8. The maximum  $f_{\text{organic}}$  for SB9 is 0.191 and 0.143 for SB8 for the maximum 10 g/L of both glycolate and formate. However based on historical measured formate concentrations from Tank 40 WAPS analyses during the nitric/formic flowsheet, the highest value reported for formate is a less than detectable value of <585 mg/L for SB4 with comparable nitrate and nitrite levels to those from Reference 70 and 71.<sup>72,73,74,75,76,77</sup> Thus the  $f_{\text{organic}}$  terms shown in line 16 of Table 4-1 and Table 4-2 of <0.012 and <0.009 along with the data presented in Section 2.3 of Reference 65 support using a  $f_{\text{organic}}$  term of 0 for these vessels. These values should also bound the  $f_{\text{organic}}$  terms expected for the planned nitric/glycolic flowsheet since glycolate levels for incoming washed sludge/salt from CSTF should not be higher than current and past formate levels, and the glycolate reactivity with hydrogen atom to form molecular hydrogen is slower than that of formate. These values are shown in line 18 of Table 4-1 and Table 4-2. Accordingly, Equation (11) for alpha radiolysis and Equation (12) for beta/gamma radiolysis from Reference 65 could add on the terms shown below for organic radiolysis.

Revised Equation (11) from Reference 65 using revised  $f_{\text{organic}}$  for SB9 (Table 4-1) or SB8 (Table 4-2):

$$R_{\text{H2, alpha total}} = 134.7 - 82.3 * [\text{NO}_{\text{eff}}]^{1/3} - 13.6 * [\text{NO}_{\text{eff}}]^{2/3} + 11.8 * [\text{NO}_{\text{eff}}] + 25.49 * f_{(\text{org})\text{Rev. (Table 4-1 or Table 4-2)}}$$

Revised Equation (12) from Reference 65 using revised  $f_{\text{organic}}$  for SB9 (Table 4-1) or SB8 (Table 4-2):

$$R_{\text{H2, beta/gamma total}} = 48.36 - 52.78 * [\text{NO}_{\text{eff}}]^{1/3} + 14.1 * [\text{NO}_{\text{eff}}]^{2/3} + 0.572 * [\text{NO}_{\text{eff}}] + 54.76 * f_{(\text{org})\text{Rev. (Table 4-1 or Table 4-2)}}$$

**Table 4-1. Calculation of  $f_{\text{organic}}$  for SB9 Conditions and Glycolate and Formate**

	Glycolate	Molar	Formate	Molar	f(org)Rev.	f(org)Rev./f(org)*
1	10000	0.133	10000	0.222	0.191	36.1
2	10000	0.133	5000	0.111	0.117	22.0
3	10000	0.133	3000	0.067	0.094	17.8
4	10000	0.133	100	0.002	0.042	7.8
5	5000	0.067	10000	0.222	0.182	34.4
6	5000	0.067	5000	0.111	0.106	20.0
7	5000	0.067	3000	0.067	0.071	13.4
8	5000	0.067	100	0.002	0.016	2.9
9	3000	0.040	10000	0.222	0.179	33.7
10	3000	0.040	5000	0.111	0.101	19.1
11	3000	0.040	3000	0.067	0.066	12.5
12	3000	0.040	100	0.002	0.010	1.9
13	0	0	10000	0.222	0.173	32.6
14	0	0	5000	0.111	0.095	17.9
15	0	0	3000	0.067	0.059	11.1
16	0	0	<585	<0.013	<0.012	2.3
17	0	0	100	0.002	0.002	0.4
18	<585	<0.0078	0	0	<0.002	0.3

\* $f_{\text{organic}} = 0.0053$  from Table 1 of Reference 65

**Table 4-2. Calculation of  $f_{\text{organic}}$  for SB8 Conditions and Glycolate and Formate**

	Glycolate	Molar	Formate	Molar	f(org)Rev.	f(org)Rev./f(org)*
1	10000	0.133	10000	0.222	0.143	28.0
2	10000	0.133	5000	0.111	0.085	16.7
3	10000	0.133	3000	0.067	0.068	13.4
4	10000	0.133	100	0.002	0.030	5.8
5	5000	0.067	10000	0.222	0.136	26.6
6	5000	0.067	5000	0.111	0.077	15.1
7	5000	0.067	3000	0.067	0.051	10.0
8	5000	0.067	100	0.002	0.011	2.2
9	3000	0.040	10000	0.222	0.133	26.0
10	3000	0.040	5000	0.111	0.074	14.4
11	3000	0.040	3000	0.067	0.048	9.3
12	3000	0.040	100	0.002	0.007	1.4
13	0	0	10000	0.222	0.128	25.2
14	0	0	5000	0.111	0.069	13.4
15	0	0	3000	0.067	0.042	8.3
16	0	0	<585	<0.013	<0.009	1.7
17	0	0	100	0.002	0.0005	0.1
18	<585	<0.0078	0	0.000	<0.001	0.2

\* $f_{\text{organic}} = 0.0051$  from Table 2 of Reference 65

Section 2.4 of Reference 65 calculates a  $f_{\text{organic}}$  term for material that is transferred from the RCT to the Recycle Pump Tank (RPT) after undergoing nitrite inhibition that involves raising the nitrite concentration to a minimum of 0.156 M. Table 4 of Reference 65 uses a historical maximum measured RCT value of TOC equal to 1,005 ppm which converts to a formate concentration of 3,770 mg/kg. This value is rounded up to 4000 mg/kg and converted to a formate molarity of 0.089M (assuming a density of 1 g/mL). Using this value and the nitrite concentration of 0.156M a  $f_{\text{organic}}$  value is calculated as 0.1442.<sup>65</sup> These calculations were repeated using the Table 3-1 glycolate and formate matrix as shown in Table 4-3 for the RPT. The maximum revised  $f_{\text{organic}}$  calculated is 0.323 for the case of 10 g/L of both glycolate and formate. However the highest value for formate in the RPT at the current acid stoichiometry of 110% Hsu for the nitric/formic flowsheet would be 4,000 mg/L which would give the same  $f_{\text{organic}}$  calculated in Table 4 of Reference 65 as  $f_{\text{organic}} = 0.1442$ . For the nitric/glycolic flowsheet it has been calculated that a 10,000 mg/L glycolate in the RPT would be the practical maximum expected.<sup>78</sup> If one assumes a conservative 20% conversion of glycolic acid to formic acid during processing, then the  $f_{\text{organic}}$  calculated for this scenario of 10,000 mg/L glycolate and 2,000 mg/L formate is 0.143 per line 4 of Table 4-3.

Therefore Equation 9 for alpha radiolysis and Equation 10 for beta/gamma radiolysis from Reference 65 could add on the revised terms shown below for organic radiolysis.

Revised Equation (9) from Reference 65 using revised  $f_{\text{organic}}$  from Table 4-3 for the RPT:

$$R_{\text{H2, alpha total}} = 134.7 - 82.3 \cdot [\text{NO}_{\text{eff}}]^{1/3} - 13.6 \cdot [\text{NO}_{\text{eff}}]^{2/3} + 11.8 \cdot [\text{NO}_{\text{eff}}] + 25.49 \cdot f_{(\text{org})\text{Rev. (Table 4-3)}}$$

Revised Equation (10) from Reference 65 using revised  $f_{\text{organic}}$  from Table 4-3 for the RPT:

$$R_{\text{H2, beta/gamma total}} = 48.36 - 52.78 \cdot [\text{NO}_{\text{eff}}]^{1/3} + 14.1 \cdot [\text{NO}_{\text{eff}}]^{2/3} + 0.572 \cdot [\text{NO}_{\text{eff}}] + 54.76 \cdot f_{(\text{org})\text{Rev. (Table 4-3)}}$$

**Table 4-3. Calculation of  $f_{\text{organic}}$  for RPT with Glycolate and Formate**

	Glycolate	Molar	Formate	Molar	$f_{(\text{org})\text{Rev.}}$	$f_{(\text{org})\text{Rev.}}/f_{(\text{org})}^*$
1	10000	0.133	10000	0.222	0.323	2.2
2	10000	0.133	5000	0.111	0.210	1.5
3	10000	0.133	3000	0.067	0.173	1.2
4	10000	0.133	2000	0.044	0.143	1.0
5	10000	0.133	100	0.002	0.080	0.6
6	5000	0.067	10000	0.222	0.310	2.1
7	5000	0.067	5000	0.111	0.192	1.3
8	5000	0.067	3000	0.067	0.133	0.9
9	5000	0.067	100	0.002	0.031	0.2
10	3000	0.040	10000	0.222	0.304	2.1
11	3000	0.040	5000	0.111	0.185	1.3
12	3000	0.040	3000	0.067	0.125	0.9
13	3000	0.040	100	0.002	0.020	0.1
14	0	0	10000	0.222	0.296	2.1
15	0	0	5000	0.111	0.174	1.2
16	0	0	3000	0.067	0.112	0.8
17	0	0	100	0.002	0.004	0.0

\* $f_{\text{organic}} = 0.1442$  from Table 4 of Reference 65

## 4.2 Comparison of Thermolytic Additive Terms

The treatment of potential thermolytic contributors to DWPF samples in Reference 65 notes that Ashby's work suggests that formate does not undergo thermolysis at temperatures below 120 °C. However the Hanford thermolysis HGR equation was used in Section 3.2 of that work to demonstrate that even if formate did undergo thermolysis in high pH feeds within DWPF, i.e., in the case of caustic boiling of DWPF feed material before acid addition, the thermolytic rates would be insignificant vs. the acid catalysis rates currently used in the facility for the nitric acid/formic acid flowsheet using SB9 input data. Input values from SB9 of 0.1 wt% for TOC and 0.15 wt% for Al were used in that calculation. It was noted that no contributions from the SRAT heel were included and that the measured TOC was used without any exclusion for formate or oxalate.

### 4.2.1 Nitric/Formic Flowsheet for Heated Tanks in DWPF

In Section 3.4 of this report for thermolysis, only the glycolate was considered as a source for thermolysis production of hydrogen and formate was neglected per the cited literature accounts. A scenario was examined to include the SB9 SRAT heel and to use only the adjusted TOC which is calculated by subtracting the carbon contribution from both formate and oxalate.

Table 4-4 shows the input parameters for this scenario using input data from Reference 79 and SB9 analytical data from DWPF in the late 2016 timeframe.<sup>80</sup> This data shows that the adjusted TOC contribution from the SRAT heel could be as high as 3,770 mg/L and the adjusted TOC from SB9 could be as high as 160 mg/L. Statistical analyses were used to determine these bounding values for this scenario.<sup>80</sup> Using a conservative ratio of 25% heel mixed with 75% of incoming slurry, the calculated adjusted TOC for this blend is 1,063 mg/L. Assuming a 1.25 concentration factor during caustic boiling would increase this TOC value to 1,328 mg/L, or 0.13 wt% adjusted TOC. The Al value used for this blend is the same value used for SB9 of 0.059 M or 0.15 wt% for a density of 1.05 g/mL. This level of soluble Al is similar to that predicted from a scoping consideration using OLI Systems Software and the SB9 chemical composition.<sup>80</sup> Other chemical components for OH<sup>-</sup>, NO<sub>3</sub><sup>-</sup>, NO<sub>2</sub><sup>-</sup>, etc. are assumed to be the same as SB9 Tank 40. While there will be additions from Actinide Removal Process (ARP) and the Modular Caustic Side Solvent Extraction Unit (MCU) (and potentially the Salt Waste Processing Facility (SWPF)) and potentially some change to the bulk chemistry, this scenario used in Table 4-4 is thought to be a reasonable assumption.

**Table 4-4. Scenario Considered for Thermolysis in Nitric/Formic Flowsheet with Heel**

DWPF Flowsheet / Organics Used	Input Data for Thermolysis
Nitric acid/Formic acid; Calculated adjusted TOC	SRAT Heel determined from SRAT Product SB9 determined from SB9 WAPS Adjusted TOC <sub>Heel</sub> = 3,770 mg/L max. Adjusted TOC <sub>SB9</sub> = 160 mg/L max. Assume 25:75 blend of heel with SB9 Assume 2,000 mg/L antifoam added at start of caustic boiling; TOC content ~ 50% Assume 1.25 concentration factor for caustic boiling. Overall adjusted TOC in blend = 2,578 mg/L, or 0.25 wt% Al = 0.059 M or 0.15 wt% for a density of 1.05 g/mL



In Reference 65 the thermolysis Equation (2) on page 10 was used along with the quoted TOC value of 0.1 wt% and an Al value of 0.15 wt% from SB9 SRAT receipt supernate using a density of 1.05 g/mL. This calculation gave an expected hydrogen generation rate of 7.6E-05 mole H<sub>2</sub>/day/kg which converts to a rate of 1.38E-05 ft<sup>3</sup>/hr/gal at 105°C using a density of 1.05 g/mL. This calculated rate was then shown to be insignificant vs. the catalytic rate (6.15E-03 ft<sup>3</sup>/hr/gal at 105°C) at several temperatures via Table 6 of Reference 65. The highest ratio of thermolysis rate to catalysis rate was shown to be 0.0022 at 105°C and this ratio decreased with decreasing temperature.

The Hanford thermolysis Equation (2) on page 10 of Reference 65 was used in this report to evaluate the impact of the scenario listed in Table 4-4. This scenario covers the existing nitric acid/formic acid DWPF flowsheet with consideration for the SRAT heel and removes formate and oxalate from the TOC term. The  $r_f$  and  $f_L$  terms were taken as 1 for conservatism.

Results for the nitric-formic flowsheet considerations are shown in Table 4-5 for the SB9 scenario involving the SRAT heel and adjusted TOC levels. These data show that the highest fraction of thermolysis to catalytic rate at 105°C is equal to 0.0057. The thermolysis to catalysis rate fractions all decrease with lowered temperatures. Thus the existing nitric-formic catalytic limit would be bounding for thermolysis during caustic boiling and all lower temperatures, using the matrix from this scenario. As discussed in Reference 65 the thermolytic calculated rate is mutually exclusive of the measured catalytic rate since it is not expected that the thermolysis terms derived from caustic Hanford waste would apply during acid catalysis.

The Hanford thermolysis equation has an uncertainty of  $\pm 1.94$  kJ/mol in the activation energy.<sup>25</sup> When this value is considered in the equation a lower bound of  $\sim 0.5X$  and an upper bound of  $\sim 2X$  can be calculated for the HGR at the highest temperature of 105°C. These uncertainties are applied to the highest temperature for the scenario of Table 4-5. As noted at the bottom of Table 4-5 the range of thermolysis HGR/catalytic HGR for the highest temperature at 105°C is 0.003 to 0.011. Thus the thermolysis HGR could be as high as 1.1% of the maximum nitric/formic catalysis limit HGR for the SB9 case. Using the inverse of these ratios, the nitric/formic catalysis limit bounds the thermolysis HGR in the range of  $\sim 325X$  to  $\sim 95X$  for this SB9 scenario.

**Table 4-5. Comparison of Thermolytic Rates to Catalytic Rates in Nitric/Formic DWPF Flowsheet**

SB9	Temperature	Thermolytic HGR	Catalytic HGR	Fraction of Catalytic
See Table 4-4 for conditions	°C	ft <sup>3</sup> /hr/gal	ft <sup>3</sup> /hr/gal	Unitless
	105	3.50E-05	6.15E-03	0.0057*
	75	2.77E-06	5.73E-04	0.0048
	50	2.34E-07	6.63E-05	0.0035
	25	1.32E-08	7.62E-06	0.0017
	5	9.15E-10	1.34E-06	0.0007

\*Range of 0.003 to 0.011 considering uncertainty of Hanford thermolysis HGR, see text.

#### 4.2.2 Nitric/Glycolic Flowsheet for Heated Tanks in DWPF

A similar scenario involving a SRAT heel, adjusted TOC and added glycolate was considered for the nitric acid/glycolic acid flowsheet. One critical parameter in these comparisons is the current reference value for the nitric acid/formic acid DWPF flowsheet catalytic limit of 0.15 lb/hr/6000 gal<sup>65</sup> vs. the documented safety analysis value of 0.024 lb/hr/6000 gal planned for the nitric acid/glycolic acid DWPF flowsheet in the future.<sup>81</sup>

Table 4-6 shows the input parameters for this scenario using input data from a 2013 heel study<sup>82</sup> and the SB9 WAPS.<sup>79</sup> This data shows that the maximum glycolate in the SRAT heel is ~ 70,000 mg/L and that 2,000 mg/L of antifoam is also in the heel. The adjusted TOC is 160 mg/L maximum in the incoming sludge. The same levels of glycolate used for this report from Table 3-1 of 10 g/L, 5 g/L and 3 g/L were also considered for the incoming sludge. It should be noted that this assumption is highly conservative since the sludge is washed during preparation in Tank 51 and glycolate is removed

A conservative ratio of 25% heel mixed with 75% of incoming slurry was used and two different levels of antifoam addition for caustic boiling were considered. The maximum level of 2,000 mg/L as was used in the nitric/formic treatment and also a reduced level of nominally 1/4X, or 500 mg/L was computed. This latter reduced antifoam addition is based on recent small scale testing at SRNL.<sup>3</sup> Assuming a 1.25 concentration factor during caustic boiling would result in a final adjusted TOC value to 1,668 mg/L, or 0.16 wt% adjusted TOC. Using the lower final antifoam addition of only 500 mg/L results in a lower final adjusted TOC value of 0.07 wt%. The Al value used for this blend is the same value used for SB9 of 0.059M or 0.15 wt% for a density of 1.05 g/mL. This level of Al is similar to that predicted from a scoping consideration using OLI and the SB9 chemical composition.<sup>80</sup> Overall concentrations of Al, hydroxide and nitrite are also listed. Other chemical components for OH<sup>-</sup>, NO<sub>3</sub><sup>-</sup>, NO<sub>2</sub><sup>-</sup>, etc. are assumed to be the same as SB9 Tank 40. While there will be additions from ARP/MCU (and potentially SWPF) and potentially some change to the bulk chemistry, this scenario used in Table 4-6 is thought to be a reasonable assumption. Calculations for this scenario used both the Eqn. 2 from this report (i.e., the same as Equation 2 from Reference 65) for the adjusted TOC, and Equations 3-6 from this report to calculate the HGR from glycolate thermolysis.

**Table 4-6. Scenario Considered for Thermolysis in Nitric/Glycolic Flowsheet with Heel**

DWPF Flowsheet / Organics Used	Input Data for Thermolysis
Nitric acid/Glycolic acid; Calculated adjusted TOC and Glycolate thermolysis	SRAT Heel determined from SRAT Product SB9 determined from SB9 WAPS Glycolate <sub>Heel</sub> = 70,000 mg/L max. Antifoam <sub>Heel</sub> = 2,000 mg/L Adjusted TOC <sub>SB9</sub> = 160 mg/L max. Use Table 3-1 levels of glycolate for incoming sludge of 10 g/L, 5 g/L and 3 g/L Assume 25:75 blend of heel with SB9 Assume 2,000 mg/L antifoam added at start of caustic boiling; TOC content ~ 50% Assume 1.25 concentration factor for caustic boiling Overall adjusted TOC in blend = 1,668 mg/L, or 0.16 wt% for maximum antifoam; or 730 mg/L, or 0.07 wt% for reduced antifoam addition Overall glycolate concentrations of 31,250 mg/L, 26,563 mg/L and 24,688 mg/L Overall [Al] = 0.059M, [OH <sup>-</sup> ] = 0.18M, [NO <sub>2</sub> <sup>-</sup> ] = 0.26M

Table 4-7 presents the results from calculations for the maximum SRS Tank Farm scenario parameters from Table 4-6 and the various levels of glycolate. Table 4-8 presents similar results calculated for the lower antifoam addition. From Table 4-7 the fraction of thermolysis rate to catalytic rate is highest at 4.1% for the maximum level of glycolate at 31.3 g/L and 105°C and the fraction decreases with decreasing temperature. The range of the thermolysis to catalysis fraction is from 2.7% to 6.4% considering the uncertainty in the Hanford thermolysis equation and a nominal +/-20% uncertainty in the glycolate thermolysis equations.<sup>54</sup> This thermolysis to catalysis fraction decreases to 3.7% at 105°C for the lowest glycolate concentration of 24.7 g/L. From Table 4-8 involving the lower addition of antifoam, the fraction of thermolysis rate to catalytic rate is highest at 2.8% for the maximum level of 31.3 g/L glycolate scenario at 105°C and the fraction decreases with decreasing temperature. The range of the thermolysis to catalysis fraction is from 2.0% to 4.1% considering the uncertainty in the HGR equations. The thermolysis to catalysis fraction decreases to 2.4% at 105°C for the lowest glycolate concentration of 24.7 g/L.

These calculations show that when using the lower catalytic limit for nitric-glycolic flowsheet of 0.024 lb/hr/6000 gal and the highest glycolate level considered, the catalytic upper limit bounds the thermolysis HGR by ~24X (at 105°C) or better at lower temperatures for the maximum antifoam addition scenario and bounds the thermolysis ~35X (at 105°C) or better at lower temperatures for the reduced antifoam scenario. Considering the uncertainty of the Hanford thermolysis equation and the glycolate thermolysis equations, these ranges for the upper limit catalytic bounds are from ~37X to ~16X for the maximum antifoam scenario and ~50X to ~25X for the reduced antifoam scenario.

**Table 4-7. Comparison of Thermolytic Rates to Catalytic Rates in Nitric/Glycolic DWPF Flowsheet with Maximum Antifoam Addition**

Glycolate	Temperature	Adj. TOC HGR	Glycolate HGR	Total HGR	Catalytic HGR	Fraction of Catalytic
g/L	°C	ft <sup>3</sup> /hr/gal	ft <sup>3</sup> /hr/gal	ft <sup>3</sup> /hr/gal	ft <sup>3</sup> /hr/gal	Unitless
31.3	105	2.24E-05	1.82E-05	4.06E-05	9.84E-04	0.041*
	75	1.77E-06	7.52E-07	2.52E-06	9.17E-05	0.028
	50	1.50E-07	3.39E-08	1.84E-07	1.06E-05	0.017
	25	8.44E-09	9.14E-10	9.36E-09	1.22E-06	0.008
	5	5.86E-10	3.17E-11	6.17E-10	2.14E-07	0.003
26.6	105	2.24E-05	1.54E-05	3.78E-05	9.84E-04	0.038
	75	1.77E-06	6.39E-07	2.41E-06	9.17E-05	0.026
	50	1.50E-07	2.88E-08	1.79E-07	1.06E-05	0.017
	25	8.44E-09	7.77E-10	9.22E-09	1.22E-06	0.008
	5	5.86E-10	2.69E-11	6.12E-10	2.14E-07	0.003
24.7	105	2.24E-05	1.42E-05	3.66E-05	9.84E-04	0.037
	75	1.77E-06	5.88E-07	2.36E-06	9.17E-05	0.026
	50	1.50E-07	2.65E-08	1.76E-07	1.06E-05	0.017
	25	8.44E-09	7.15E-10	9.16E-09	1.22E-06	0.008
	5	5.86E-10	2.48E-11	6.10E-10	2.14E-07	0.003

\*Range of 0.027 to 0.064 considering uncertainty of Hanford thermolysis HGR

**Table 4-8. Comparison of Thermolytic Rates to Catalytic Rates in Nitric/Glycolic DWPF Flowsheet with Reduced Antifoam Addition**

Glycolate	Temperature	Adj. TOC HGR	Glycolate HGR	Total HGR	Catalytic HGR	Fraction of Catalytic
g/L	°C	ft <sup>3</sup> /hr/gal	ft <sup>3</sup> /hr/gal	ft <sup>3</sup> /hr/gal	ft <sup>3</sup> /hr/gal	Unitless
31.3	105	9.81E-06	1.82E-05	2.80E-05	9.84E-04	0.028*
	75	7.75E-07	7.52E-07	1.53E-06	9.17E-05	0.017
	50	6.56E-08	3.39E-08	9.95E-08	1.06E-05	0.009
	25	3.69E-09	9.14E-10	4.61E-09	1.22E-06	0.004
	5	2.56E-10	3.17E-11	2.88E-10	2.14E-07	0.001
26.6	105	9.81E-06	1.54E-05	2.52E-05	9.84E-04	0.026
	75	7.75E-07	6.39E-07	1.41E-06	9.17E-05	0.015
	50	6.56E-08	2.88E-08	9.44E-08	1.06E-05	0.009
	25	3.69E-09	7.77E-10	4.47E-09	1.22E-06	0.004
	5	2.56E-10	2.69E-11	2.83E-10	2.14E-07	0.001
24.7	105	9.81E-06	1.42E-05	2.40E-05	9.84E-04	0.024
	75	7.75E-07	5.88E-07	1.36E-06	9.17E-05	0.015
	50	6.56E-08	2.65E-08	9.21E-08	1.06E-05	0.009
	25	3.69E-09	7.15E-10	4.41E-09	1.22E-06	0.004
	5	2.56E-10	2.48E-11	2.81E-10	2.14E-07	0.001

\*Range of 0.020 to 0.041 considering uncertainty of Hanford thermolysis HGR and the Glycolate HGR, see text.

The predicted ranges of the thermolysis to catalysis fractions from Table 4-5, Table 4-7, Table 4-8 and the associated uncertainty ranges can be compared to the NFPA guideline<sup>83</sup> that DWPF operates under for the SRAT/SME.<sup>84</sup> In general the combustible concentration limit during processing is maintained at or below 60 percent of the composite lower flammability level (CLFL) where automatic instrumentation with safety interlocks are provided and at 25 percent of the CLFL in the absence of such instrumentation. The current nitric-formic DWPF flowsheet uses the 60% CLFL case using at least one gas chromatograph (GC) with associated interlock.<sup>84</sup> Two GCs are provided to determine the hydrogen concentrations in the SRAT off-gas system and calculate a CLFL based on a bounding value of Isopar L and ADPs.<sup>84</sup> Since it is expected that the planned nitric-glycolic flowsheet will have much lower catalytic HGRs,<sup>85,3</sup> safety significant protection provided by constant monitoring from a GC instrument for the SRAT and SME during operation may no longer be required and the 25% CLFL limit would be applied.<sup>86</sup>

Table 4-5 shows that the predicted range for the thermolysis rate to maximum catalysis rate percentages for the adjusted TOC scenario involving the SRAT heel at maximum temperature of 105°C is 0.3% to 1.1%. This range is likely well under the hydrogen contribution to the current operating limit of 60% CLFL used in the DWPF for the formic-nitric flowsheet.

Considering the nitric-glycolic DWPF flowsheet the thermolysis rate to maximum catalysis rate percentages for the highest glycolate and maximum temperature of 105°C are 2.7% to 6.4% for the maximum antifoam addition (Table 4-7) and 2.0% to 4.1% for the reduced antifoam addition (Table 4-8). Thus due to the expected lower catalysis rate maximum for the nitric-glycolic flowsheet, the predicted thermolysis HGRs make up a slightly larger fraction of the safety margin of 25% CLFL with respect to hydrogen generation in the SRAT and SME (vs. the nitric/formic flowsheet using 60% of CLFL). Current planned testing at SRNL is designed to investigate the validity of the Hanford thermolysis equations and the glycolate thermolysis equations with respect to glycolate thermolytic decomposition using actual real waste samples from the SRS Tank Farm.<sup>2</sup>

As noted previously in this section, since the predicted thermolysis rates are mutually exclusive of the acid catalysis rates, the scenarios considered for either the nitric/formic flowsheet or the nitric/glycolic flowsheet would most likely apply to caustic boiling of DWPF feeds before acid is added.

#### 4.3 Comparison of Thermolytic Additive Terms for Nonheated Tanks and Heated Tanks to Radiolytic Rates

The DWPF vessels indicated in Section 2.2 through 2.4 of Reference 65 consisting of the SEFT, PRFT, SPT, PPT, LWPT, LWHT and the RPT do not consider catalytic hydrogen. These vessels are referred to as ‘colder’ vessels relative to the process vessels that are heated. For these vessels a hypothetical maximum temperature of 50°C was used in Reference 65 to calculate thermolysis HGRs for comparison to radiolytic HGRs that are documented in Reference 87. It should be noted that the radiolytic HGRs calculated from Reference 87 are conservative in that they do not credit any scavenging from nitrate and nitrite salts. These radiolytic HGRs also do not contain any contribution from organics radiolysis. Using SB9 input data the thermolysis rate at 50°C was calculated to be 9.2E-08 ft<sup>3</sup>/hr/gal compared to expected radiolytic rates on the order of 10<sup>-5</sup> ft<sup>3</sup>/hr/gal.<sup>65</sup> A salt batch input data set was also used to calculate a thermolysis rate at 50°C of 2.4E-08 ft<sup>3</sup>/hr/gal compared to expected radiolytic rates on the order of 10<sup>-6</sup> to 10<sup>-5</sup> ft<sup>3</sup>/hr/gal.<sup>65</sup> This data showed that thermolysis rates at 50°C were therefore negligible compared to radiolytic rates. These two data sets are shown as the first two rows of data in Table 4-9. Similar calculations involving 50°C for the nitric/formic and nitric/glycolic scenarios at the highest glycolate blend concentration of 31.3 g/L are compared to the radiolytic rates in Table 4-9. The radiolytic rates are all given in the temperature range of 42.4°C to 50°C.<sup>87</sup> These data show that for either the nitric/formic or the nitric/glycolic scenarios the predicted thermolysis HGRs at 50°C are all below the predicted radiolytic HGR rates. Similar HGRs are shown for the heated tanks at a temperature of 105°C for these same scenarios which indicates that the 105°C thermolysis rates are comparable to the radiolytic rates for sludge tanks and the LWPT salt tanks. The 105°C HGRs are an order of magnitude higher than the radiolytic rate for the LWHT salt tank.

**Table 4-9. Comparison of Thermolysis Rates at 50°C and at 105°C to Radiolytic Rates in Temperature Range of 42.4°C to 50°C.**

	Nitric/Formic Flowsheet	Thermolytic HGR at 50°C (ft <sup>3</sup> /hr/gal)	Thermolytic HGR at 105°C (ft <sup>3</sup> /hr/gal)	Radiolytic HGR Range <sup>87</sup> (sludge) (ft <sup>3</sup> /hr/gal)	Radiolytic HGR Range <sup>87</sup> (salt) (ft <sup>3</sup> /hr/gal)
1	Reference 65 SB9	9.2E-08	NA	2.7E-05 to 9.5E-05	NA
2	Reference 65 Salt	2.4E-08	NA	NA	2.0E-06 (LWHT) to 4.9E-05 (LWPT)
3	Adj. TOC, SRAT Heel	2.34E-07	3.50E-05	2.7E-05 to 9.5E-05	2.0E-06 (LWHT) to 4.9E-05 (LWPT)
--	<b>Nitric/Glycolic Flowsheet</b>	--		--	--
4	Adj. TOC, Max. Glycolate, Max. Antifoam	1.84E-07	4.06E-05	2.7E-05 to 9.5E-05	2.0E-06 (LWHT) to 4.9E-05 (LWPT)
5	Adj. TOC, Max. Glycolate, Reduced Antifoam	9.95E-08	2.800E-05	2.7E-05 to 9.5E-05	2.0E-06 (LWHT) to 4.9E-05 (LWPT)

## 5.0 Conclusions

### Potential Impacts of Formate and Glycolate Radiolysis to the SRS Tank Farm

- Addition of organic radiolysis predictive terms for the highest level of 10 g/L formate to measured HGR for five selected SRS samples from 1998 to 2000 indicates that predicted total HGR is bounded by the current baseline equations except for SRS Tank 33 that contained low nitrite.
- Since the glycolate rate constant for hydrogen production is only ~ 20% of formate, consideration of both glycolate and formate at the 10 g/L level appears also to be bounded by the baseline equations also with the exception of SRS Tank 33.
- Comparison of TtLFL values for either 10 g/L formate or for 10 g/L formate and glycolate to the baseline TtLFL values from water radiolysis only, suggests that only two of the SRS HHW tanks would have calculated TtLFL values less than 7 days. The TtLFL values are near 6 days for SRS Tanks 33 and 39 when organic radiolysis additive HGR terms are considered.

### Potential Impacts of Glycolate Thermolysis to the SRS Tank Farm

- SRS Tank Farm HGRs predicted by the Hanford thermolysis equations are higher for most tanks than predictions generated by the Ashby rate equations.
- The Hanford equations predict average temperature-adjusted HGRs below 1 ft<sup>3</sup>/hr at 75°C and the Ashby equations give similar values at 90°C. These levels of HGRs are similar to water radiolysis temperature-adjusted average HGRs in the range of 0.65 to 0.75 ft<sup>3</sup>/hr.

### Potential Impacts of Overall Additive Radiolysis and Thermolysis Terms to the SRS Tank Farm

- Comparing HGR with added glycolate and formate radiolysis and glycolate thermolysis suggests that a threshold temperature of ~ 50°C could apply to the 10 g/L level each of these organics, a threshold limit of ~ 75°C is predicted for the 5 g/L each of these organics, and an upper temperature of 90°C could apply to the lower 3 g/L each of these organics. All three of the different organic concentration levels show visible separation in the plots between the thermolysis terms and the organic radiolysis terms for the 100°C data.
- Similar conclusions to these threshold temperatures are drawn from a detailed comparison of additive terms and past tank sampling from 1998 to 2000 with the exception of Tank 33 due to its low nitrite concentration during that time.
- Due to the wide range of existing water radiolysis HGR values (1.5E-03 ft<sup>3</sup>/hr to 4.84 ft<sup>3</sup>/hr) it is difficult to assign a single temperature and organic concentration threshold value that would apply for all tanks. Even at the approximate levels identified above, two of the rapid generation tanks drop below TtLFL values of 7 days at all three of the different threshold temperature plus organics levels cited.
- The nitrite anion is identified from this work as playing a key role in both the organic radiolysis, where it serves as effective scavenger to prevent molecular hydrogen formed from indirect organic radiolysis, and in the glycolate thermolysis, where the literature indicates that in simplified caustic waste simulants, it promotes glycolate thermolysis to produce hydrogen.

### Potential Impacts of Formate and Glycolate Radiolytic and Thermolysis Terms to the DWPF

- In Sections 2.1 and 2.2 of Reference 65 a conservative value for  $f_{\text{organic}}$  is taken as 1 due to the expected significant levels of formate present. Therefore the DWPF process vessels identified as SRAT, SME, MFT, SMECT, RCT, DWTT, SEFT and PRFT would use the R value equations specified in Reference 65 as Equation (7) for alpha heat loading and Equation (8) for beta/gamma heat loading without any adjustment from the formate and glycolate matrix considered in this report.
- The calculated  $f_{\text{organic}}$  terms from Section 2.3 of Reference 65 are significantly increased using the formate and glycolate matrix of this report for DWPF SPT/PPT/LWPT/LWHT vessels. These are the vessels that are associated with untreated sludge/salt from CSTF. The SB9  $f_{\text{organic}}$  term of 0.0053 increases to 0.191 and the SB8  $f_{\text{organic}}$  term of 0.0051 increases to 0.143 for the highest level of 10 g/L each of formate and glycolate concentrations. However review of historic formate Tank 40 concentrations from WAPS reports indicates that the highest formate value reported is less than detectable < 585 mg/L. Substitution of this formate value into the SB8 and SB9 calculations results in  $f_{\text{organic}}$  of < 0.012. By analogy if glycolate concentrations in Tank 40 for the planned nitric/glycolic flowsheet are comparable to historic formate concentrations of < 585 mg/L, then the  $f_{\text{organic}}$  term is < 0.009. Thus these calculations along with the data presented in Section 2.3 of Reference 65 support using a  $f_{\text{organic}}$  term of 0 for these vessels.
- The  $f_{\text{organic}}$  term increases also for the RPT considering the formate and glycolate levels of this report. The RPT  $f_{\text{organic}}$  term of 0.1442 increases to 0.323 for the highest level of 10 g/L each of formate and glycolate concentrations. However current nitric/formic flowsheet conditions indicate an upper limit of ~ 4,000 mg/L formate expected in the RPT with a  $f_{\text{organic}}$  = 0.1442. The calculated practical maximum limit for planned nitric/glycolic flowsheet indicate 10,000 mg/L glycolate and 2,000 mg/L formate resulting in a  $f_{\text{organic}}$  of 0.143.

### Thermolysis Impacts to the Nitric/Formic DWPF Flowsheet Using a Catalytic Limit of 0.15 lb/hr/6000 gal:

- Thermolysis rates using the Hanford correlation and its associated uncertainty and the adjusted TOC resulting from a SB9 SRAT heel blended with the adjusted TOC from DWPF incoming sludge give calculated thermolysis rate to formate catalysis rate ratios in the range of 0.003 to 0.011, or ~ 0.3% to 1.1%. Thus the same conclusion as was made in Reference 65 holds for the SB9 case scenario considered in this work. Thermolysis rates compared to catalysis rates at the ~ 105°C temperature of DWPF processing indicates that the catalytic rate is significantly bounding and remains bounding at lower temperatures.

### Thermolysis Impacts to the Nitric/Glycolic DWPF Flowsheet Using a Catalytic Limit of 0.024 lb/hr/6000 gal:

- Thermolysis rates using outputs from the Hanford correlation for adjusted TOC and the glycolate thermolysis equations applied to the nitric/glycolic SRAT heel plus incoming sludge that could contain up to 10 g/L glycolate give calculated thermolysis rate to formate catalysis rate ratios in the range of 0.027 to 0.064, or ~ 3.7 to 6.4% for maximum antifoam and 0.020 to 0.041, or ~ 2 to 4.1% for a reduced antifoam addition. These values indicate that the predicted thermolysis rates would be much lower than the potential 25% CLFL considered for the nitric/glycolic flowsheet for SRAT and SME flammability control.

Thermolysis HGRs for Nonheated Tanks Predicted at 50°C and Heated Tanks Predicted at 105°C Compared to Radiolytic HGRs:

- All of the predicted 50°C thermolysis rates determined for the nitric/formic or the nitric/glycolic flowsheets for nonheated tanks are shown to be lower than current conservative radiolytic HGRs from water radiolysis that are calculated without consideration for nitrate and nitrite scavengers. HGRs for heated tanks at a temperature of 105°C for these same scenarios are comparable to the radiolytic rates for sludge tanks and the LWPT salt tanks. The 105°C HGRs are an order of magnitude higher than the radiolytic rate for the LWHT salt tank.

## **6.0 Recommendations, Path Forward or Future Work**

- Formate anion should be measured and tracked in the WCS Tank Farm chemistry information along with the other existing anions such as nitrite and nitrate.<sup>63</sup> This would allow for accurate calculation in the future of the organic radiolysis additive terms, if needed.
- Formate thermolysis was not considered in this work due to the findings reported by Ashby<sup>54</sup> and Meisel.<sup>22</sup> However those studies performed at temperatures up to 120°C were limited in scope to a simplified simulants prepared from the sodium salts of hydroxide, aluminate, nitrate and nitrite. Alkaline thermolysis testing of hydroxycarboxylic acids and polyols at higher temperatures up to 275°C also show no indication of formate thermolysis.<sup>55,56</sup> Experimental testing of more fully developed simulants or actual SRS Tank Farm caustic samples containing added levels of soluble formate anion could be conducted as a function of temperature up to SRS evaporator temperatures, with high sensitivity hydrogen analysis to further investigate the extent of formate thermolysis in SRS waste. Laboratory testing is in progress to investigate thermolysis from actual SRS radioactive tank samples containing formate.<sup>88</sup>
- A refined understanding of glycolate thermolysis vs. the limited conditions of Ashby should be explored by performing experimental testing of more complex caustic waste simulants or actual SRS Tank Farm caustic samples containing added levels of soluble glycolate as a function of temperature up to SRS evaporator temperatures with high sensitivity hydrogen analysis. Simulant testing is planned for this purpose which may lead to further radioactive sample testing.<sup>2</sup>



## 7.0 References

- <sup>1</sup> E. W. Holtzscheiter, "Literature Review: Glycolate/Formate Impact to Tank Farm Radiolytic Hydrogen Generation", X-TAR-S-00006, Rev. 0, 2017.
- <sup>2</sup> S. T. Isom, "Evaluation of Glycolate Impact to Tank Farm and Radiolytic Hydrogen Generation", X-TTR-S-00060, Rev. 1, 2017.
- <sup>3</sup> J. D. Newell, J. M. Pareizs, C. J. Martino, S. H. Reboul, C. J. Coleman, T. B. Edwards, and F. C. Johnson, "Actual Waste Demonstration of the Nitric-Glycolic Flowsheet for Sludge Batch 9 Qualification", SRNL-STI-2016-00327, Rev. 1, 2017.
- <sup>4</sup> D. D. Walker, "Organic Compounds in Savannah River Site High-Level Waste", WSRC-TR-2002-00391, Rev. 0, 2002.
- <sup>5</sup> C. J. Martino, "Analysis of Tank 38H (HTF-38-11-69, 70) and Tank 43H (HTF-43-11-71,72) Samples for Support of the Enrichment Control and Corrosion Control Programs", SRNL-L3100-2011-00147, Rev. 0, 2011.
- <sup>6</sup> A. V. Staub, "Potentially Inadequate Recognition of the Effect of Organics on Hydrogen Generation Rates in Saltstone", PI-2017-0002, 2017.
- <sup>7</sup> W. A. Condon, "Potentially Inadequate Recognition of the Effect of Organics on Hydrogen Generation Rates in CSTF", PI-2017-0003, 2017.
- <sup>8</sup> K. M. Brotherton, "Potentially Inadequate Recognition of the Effect of Organics on Hydrogen Generation Rates in DWPF Process Vessels", PI-2017-0004, 2017.
- <sup>9</sup> B. R. Pickenheim, N. E. Bibler, D. P. Lambert, and M. S. Hay, "Glycolic Acid Physical Properties, Impurities, and Radiation Effects Assessment", SRNL-STI-2010-00314, Rev. 1, 2011.
- <sup>10</sup> K. Adu-Wusu, "Literature Review on Impact of Glycolate on the 2H Evaporator and the Effluent Treatment Facility (ETF)", SRNL-STI-2012-00132, Rev. 0, 2012.
- <sup>11</sup> C. L. Crawford and N. E. Bibler, "Radiolytic Hydrogen Generation in Savannah River Site (SRS) High Level Waste Tanks – Comparison of SRS and Hanford Modeling Predictions", WSRC-TR-2004-00468, Rev. 0, 2004.
- <sup>12</sup> C. L. Crawford, C. J. Martino, and J. I. Mickalonis, "Task Technical and Quality Assurance Plan for Glycolate Impacts on Savannah River Site Tank Farm Hydrogen Generation and Corrosion", SRNL-RP-2017-00082, Rev. 0, 2017.
- <sup>13</sup> "Technical Reviews", Conduct of Engineering Manual E7, Procedure 2.60, Rev. 17, 2016.
- <sup>14</sup> "Savannah River National Laboratory Technical Report Design Check Guidelines", WSRC-IM-2002-00011, Rev. 2, 2004.
- <sup>15</sup> C. S. Boley and J. R. Hester, "Hydrogen Generation Rates for Tank Farm Applications", WSRC-TR-98-00303, Rev. 0, 1998.
- <sup>16</sup> C. S. Boley, "G-Value Prediction for Hydrogen Generation Rates for High Level Waste (U)", X-CLC-H-00100, Rev. 0, 1998.
- <sup>17</sup> N. E. Bibler and D. D. Walker, "The Dependence of Radiolytic H<sub>2</sub> Generation on the Nitrate Concentration in High-Level Solutions (U)", WSRC-RP-91-1171, 1991.
- <sup>18</sup> N. E. Bibler and C. L. Crawford, "Hydrogen Production in Radioactive Solutions in the Defense Waste Processing Facility (U)", WSRC-TR-95-0090, 1995.
- <sup>19</sup> C. L. Crawford and D. D. Walker, "Hydrogen Generation by Radiolysis of Tetraphenylborate Solutions and Slurries (U)", WSRC-TR-96-0109, Rev. 0, 1996.
- <sup>20</sup> N. E. Bibler, J. M. Pareizs, T. L. Fellingner, and C. J. Bannochie, "Measurement and Prediction of Radiolytic Hydrogen Production in Defense Waste Processing Slurries at Savannah River Site", WSRC-STI-2006-00114 Rev. 1, 2007.
- <sup>21</sup> G. V. Buxton, C. L. Greenstock, W. P. Helman, and A. B. Ross, "Critical Review of Rate Constants for Reactions of Hydrated Electrons, Hydrogen Atoms and Hydroxyl Radicals ( $\cdot\text{OH}/\cdot\text{O}$ ) in Aqueous Solution," Journal of Physical and Chemical Reference Data (1988) 17, No. 2, 513-886.
- <sup>22</sup> D. Meisel, C. D. Jonah, S. Kapoor, M. S. Matheson, and M. C. Sauer, Jr., "Radiolytic and Radiolytically Induced Generation of Gases from Synthetic Wastes", ANL-93/43, 1993.
- <sup>23</sup> S. A. Bryan, L. R. Pederson, and C. M. King, "Thermal and Radiolytic Gas Generation in Hanford High-Level Waste," WM'00 Conference, February 27 - March 2, 2000, Tucson, AZ, 2000, <http://www.wmsym.org/archives/2000/pdf/41/41-07.pdf>.

- <sup>24</sup> D. Meisel, H. Diamond, E. P. Horwitz, C. D. Jonah, M. S. Matheson, M. C. Sauer, Jr., J. C. Sullivan, F. Barnabas, E. Cerny, and Y. D. Cheng, "Radiolytic Generation of Gases from Synthetic Waste Annual Report – FY 1991", ANL-91/41, 1991.
- <sup>25</sup> T. A. Hu, "Empirical Rate Equation Model and Rate Calculations of Hydrogen Generation for Hanford Tank Waste", HNF-3851, Rev. 1, 2004.
- <sup>26</sup> R. J. Yarbrough, "Steady-State Flammable Gas Release Rate Calculation and Lower Flammability Level Evaluation for Hanford Tank Waste", RPP-5926, Rev. 17, 2016,  
<http://pdw.hanford.gov/arpir/index.cfm/viewDoc?accession=0074988H>.
- <sup>27</sup> D. J. Sherwood and L. M. Stock, "Modifying the Hu Correlation to Predict Hydrogen Formation in the Hanford Waste Treatment and Immobilization Plant", 24590-WTP-RPT-RT-04-0002, Revision 0, 2004.
- <sup>28</sup> J. W. T. Spinks and R. J. Woods, "An Introduction to Radiation Chemistry", 3<sup>rd</sup> Edition, Wiley-Interscience, 1990.
- <sup>29</sup> T. A. Hu, "Improved Model for Hydrogen Generation Rate of Radioactive Waste at the Hanford Site", Nuclear Technology (2012) 178, No. 1, 39-54.
- <sup>30</sup> L. M. Stock and J. E. Meacham, "Occurrence and Chemistry of Organic Compounds in Hanford Site Waste Tanks", RPP-21854, Rev. 0, 2004.
- <sup>31</sup> R. T. Pabalan, M. S. Jarzempa, T. A. Abrajano Jr., D. A. Pickett, D. S. Moulton, N. Sridhar, J. Weldy, C. S. Brazel, J. T. Persyn, B. Li, J. P. Hsu, and J. Erwin, "Hanford Tank Waste Remediation System High-Level Waste Chemistry Manual", Center for Nuclear Waste Regulatory Analyses, San Antonio, TX, Rev. 1, 1998,  
<https://www.nrc.gov/docs/ML0336/ML033640258.pdf>
- <sup>32</sup> D. M. Camaioni, W. D. Samuels, J. C. Linehan, A. K. Sharma, S. T. Autrey, M. A. Lilga, M. O. Hogan, S. A. Clauss, K. L. Wahl, and J. A. Campbell, "Organic Tanks Safety Program Waste Aging Studies Final Report", PNNL-11909, Rev. 1, 1998.
- <sup>33</sup> S. Fiskum, L. Snow, M. Edwards, R. Shimskey, and R. Peterson, "Hanford Tank Waste – What is in it? Where is it going? - 10277", WM2010 Conference, March 7-11, 2010, Phoenix, AZ, 2010,  
<http://www.wmsym.org/archives/2010/pdfs/10277.pdf>.
- <sup>34</sup> V. Jain, H. Shah, J. E. Occhipinti, W. R. Wilmarth, and R. E. Edwards, "Evaluation of Mercury in Liquid Waste Processing Facilities Phase I Report", SRR-CES-2015-00012, Rev. 1, 2015.
- <sup>35</sup> C. J. Bannochie, T. L. Fellingner, P. Garcia-Strickland, H. B. Shah, V. Jain, and W. R. Wilmarth, "Mercury in Aqueous Tank Waste at the Savannah River Site: Facts, Forms, and Impacts", Separation Science and Technology (2017) online article 28 Mar 2017, 1-13,  
<http://www.tandfonline.com/doi/pdf/10.1080/01496395.2017.1310239?needAccess=true>.
- <sup>36</sup> J. K. Dunleavy, "Final Analysis Mercury as a Catalyst Poison", Platinum Metals Rev. (2006) 50, No. 3, 156.
- <sup>37</sup> D. C. Koopman, "Statistical Evaluation of Processing Data from the Rh-Ru-Hg Matrix Study", SRNL-STI-2009-00084, Rev. 0, 2009.
- <sup>38</sup> J. T. Willett, "Mercury Compounds as Catalysts for the Polyurethane Reaction", US Patent US3419509 A, 1968.
- <sup>39</sup> E. C. Ashby, E. K. Barefield, C. L. Liotta, H. M. Neumann, F. Doctorovich, A. Konda, K. Zhang, J. Hurley, D. Boatright, A. Annis, G. Pansino, M. Dawson, and M. Juliao, "Mechanistic Studies Related to the Thermal Chemistry of Simulated Nuclear Wastes That Mimic the Contents of a Hanford Site Double-Shell Tank", ACS Symposium Series (1994) 554, Chapter 16 Emerging Technologies in Hazardous Waste Management IV, 249.
- <sup>40</sup> E. C. Ashby, C. Jonah, D. Meisel, L. R. Pederson, and D. M. Strachan, "Gas Generation and Retention in Tank 101-SY: A Summary of Laboratory Studies, Tank Data, and Information Needs", PNL-8124, 1992.
- <sup>41</sup> E. C. Ashby, F. Doctorovich, C. L. Liotta, H. M. Neumann, E. K. Barefield, A. Konda, K. Zhang, J. Hurley, and D. D. Siemer, "Concerning the Formation of Hydrogen in Nuclear Waste. Quantitative Generation of Hydrogen via a Cannizzaro Intermediate", J. Am. Chem. Soc. (1993) 115, No. 3, 1171-1173.
- <sup>42</sup> E. K. Barefield, D. Boatright, A. Deshpande, F. Doctorovich, C. L. Liotta, H. M. Neumann, and S. Seymore, "Mechanisms of Gas Generation from Simulated SY Tank Farm Wastes: FY 1995 Progress Report", PNNL-11247, 1996.
- <sup>43</sup> E. K. Barefield, C. L. Liotta, and H. M. Neumann, "Studies Related to Chemical Mechanisms of Gas Formation in Hanford High-Level Nuclear Wastes", Project ID Number 54807, 1998.
- <sup>44</sup> H. Babad, G. D. Johnson, J. A. Lechelt, D. A. Reynolds, L. R. Pederson, D. M. Strachan, D. Meisel, C. Jonah, and E. C. Ashby, "Evaluation of the Generation and Release of Flammable Gases in Tank 241-SY-101", WHC-EP-0517, 1991.
- <sup>45</sup> D. Meisel, H. Diamond, E. P. Horwitz, C. D. Jonah, M. S. Matheson, M. C. Sauer, Jr., and J. C. Sullivan, "Radiation Chemistry of Synthetic Waste", ANL-91/40, 1991.

- <sup>46</sup> D. Meisel, M. C. Sauer, Jr., J. C. Sullivan, C. D. Jonah, H. Diamond, M. S. Matheson, F. Barnabas, E. Cerny, and Y. Cheng, "Radiolytic and Radiolytically Induced Generation of Gases in Simulated Waste Solutions", ANL/CP-74531, 1990.
- <sup>47</sup> S. Kapoor, F. Barnabas, C.D. Jonah, M. C. Sauer, Jr., and D. Meisel, "On the Generation of H<sub>2</sub> from Formaldehyde in Basic Aqueous Solutions", ANL/CHM/PP-76828, 1994.
- <sup>48</sup> C. D. Jonah, D. Meisel, and M. C. Sauer, Jr., "The Radiolytic and Radiolytically Induced Gas Generation in Hanford Waste Tanks", ANL/CHM/PP-77923, 1994.
- <sup>49</sup> D. Meisel, A. Cooka, D. Camaioni, and T. Orlando, "Chemistry, Radiation, and Interfaces in Suspensions of Nuclear Waste Simulants", ANL/CHM/CP-92698, 1997.
- <sup>50</sup> S.A. Bryan and L. R. Pederson, "Composition, Preparation, and Gas Generation Results from Simulated Wastes of Tank 241-SY-101", PNL-10075, 1994.
- <sup>51</sup> L.R. Pederson and S. A. Bryan, "Status and Integration of Studies of Gas Generation in Hanford Wastes", PNNL-11297, 1996.
- <sup>52</sup> D. M. Strachan, L. R. Pederson, S. A. Bryan, E. C. Ashby, C. Liotta, E. K. Barefield, D. Meisel, C. D. Jonah, and M. C. Sauer, Jr., "Chemical Mechanisms for Gas Generation in Tank 241-SY-101", ANL/CHM/CP-79536, 1993.
- <sup>53</sup> A. Costine and J. S. C. Loh, "Understanding Hydrogen in Bayer Process Emissions. 4. Hydrogen Production during the Wet Oxidation of Industrial Bayer Liquor", Ind. Eng. Chem. Res. (2016) 55, No. 16, 4415-4425.
- <sup>54</sup> E. C. Ashby, A. Annis, E. K. Barefield, D. Boatright, F. Doctorovich, C. L. Liotta, H. M. Neumann, A. Konda, C. F. Yao, K. Zhang, and N. G. McDuffie, "Synthetic Waste Chemical Mechanism Studies", WHC-EP-0823, 1994.
- <sup>55</sup> A. Costine, J. S. C. Loh, G. Power, M. Schibeci, and R. G. McDonald, "Understanding Hydrogen in Bayer Process Emissions. 1. Hydrogen Production during the Degradation of Hydroxycarboxylic Acids in Sodium Hydroxide Solutions", Ind. Eng. Chem. Res. (2011) 50, No. 22, 12324-12333.
- <sup>56</sup> A. Costine, J. S. C. Loh, F. Busetti, C. A. Joll, and A. Heitz, "Understanding Hydrogen in Bayer Process Emissions. 3. Hydrogen Production during the Degradation of Polyols in Sodium Hydroxide Solutions", Ind. Eng. Chem. Res. (2013) 52, No. 16, 5572-5581.
- <sup>57</sup> R. M. Chamberlin and J. B. Arterburn, "Dynamic Effects of Tank Waste Aging on Radionuclide Complexant Interactions", LA-UR-00-5998, 2000.
- <sup>58</sup> J. B. Arterburn, M. Pannala, A. M. Gonzalez, and R. M. Chamberlin, "Palladium-Catalyzed Transfer Hydrogenation in Alkaline Aqueous Medium", Tetrahedron Letters 41, (2000) No 41, 7847-7849.
- <sup>59</sup> S. H. Reboul and H. M. Ajo, "Noble Metals in As-Received Tank 51 SB5 Qualification Sample", SRNL-PSE-2008-00115, Rev. 0, 2008.
- <sup>60</sup> C. H. Keilers, Jr., R. Brigmon, T. Britt, M. Clark, S. Fink, D. Hobbs, W. King, C. Nash, B. Wiersma, and J. Zamecnik, "Flammable Gas Generation Mechanisms for High Level Liquid Waste Facilities", X-ESR-G-00062, Rev. 0, 2017.
- <sup>61</sup> E. K. Barefield, D. Boatright, A. Deshpande, F. Doctorovich, C. L. Liotta, H. M. Neumann, and S. Seymore, "Mechanisms of Gas Generation from Simulated SY Tank Farm Wastes: FY 1994 Progress Report", Flammable Gas Safety Program, 1994.
- <sup>62</sup> D. M. Camaioni, W. D. Samuels, B. D. Lenihan, S. A. Clauss, K. L. Wahl, and J. A. Campbell, "Organic Tanks Safety Program Waste Aging Studies", PNL-10161, 1994.
- <sup>63</sup> February 2017 Waste Characterization Spreadsheet, Waste Characterization System: WCS, \\Wg17\WCS1.5PROD\WCS 1.5 v011.4.xls, February 7, 2017.
- <sup>64</sup> C. J. Martino and C. J. Coleman, "Evaporator Feed Qualification Analysis of Tank 38H and 43H Samples: January 2010 through April 2013", SRNL-STI-2012-00464, Rev. 0, 2013.
- <sup>65</sup> A. T. Clair, "Inclusion of Organic Contribution to Radiolytic and Thermolytic Hydrogen Generation in DWPF", X-ESR-S-00320, Rev. 2, 2017.
- <sup>66</sup> S. K. Guardiano, L. C. Terheggen, and C. B. Sudduth, "Inclusion of Organic Contribution to Radiolytic and Thermolytic Hydrogen Generation at CSTF", X-ESR-G-00061, Rev. 0, 2017.
- <sup>67</sup> J. R. Hester, "Reliability of WCS Hydrogen Generation Rate Estimates", HLW-STE-2002-00361, Rev. 0, 2002.
- <sup>68</sup> R. F. Swingle, "Analysis of Organic Samples from Waste Tanks 26F, 33F, 46F, and 43H – Summer 1999", WSRC-TR-99-00397, Rev. 0, 1999.
- <sup>69</sup> H. Bui, "CSTF Flammability Control Program- Program Description Document", WSRC-TR-2003-00087, Rev. 29, 2016.

- 
- <sup>70</sup> J. M. Pareizs, J. D. Newell, C. J. Martino, C. L. Crawford, and F. C. Johnson, “Sludge Washing and Demonstration of the DWPF Nitric/Formic Flowsheet in the SRNL Shielded Cells for Sludge Batch 9 Qualification”, SRNL-STI-2016-00355, Rev. 0, 2016.
- <sup>71</sup> J. M. Pareizs and C. L. Crawford, “Sludge Washing and Demonstration of the DWPF Flowsheet in the SRNL Shielded Cells for Sludge Batch 8 Qualification”, SRNL-STI-2013-00116, Rev. 0, 2013.
- <sup>72</sup> C. J. Bannochie, T. L. Fellingner and J. M. Pareizs, “Tank 40 Final SB3 Chemical Characterization Results”, WSRC-TR-2005-00049, Rev. 0, 2005.
- <sup>73</sup> C. J. Bannochie, “Tank 40 Final SB4 Chemical Characterization Results”, WSRC-STI-2007-00674, Rev. 0, 2008.
- <sup>74</sup> C. J. Bannochie and D. R. Click, “Tank 40 Final SB5 Chemical Characterization Results Prior to Np Addition”, SRNL-STI-2009-00060, Rev. 2, 2010.
- <sup>75</sup> C. J. Bannochie, “Tank 40 Final SB6 Chemical Characterization Results”, SRNL-STI-2010-00441, Rev. 0, 2010.
- <sup>76</sup> C. J. Bannochie, “Tank 40 Final SB7b Chemical Characterization Results”, SRNL-STI-2012-00097, Rev. 1, 2012.
- <sup>77</sup> C. J. Bannochie, “Tank 40 Final Sludge Batch 8 Chemical Characterization Results”, SRNL-STI-2013-00504, Rev. 0, 2013.
- <sup>78</sup> S. T. Isom, “Input to Consolidated Hazards Assessment for Glycolic Acid Impact to the Recycle Waste System in the Defense Waste Processing Facility”, X-ESR-S-00252, Rev. 0, 2015.
- <sup>79</sup> C. J. Bannochie, W. P. Kubilius and J. M. Pareizs, “Tank 40 Final Sludge Batch 9 Chemical and Fissile Radionuclide Characterization Results”, SRNL-STI-2017-00239, Rev. 0, 2017.
- <sup>80</sup> C. L. Crawford, “Impacts formate and glycolate to SRS Tank Farm”, B9108-00026-42, SRNL E-Notebook (Production), Savannah River National Laboratory, June 2017.
- <sup>81</sup> A. T. Clare, “Maximum Catalytic Hydrogen Generation Rate in the DWPF Nitric-Glycolic Flowsheet”, DWPF-I-PC-0046, Rev. 0, 2016.
- <sup>82</sup> D. P. Lambert, J. R. Zamecnik and D. R. Best, “FY13 Glycolic-Nitric Acid Flowsheet Demonstrations of the DWPF Chemical Process Cell with Simulants”, SRNL-STI-2013-00343, Rev. 0, 2014.
- <sup>83</sup> NFPA 69, Standard on Explosion Prevention Systems, 2002 Edition.  
<http://hamyarenergy.com/static/fckimages/files/NFPA/Hamyar%20Energy%20NFPA%2069%20-%202002.pdf>
- <sup>84</sup> “Final Safety Analysis Report Savannah River Site Defense Waste Processing Facility”, WSRC-SA-6, Rev. 35, Volume 8, 2016.
- <sup>85</sup> C. J. Martino, J. D. Newell, and M. S. Williams, “Nitric-Glycolic Flowsheet Testing for Maximum Hydrogen Generation Rate”, SRNL-STI-2015-00130, Rev. 0, 2016.
- <sup>86</sup> S. T. Isom, “Input to Consolidated Hazards Analysis for the Glycolic Acid Impact to the Chemical Processing Cell in the Defense Waste Processing Facility”, X-ESR-S-00276, Rev. 0, 2016.
- <sup>87</sup> E. F. Riddick, “Radiolytic and Catalytic Hydrogen Generation Rates for DWPF Waste Streams and Vessels (U)”, S-CLC-S-00149, Rev. 0, 2014.
- <sup>88</sup> C. J. Martino, J. D. Newell and J. M. Pareizs, “Task Technical and Quality Assurance Plan for Testing to Support Hydrogen Generation Rate in the Savannah River Site Tank Farm and Defense Waste Processing Facilities”, SRNL-RP-2017-00305, Rev. 0, 2017.

**Appendix A Radiolysis HGR Equations for SRS Baseline Methodology Involving Water Radiolysis  
and Organic Radiolysis Via Competition Kinetics**

## SRS Baseline

$$G(H_2)_{total} = G(H_2)_{Water Radiolysis} + G(H_2)_{Organic Radiolysis Competition Kinetics}$$

### Water Radiolysis

Beta/gamma  $G(H_2)=0.466$  and alpha  $G(H_2)=1.3$  terms;  $NO_{eff} = [NO_3^-] + 0.5*[NO_2^-]$

G-value correlations increased 10% to R-value terms (Reference 16)

G-value convert to R-value with constant 94.37 (based on 25°C)

R-value ( $ft^3/1E+06$  Btu) x Btu/hr/1E+06 =  $ft^3/hr$   $H_2$  generation rate (Reference 63)

Equations from Reference 16:

$$G_{\beta/\gamma} = 0.466 - 0.51*[NO_{eff}^-]^{1/3} + 0.14*[NO_{eff}^-]^{2/3} + 0.0055*[NO_{eff}^-] \quad (4)$$

$$G_{\alpha} = 1.3 - 0.79*[NO_{eff}^-]^{1/3} - 0.13*[NO_{eff}^-]^{2/3} + 0.11*[NO_{eff}^-] \quad (1)$$

$$R_{\alpha} = 134.7 - 82.3*[NO_{eff}^-]^{1/3} - 13.6*[NO_{eff}^-]^{2/3} + 11.8*[NO_{eff}^-] \quad (7)$$

$$R_{\beta/\gamma} = 48.36 - 52.78*[NO_{eff}^-]^{1/3} + 14.1*[NO_{eff}^-]^{2/3} + 0.572*[NO_{eff}^-] \quad (8)$$

### Organic Radiolysis (Competition Kinetics from Reference 20)

Beta/gamma  $G(H_2)_{organic} = G(H\cdot) = 0.58 \times f_{organic}$  and alpha  $G(H_2)_{organic} = G(H\cdot) = 0.27 \times f_{organic}$

where,

$G(H\cdot)$  is the radiolytic yield of H atoms per 100 eV of energy absorbed

$f_{organic}$  is the fraction of hydrogen radicals that react with organics to produce  $H_2$ .

The  $f_{organic}$  is based on the ratio of the reactivity of organics to total reactivity of organics plus other scavengers, i.e.,  $NO_2^-$ ,  $NO_3^-$  and  $OH^-$ . See Table 3-2 for an example calculation involving formate and glycolate.

G-value convert to R-value with constant 94.37 (based on 25°C)

R-value ( $ft^3/1E+06$  Btu) x Btu/hr/1E+06 =  $ft^3/hr$   $H_2$  generation rate (Reference 63)

**Appendix B. Radiolysis HGR Equations for SRS Baseline Methodology Involving Water Radiolysis  
and Organic Radiolysis Via ANL Correlation**

## SRS Baseline and ANL Correlation

$$G(H_2)_{\text{total}} = G(H_2)_{\text{Water Radiolysis}} + G(H_2)_{\text{Organic Radiolysis ANL Correlation}}$$

### Water Radiolysis

Beta/gamma  $G(H_2)=0.466$  and alpha  $G(H_2)=1.3$  terms;  $NO_{\text{eff}} = [NO_3^-] + 0.5*[NO_2^-]$

G-value correlations increased 10% to R-value terms (Reference 16)

G-value convert to R-value with constant 94.37 (based on 25°C)

R-value ( $\text{ft}^3/1\text{E}+06 \text{ Btu}$ ) x  $\text{Btu/hr}/1\text{E}+06 = \text{ft}^3/\text{hr}$   $H_2$  generation rate (Reference 63)

Equations from Reference 16:

$$G_{\beta/\gamma} = 0.466 - 0.51 * [NO_{\text{eff}}^-]^{1/3} + 0.14 * [NO_{\text{eff}}^-]^{2/3} + 0.0055 * [NO_{\text{eff}}^-] \quad (4)$$

$$G_{\alpha} = 1.3 - 0.79 * [NO_{\text{eff}}^-]^{1/3} - 0.13 * [NO_{\text{eff}}^-]^{2/3} + 0.11 * [NO_{\text{eff}}^-] \quad (1)$$

$$R_{\alpha} = 134.7 - 82.3 * [NO_{\text{eff}}^-]^{1/3} - 13.6 * [NO_{\text{eff}}^-]^{2/3} + 11.8 * [NO_{\text{eff}}^-] \quad (7)$$

$$R_{\beta/\gamma} = 48.36 - 52.78 * [NO_{\text{eff}}^-]^{1/3} + 14.1 * [NO_{\text{eff}}^-]^{2/3} + 0.572 * [NO_{\text{eff}}^-] \quad (8)$$

### Organic Radiolysis (based on ANL glycolate testing Reference 24)

$$G(H_2)_{\text{Organic Radiolysis ANL Correlation}} = R_x \times [RH]$$

$$R_{\text{glycolate}} = 0.055 \text{ for glycolate}$$

$R_{\text{formate}} = 0.055 \times 0.5 \times [\text{rate}(\text{formate} + H\cdot = 2.1\text{E}+08 \text{ M}^{-1}\text{s}^{-1}) / \text{rate}(\text{glycolate} + H\cdot = 4.6\text{E}+07 \text{ M}^{-1}\text{s}^{-1})]$  for formate; Note: the '0.5' factor above is used due to the presence of only 1 C-H bond in formate vs. 2 C-H bonds in glycolate.

G-value convert to R-value with constant 94.37 at 25°C

R-value ( $\text{ft}^3/1\text{E}+06 \text{ Btu}$ ) x  $\text{Btu/hr}/1\text{E}+06 = \text{ft}^3/\text{hr}$   $H_2$  generation rate (Reference 63)



## **Appendix C. Radiolysis HGR Equations for Hanford**

## Hanford Baseline from Reference 29

### Water Radiolysis

Beta/gamma  $G(H_2) = 0.45$  and alpha  $G(H_2) = 1.4$  terms;

$[NO_3^-]$ ,  $[NO_2^-]$ ,  $[Na^+]_{ex}$  (0 to 10-14 range for SRS Salt)

G-value correlations multiplied by liquid fraction ( $L_f$ ) (0.3 up to 1.0 SRS)

G-value convert to R-value with constant 94.37 (based on 25°C)

R-value ( $ft^3/1E+06$  Btu) x Btu/hr/1E+06 =  $ft^3/hr$   $H_2$  gen rate (Reference 63)

$$G_{(H_2)_{H_2O}}^{\beta/\gamma} = \frac{0.32}{1 + 2.4[NO_3^-] + 0.62[NO_2^-] + 0.31[Na^+]_{ex}^2} + \frac{0.13}{1 + 139[NO_3^-] + 54[NO_2^-]}$$

$$G_{(H_2)_{H_2O}}^{\alpha} = \frac{1.05}{1 + 2.4[NO_3^-] + 0.63[NO_2^-]} + \frac{0.35}{1 + 3900[NO_3^-] + 1400[NO_2^-]}$$

### Organic Radiolysis from Reference 29

Beta/gamma  $G(H_2)$  based on TOC and Temperature

Alpha  $G(H_2)$  based on TOC and Temperature; 0.5X factor relative to beta/gamma

G-value correlations multiplied by liquid fraction ( $L_f$ ) (0.3 up to 1.0 SRS)

G-value convert to R-value with constant 94.37 (based on 25°C)

R-value ( $ft^3/1E+06$  Btu) x Btu/hr/1E+06 =  $ft^3/hr$   $H_2$  gen rate (Reference 63)

$$G_{(H_2)_{ORG}}^{\beta/\gamma} = a_{rad} \times \exp^{(-E_{rad}/RT)} \times (r_f \times [TOC])$$

$$G_{(H_2)_{ORG}}^{\alpha} = 0.5 \times a_{rad} \times \exp^{(-E_{rad}/RT)} \times (r_f \times [TOC])$$

Where,

$E_{rad} = 48,800$  J/mole, the activation energy in organic radiolysis

$a_{rad} = 1.11 \times 10^7$   $H_2/100$  eV, the pre-exponential term in organic radiolysis

$r_f = 0.6$  DSTs and 0.3 for SSTs, the reactivity coefficient of [TOC]

$R = 8.314$  J/mole/K, gas constant

$T$  = absolute temperature of waste in (K)

[TOC] = total organic carbon concentration in the liquid waste (wt%)

**Appendix D. Fraction of Organics Reacting with Hydrogen Atom with Formate and Glycolate  
Equal to 10 g/L**

**Table D-1. Fraction of Organics Reacting with Hydrogen Atom for All Tanks with Formate and Glycolate Equal to 10 g/L\***

Tank	f(gly.)	f(form.)	f(organic)	[NO <sub>2</sub> <sup>-</sup> ], M	[NO <sub>3</sub> <sup>-</sup> ], M	[OH <sup>-</sup> ], M
1	0.003	0.021	0.024	2.75	2.00	9.30
2	0.003	0.020	0.022	3.04	2.25	7.18
3	0.003	0.026	0.029	2.26	1.71	6.76
4	0.017	0.131	0.148	0.41	0.30	0.66
7	0.016	0.122	0.138	0.45	0.38	0.55
8	0.007	0.057	0.064	0.98	0.86	3.24
9	0.003	0.019	0.022	3.20	1.90	3.80
10	0.017	0.129	0.146	0.40	3.02	1.07
11	0.032	0.241	0.273	0.16	0.83	1.08
13	0.013	0.095	0.108	0.58	0.59	1.18
14	0.003	0.021	0.024	2.90	3.70	4.10
15	0.005	0.040	0.046	1.52	0.90	0.94
21	0.011	0.080	0.091	0.67	1.16	2.45
22	0.029	0.222	0.251	0.22	0.05	0.11
23	0.015	0.116	0.132	0.46	1.37	0.92
24	0.003	0.024	0.028	2.37	1.72	7.74
25	0.006	0.047	0.053	1.22	2.58	3.43
26	0.009	0.068	0.077	0.81	1.62	2.52
27	0.004	0.030	0.034	1.90	1.79	7.16
28	0.004	0.029	0.033	1.91	1.76	8.16
29	0.024	0.181	0.205	0.27	0.34	0.58
30	0.003	0.025	0.029	2.23	1.52	8.80
31	0.003	0.024	0.027	2.58	2.57	4.13
32	0.006	0.042	0.048	1.34	1.85	4.36
33	0.008	0.060	0.068	0.91	1.25	3.20
34	0.005	0.040	0.046	1.39	1.54	5.21
35	0.007	0.056	0.063	1.06	2.01	1.44
36	0.004	0.029	0.033	1.94	1.44	8.29
37	0.006	0.045	0.051	1.29	1.47	3.06
38	0.006	0.044	0.050	1.35	0.62	1.63
39	0.020	0.155	0.175	0.30	1.66	1.56
40	0.023	0.174	0.197	0.30	0.10	0.18
41	0.026	0.198	0.224	0.25	0.09	0.18
42	0.003	0.025	0.029	2.29	2.01	7.60
43	0.005	0.037	0.042	1.62	0.74	2.02
44	0.006	0.046	0.052	1.11	1.27	7.72
45	0.005	0.034	0.039	1.46	1.17	12.16
46	0.004	0.033	0.037	1.64	1.13	9.32
47	0.004	0.028	0.032	1.98	1.79	8.67
48	0.012	0.095	0.107	0.58	0.21	1.31
49	0.009	0.066	0.074	0.84	1.81	2.57
50	0.010	0.079	0.090	0.69	1.84	2.05
51	0.023	0.172	0.194	0.30	0.12	0.22
<b>Min.</b>	0.003	0.019	0.022**	0.16	0.05	0.11
<b>Max.</b>	0.032	0.241	0.273**	3.20	3.70	12.16

\*Closed Tanks not shown; Organics = 10 g/L each for glycolate and formate

\*\* These minimum and maximum  $f_{\text{organic}}$  terms increase by ~ 3% (from 0.022 to 0.023) for the minimum value and by ~ 14% (from 0.273 to 0.311) for the maximum value if the hydroxide anion (OH<sup>-</sup>) is removed from the calculations